MODERN DEVELOPMENT OF MAGNETIC RESONANCE

abstracts

2014

KAZAN * RUSSIA


MODERN DEVELOPMENT OF MAGNETIC RESONANCE
KAZAN 2014

MODERN DEVELOPMENT OF MAGNETIC RESONANCE

ABSTRACTS OF THE
INTERNATIONAL CONFERENCE

Editor:
KEV M. SALIKHOV

KAZAN, SEPTEMBER 23–27, 2014

Prof. Kev M. Salikhov
Zavoisky Physical-Technical Institute,
Russian Academy of Sciences, Kazan, Russian Federation
Phone: 7 (843) 2720503
E-mail: salikhov@kfti.knc.ru

Published by Zavoisky Physical-Technical Institute, Kazan
www.kfti.knc.ru

CHAIRMAN

Kev Salikhov,
Full Member of the Russian Academy of Sciences

PROGRAM COMMITTEE

Albert Aganov (Russia)
Vadim Atsarkin (Russia)
Pavel Baranov (Russia)
Marina Bennati (Germany)
Bernhard Blümich (Germany)
Michael Bowman (USA)
Marina Brustolon (Italy)
Sabine Van Doorslaer (Belgium)
Jack Freed (USA)
Ilgiz Garifullin (Russia)
Graeme Hanson (Australia)
Martina Huber (The Netherlands)
Walter Kockenberger (UK)
Wolfgang Lubitz (Germany)
Klaus Möbius (Germany)
Hitoshi Ohta (Japan)
Igor Ovchinnikov (Russia)
Kev Salikhov (Russia)
Vladimir Skirda (Russia)
Murat Tagirov (Russia)
Takeji Takui (Japan)
Valery Tarasov (Russia)
Dmitrii Tayurskii (Russia)
Yurii Tsvetkov (Russia)
Violeta Voronkova (Russia)

LOCAL ORGANIZING COMMITTEE

Tarasov V.F., chairman
Adzhaliev Yu.A.
Akhmin S.M.
Chuclanov A.P.
Falin M.L.
Galeev R.T.
Gerasimov K.I.
Goleneva V.M.
Gubaidulina A.Z.
Guseva R.R.
Kupriyanova O.O.
Kurkina N.G.
Latypov V.A.
Lvov S.G.
Mosina L.V.
Voronkova V.K.
Voronova L.V.
Yanduganova O.B.
Yurtaeva S.V.
Ziganshina S.A.

SCIENTIFIC SECRETARY

Violeta K. Voronkova

The conference is organized under the auspices of the AMPERE Society

ORGANIZERS

Kazan E. K. Zavoisky Physical-Technical Institute
of the Kazan Scientific Center of the Russian Academy of Sciences
The Academy of Sciences of the Republic of Tatarstan
Kazan Federal University

SUPPORTED BY

The Government of the Republic of Tatarstan
The Russian Foundation for Basic Research
Bruker BioSpin Moscow

CONFERENCE LOCATION

The Academy of Sciences of the Republic of Tatarstan
Kazan, ul. Baumana 20

CONTENTS

ZAVOISKY AWARD LECTURES

Measuring the Nanoworld
G. Jeschke 2

RNA and DNA: Flexible Molecules for Cellular Regulation
T. F. Prisner 3

PLENARY LECTURES

Dipolar Spectroscopy: New Methodical Aspects and Applications
P. E. Spindler, P. Schöps, A. Marko, B. Endeward, T. F. Prisner 6

The Long Way that Leads from Short Distances to Biomolecular Structure
G. Jeschke 7

ODMR as a Tools to Study Nanosystems
N. G. Romanov, P. G. Baranov 8

Distance Measurements in Nucleic Acids Using Advanced SDSL with Nitroxyl and Trityl Radicals
E. Bagryanskaya, O. Krumkacheva, M. Fedin, A. Kuzhelev, V. Tormushev, I. Kirilyuk, Y. Polienko, E. Babaylova, G. Karpova, G. Shevelev, A. Lomzov, D. Pyshny 9

Solid State NMR Studies of Heterogeneous Catalysts
G. Buntkowsky, T. Gutmann, H. Breitzke 11

Spin Relaxation in Disordered Media
F. S. Dzheparov 12

Electrons Localization in Ge/Si Nanoheterostructures Studied by ESR
A. V. Dvurechenskii, A. F. Zinovieva, A. V. Nenashev 13

Molecular Motions in Frozen Phospholipid Bilayers in Presence of Cryoprotectors: Spin Label EPR Study
K. B. Konov, N. P. Isaev, D. V. Leonov, S. A. Dzuba 14

Time-Resolved and Field Dependent CIDNP of Biologically Important Molecules
A. V. Yurkovskaya, O. B. Morozova 15

Electronic Structure and Magnetic Anisotropy in 3d-Transition Metal Single Ion Magnets from the First Principles
E. A. Suturina, M. Atanasov, F. Neese 16

Spin Labeling: 50 Years of History
G. I. Likhtenshtein 17

SECTION 1
CHEMICAL AND BIOLOGICAL SYSTEMS

What Iron Electron Configuration – d^7 or d^9 is Characteristic of Electronic Structure of Dinitrosyl Iron Complexes with Thiolate Ligands in the Solutions
A. F. Vanin 20

Nitroxide Biradicals with Acetylene Groups in the Bridge: Structure, Internal Mobility, EPR, and DFT Calculations
O. I. Gromov, E. N. Golubeva, A. I. Kokorin 21

EPR Study of Tetranitroxide Derivatives of C60
R. B. Zaripov, G. R. Nureeva, L. I. Savostina, V. K. Voronkova, K. M. Salikhov, V. P. Gubskaya, I. A. Nuretdinov 22

SECTION 2
MODERN METHODS OF MAGNETIC RESONANCE

Solid-State NMR in Heterogeneous Catalysis
O. B. Lapina, A. A. Shubin, V. V. Terskikh 26

Nuclear Spin Isomers of Molecules for Signal Enhancement in NMR and MRI
I. V. Koptyug, V. V. Zhivonitko, K. V. Kovtunov, I. V. Skovpin, D. A. Barskiy, O. G. Salnikov 27

Detecting a New Source for Photochemically Induced Dynamic Nuclear Polarization
G. Kothe, M. Lukaschek, G. Link, S. Kacprzak, B. Illarionov, M. Fischer, W. Eisenreich, A. Bacher, S. Weber 28

The Influence of the Magnetic Nuclei in Intersystem Crossing of Pentacene
Yu. E. Kandrashkin 29

SECTION 3
THEORY OF MAGNETIC RESONANCE

Proton Spin Dynamics in Polymer Melts: New Perspectives for Experimental Investigations of Polymer Dynamics
N. Fatkullin, S. Stapf, M. Hofmann, R. Meier, E. A. Rössler 32

Entanglement and Quantum Discord in NMR Experiments
E. B. Fel'dman 33

SECTION 4
STRONGLY CORRELATED ELECTRON SYSTEMS

Order-by-Disorder in the Frustrated Quantum Spin Magnet $CoAl_2O_4$
V. Kataev, S. Zimmermann, A. Alfonsov, E. Vavilova, M. Iakovleva, H.-J. Grafe, H. Luetkens, H.-H. Klauss, A. Maljuk, T. Dey, S. Wurmehl, B. Büchner 36

Effects of Disorder in Doped Honeycomb Iridates
E. Vavilova, V. Kataev, G. Prando, A. Alfonsov, H.-J. Grafe, B. Büchner, H. Wu, Q. Huang, K. Baroudi, C. Yim, R. J. Cava 37

Investigation of the Heterostructure $YbMnO_3/SrTiO_3$ by ESR Method
R. M. Eremina, I. V. Yatsyk, D. V. Mamedov, T. P. Gavrilova, I. I. Fazlizhanov, V. I. Chichkov, N. V. Andreev 38

SECTION 5
LOW-DIMENSIONAL SYSTEMS AND NANO-SYSTEMS

Spin Splitting of Edge π-Electronic States of Nanographites at their Interaction with Acceptor Molecules: ESR, CESR and MS Studies
A. M. Ziatdinov, N. S. Saenko 40

Peculiarities of Magnetic Properties of New 2D Honeycomb Lattice Tellurates $A_2Ni_2TeO_6$ (A = Li, Na)
E. A. Zvereva, V. Y. Kudryashov, V. B. Nalbandyan, I. L. Shukaev, A. N. Vasiliev 42

Tunnel Magnetoresistance of Magnetic Point Contacts
N. Useinov, L. Tagirov 44

Potentials of NMR for Transport and Structural Characterization of Nanoporous Solids
R. Valiullin 46

SECTION 6
OTHER APPLICATIONS OF MAGNETIC
RESONANCE. RELATED PHENOMENA

Goethite (α-FeOOH) Magnetic Transition by ESR and Auxiliary Techniques
D. F. Valezi, M. T. Piccinato, P. W. C. Sarvezuk, F. F. Ivashita, A. Paesano Jr., J. Varalda, D. H. Mosca, C. L. B. Guedes, E. Di Mauro 48

Formation of the Train of Short Pulses from a Single Photon Field
R. N. Shakhmuratov 49

Pulse EPR Study of Photo-Induced States of Systems on the Basis of Zinc Porphyrin
A. Sukhanov, V. Voronkova, E. Mikhalitsyna, V. Tyurin, K. Salikhov 50

Mechanism of Photoreaction in Aqueous Solutions Involving Radicals of S-Methylcysteine and S-Methylglutathione Studied by Time Resolved and Magnetic Field Dependence CIDNP
M. S. Panov, O. B. Morozova, A. V. Yurkovskaya 51

Pulsed Electron-Electron Double Resonance Spectroscopy on a High-Spin Mn^{2+} Ion Non-Covalently Attached to a Nitroxide Radical
D. Akhmetzyanov, J. Plackmeyer, B. Endeward, V. Denysenkov, A. Marko, T. F. Prisner 52

Transceiver System for New Specialized Medical Magnet-Resonance Tomographs
A. A. Bayazitov, Ya. V. Fattakhov, A. R. Fakhrutdinov, V. N. Anashkin, V. A. Shagalov, P. Chumarov 53

Aggregation of Antimicrobial Peptide Alamethicin in Bacteria Cell Observed by EPR
N. P. Isaev, R. I. Samoilova, M. De Zotti, F. Formaggio, C. Toniolo, J. Raap 55

Management of Relative Phases of Excited Dipoles with Pulse of Weak Magnetic Field and Photon Echo Measurement of *g*-factors both Ground and Excited States Er^{3+} in $LuLiF_4$
V. N. Lisin, A. M. Shegeda 56

POSTERS

EPR and NMR Investigations of the Thermal Annealing Effect on the Structure of MACG
M. M. Akhmetov, V. Yu. Petukhov, G. G. Gumarov, G. N. Konygin, D. S. Rybin, M. M. Bakirov, A. B. Konov 60

EPR Investigations of Disprosium Dimer with the Field-Induced Slow Magnetic Relaxation
A. Baniodeh, R. Galeev, A. Sukhanov, R. Eremina, V. Voronkova, Ch. E. Anson, A. Mondal, A. K. Powell 62

Self-Organization Features of the Copper(II) Bromide Compound with 3-Amino-4-Ethoxycarbonylpyrazole
A. S. Berezin, V. A. Nadolinny, L. G. Lavrenova 63

Phase Separation in $La_{0.75}Gd_{0.25}MnO_3$ Detected by ESR
R. M. Eremina, I. V. Yatsyk, D. V. Mamedov, T. P. Gavrilova, A. G. Badelin 65

ESR of Nd^{3+} and Dy^{3+} Ions in $CsCaF_3$ Single Crystals
M. L. Falin, V. A. Latypov, S. L. Korableva 67

ESR of Er^{3+} Ions at Cubic Sites in $CsCaF_3$ and Cs_2NaYF_6 Single Crystals
M. L. Falin, V. A. Latypov, A. V. Lovchev, N. M. Khaidukov 68

EPR Study of Nitric Oxide Production in Spinal Cord of Rats after Spinal Cord Injury in Acute and Chronic Periods
Kh. L. Gainutdinov, G. G. Iafarova, V. V. Andrianov, T. V. Baltina, V. S. Iyudin 70

Separation of the Contribution of Exchange Interaction to the Shape of EPR Spectra of Nitroxide Radicals in Solutions
R. T. Galeev, M. M. Bakirov, K. M. Salikhov 72

Evaluation of Serum Blood Cytochrome *c* Oxidase in Sportsmen by Low Temperature EPR
M. I. Ibragimova, A. I. Chushnikov, G. V. Cherepnev, V. Yu. Petukhov, I. V. Yatsyk 73

Lability of the Spin State of Fe(III) Complexes with Tetradentate N_2O_2 Schiff Base Ligands
T. A. Ivanova, L. V. Mingalieva, I. V. Ovchinnikov, I. F. Gilmutdinov, O. A. Turanova, G. I. Ivanova, V. A. Shustov 74

Investigation of Posphorus-Related Centers in Synthetic Diamonds Grown at HPHT Conditions in P-C Medium
A. Komarovskikh, V. Nadolinny, Yu. Palyanov, I. Kupriyanov 75

The Influence of Sucrose and Trehalose on a Mobility of Lipid Membrane
K. B. Konov, N. P. Isaev, S. A. Dzuba 77

PELDOR Theory for Overlapping EPR Spectra
K. M. Salikhov, I. T. Khairuzhdinov, R. B. Zaripov 79

Spin Exchange between Charged Paramagnetic Particles in Diluted Solutions
K. M. Salikhov, A. E. Mambetov, M. M. Bakirov, I. T. Hairuzhdinov, R. T. Galeev, R. B. Zaripov, B. Bales 80

High-Frequency EPR Spectroscopy of Iron in Beryl
G. S. Shakurov, V. G. Thomas, D. A. Fursenko, E. S. Zhukova, B. P. Gorshunov 82

EPR and Group-Theoretical Studies of the Transition to Incommensurate Phase of $MgGeF_6 \cdot 6H_2O$ Crystals
P. G. Skrylnik, A. M. Ziatdinov 83

Combined Magneto-Electric Spin Resonance of Impurity Ions in Synthetic Forsterite
V. Tarasov, N. Solovarov, A. Sukhanov, R. Zaripov 85

NMR Characterization of Gasoline-Ethanol Blends
A. Turanov, A. K. Khitrin 86

EPR Study of Molecular Structure of Exchange Coupled (Mn^{2+}-Ag^{2+}) Pairs Formed in the BaF_2 Crystals
V. A. Ulanov, R. R. Zainullin, E. R. Zhiteitsev, M. M. Zaripov 88

Paramagnetic Resonance and Structural Phase Transition in $Pb_5Ge_3O_{11}$
V. A. Vazhenin, E. L. Rumyantsev, M. Yu. Artyomov, A. P. Potapov 90

A Spin Crossover Dendrimeric Iron(III) Complex with Magnetic Ordering
V. Vorobyeva, N. Domracheva, A. V. Pyataev 91

The Formation of Epsilon-Fe_2O_3/SiO_2 Nanoparticles: Investigation via FMR *in situ*
S. S. Yakushkin, G. A. Bukhtiyarova, O. N. Martyanov 92

EPR of Tetragonal and Monoclinic Nickel Centers in BaF_2 Crystals
R. R. Zainullin, G. S. Shakurov, V. A. Ulanov 93

Temperature Dependence of the Electron Paramagnetic Resonance Parameters of Semiconducting Compound
A. M. Zuzin, V. V. Radaykin, M. A. Bakulin, S. A. Savostina 95

Effect of Frequency on the Anisotropy of the Dispersion Curves in Two-Layer Magnetic Films
A. M. Zuzin, V. V. Radaykin, S. N. Sabaev, M. A. Bakulin, S. V. Bezborodov 97

Spectra of Spin Wave Resonance in Films with a Linear Distribution of the Field Anisotropy Thickness
A. M. Zuzin, V. V. Radaykin, S. N. Sabaev, M. A. Bakulin, N. V. Yantsen 99

Spin Dynamics in Systems with Honeycomb Structure Probed by NMR and NQR
M. F. Iakovleva, E. L. Vavilova, M. I. Stratin, E. A. Zvereva, M. A. Evstigneeva, V. B. Nalbandyan, V. E. Kataev, A. Muller 101

AUTHOR INDEX 102

ZAVOISKY AWARD LECTURES

Measuring the Nanoworld

G. Jeschke

Lab. Phys. Chem., ETH Zürich, Zürich 8093, Switzerland, gjeschke@ethz.ch

As everybody knows, the attraction or repulsion between two magnets depends on distance. From classical physics we also know that a rotating charge behaves like a magnet. Quantum physics tells us that an electron appears to rotate- it has spin- and that spin causes a magnetic moment. In an external magnetic field the spins of two unpaired electrons can be parallel or antiparallel. We know the size and distance dependence of this energy difference from first principles. Hence, if we measure the difference we can determine the distance between the unpaired electrons. Such measurements are sensitive in a range between about 1 and 10 nanometers, which is 100‘000 to 10‘000 times smaller than the typical width of a strand of human hair.

Chemists can make spin labels, which are stable small molecules that carry just one unpaired electron. They can also attach these labels to selected sites in a synthetic polymer macromolecule. Biochemists can attach them to selected sites in a protein macromolecule. Since the typical size of polymer and protein macromolecules is in the range between about 2 and 20 nanometers, distance measurements on such pairs of spin labels can tell us how the macromolecules are shaped.

Furthermore, if the measurement is done in the right way and if appropriate mathematics is used to analyze the data, we can determine not only average shape of the molecule, but also its flexibility. I will show this for a class of relatively rigid organic molecules, so called oligo(phenyleneethinylene)s.

Such information is of interest for people who want to design complicated molecules that perform well specified movements. Many proteins work that way. For example, the function of Bax, a protein that is normally found in the cell plasma, depends on such movement. When Bax receives a signal to destroy the cell, it changes structure and inserts into the membrane of a mitochondrium, the power plant of the cell. By creating a hole in the mitochondrial membrane, Bax initiates cell death. Distance distribution measurements on Bax have told us how this may happen.

RNA and DNA: Flexible Molecules for Cellular Regulation

T. F. Prisner

Institute of Physical and Theoretical Chemistry and Center for Biomolecular Magnetic Resonance, Goethe University, Frankfurt am Main 60438, Germany

Nucleic acid molecules can adopt a variety of structures and exhibit a large degree of conformational flexibility to fulfill their various functions in cells. Here we describe the use of Pulsed Electron Electron Double Resonance (PELDOR or DEER) to investigate nucleic acid molecules where two modified cytosine analogs have been incorporated as spin probes. Because this new type of spin labels are rigidly incorporated into double stranded DNA and RNA molecules no additional flexibility of the spin label itself is introduced and the magnetic dipole-dipole interactions between both spin labels encodes for the distance as well as for the mutual orientation between both spin labels. Multi-frequency/multi-field PELDOR experiments allow extracting this information which in turn gives very precise and valuable information on the structure and conformational flexibility of the nucleic acid molecules itself. We describe in detail our procedure to obtain the conformational ensembles and show accuracy and limitations with test examples and application to double-stranded DNA.

PLENARY LECTURES

Dipolar Spectroscopy: New Methodical Aspects and Applications

P. E. Spindler, P. Schöps, A. Marko, B. Endeward, and **T. F. Prisner**

Institute of Physical and Theoretical Chemistry and Center for Biomolecular Magnetic Resonance, Goethe University, Frankfurt am Main 60438, Germany

Dipolar Spectroscopy uses the magnetic dipole-dipole interaction between two unpaired electron spins to measure distances in the 1–8 nm range on macromolecules. Single and double frequency pulse EPR techniques exist to accomplish this goal with applications in structural biology and material sciences. Some limitations of the method arise from the fact that not the whole EPR signal of the spinlabels can be excited by the microwave pulses, that short transversal relaxation times of the spinlabels limit the observation time window and that intermolecular contributions, resulting from dipolar interactions to other molecules, complicate the analysis for broad distance distributions or long distances. We will show new approaches how to tackle these problems by the use of adiabatic broadband pulses, new pulse sequences and high magnetic fields.

The Long Way that Leads from Short Distances to Biomolecular Structure

G. Jeschke

Lab. Phys. Chem., ETH Zürich, Zürich 8093, Switzerland, gjeschke@ethz.ch

Dead-time free dipolar evolution data arising from a pair of electron spins can be converted to distance distributions on a nanometer length scale. As this length scale matches typical dimensions of biomacromolecules and biomacromolecular complexes, such distance distributions are very valuable constraints for modeling structure. This applies particularly to membrane proteins, large complexes, and proteins with functionally important disordered domain, whose structures are difficult or impossible to solve with established high-resolution methods such as x-ray crystallography and high-resolution NMR. Our approach to this problem is based on site-directed spin labeling and distance distribution measurements with the double electron electron resonance (DEER) experiment, also called PELDOR. The main limitations are sensitivity, accuracy of modelling the spin label, and the relatively small number of constraints that can be obtained in the current one-sample-one-constraint paradigm. After shortly reviewing our early efforts in pushing the respective limits, I will discuss current developments based on ultra-wideband excitation of Gd(III) labels, Monte Carlo/Universal Force Field rotamer libraries of spin label side chains, and the concept of orthogonal spin labeling. I will then show on three examples how the constraints can be used in modeling of structures. For the major light harvesting complex LHCII of green plants we have obtained an ensemble model of the disordered part of the N-terminal domain by using exclusively DEER constraints (Fig. 1). For an integrin, we have determined relative domain orientation and an ensemble model for the interdomain linker by combining DEER and small-angle X-ray scattering data. Finally, high-resolution structures of two co-existing conformations were obtained for a ribonucleoprotein complex by combining DEER and NMR constraints.

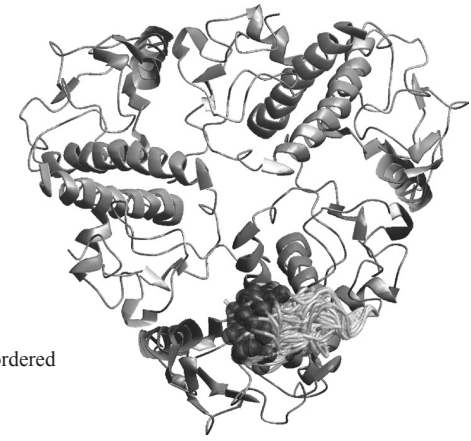

Fig. 1. An ensemble model of the disordered part of the N-terminal domain.

ODMR as a Tools to Study Nanosystems

N. G. Romanov and **P. G. Baranov**

Microwave Spectroscopy of Crystals Laboratory, Ioffe Physical-Technical Institute,
Russian Academy of Sciences, Saint Petersburg 194021, Russian Federation,
nikolai.romanov@mail.ioffe.ru

In optically detected magnetic resonance (ODMR), resonant transitions between spin sublevels are observed by monitoring variations in emitted (or absorbed) light instead of direct measurements of microwave energy absorption. This becomes possible if a spin-dependent process exists, which couples microwave and optical transitions. Absorption of a microwave quantum results in variation of light by an optical photon, providing a huge increase in sensitivity. In addition, in ODMR two channels of selectivity appear, i.e. spatial selectivity since only optically active part of the sample can give a signal and selectivity by choosing an appropriate detection wavelength. These advantages of ODMR make it very feasible for a study of nanostructures [1] and even single defects [2].

In this paper, we consider the results of ODMR study of different nanostructures and nanosystems, i.e. MBE grown semiconductor quantum dots, quantum wells and superlattices, free-standing colloidal nanocrystals and self-organized nanocrystals inside crystalline matrixes. Special attention will be paid to specific spin-dependent processes, which allow application of ODMR, ODMR techniques and information, which can be obtained and used for characterization of nanostructures.

Resent results of application of ODMR for a study of quantum wells and quantum dots based on diluted magnetic semiconductors (CdMn)Se and (CdMn)Te will be reported. These studies allowed to reveal fine structure splitting of Mn ions due to low dimensionality, formation of exchange-coupled complexes Mn-localized hole in quantum wells with excess hole concentration, and directional electron tunneling towards wider wells in multiple quantum well structures.

The work was supported by Russian Science Foundation (grant 03-03-32331).

1. Baranov P.G., Romanov N.G.: Appl. Magn. Reson. **21**, 165–193 (2001)
2. Gruber A., Dräbenstedt A., Tietz C., Fleury L., Wrachtrup J., von Borczyskowski C.: Science **276**, 2012–2014 (1997)

Distance Measurements in Nucleic Acids Using Advanced SDSL with Nitroxyl and Trityl Radicals

E. Bagryanskaya[1,2], **O. Krumkacheva**[2], **M. Fedin**[2], **A. Kuzhelev**[1,3], **V. Tormushev**[1], **I. Kirilyuk**[1], **Y. Polienko**[1], **E. Babaylova**[4], **G. Karpova**[4], **G. Shevelev**[4], **A. Lomzov**[4], and **D. Pyshny**[4]

[1] N. N. Vorozhtsov Novosibirsk Institute of Organic Chemistry, Novosibirsk, Russian Federation, egbagryanskaya@nioch.nsc.ru
[2] International Tomography Center SB RAS, Novosibirsk, Russian Federation
[3] Novosibirsk State University Novosibirsk, Russian Federation
[4] Institute of Chemical Biology and Experimental Medicine, Novosibirsk, Russian Federation

Site-directed spin labeling (SDSL) is widely applied for structural studies of biopolymers by EPR. In particular, huge attention has been drawn recently to pulsed dipolar EPR spectroscopy (PELDOR/DEER and Double Quantum Coherence (DQC) methods) allowing distance measurements in many biologically-important systems. Although significant progress has been achieved in this field, a number of challenges still remain and resolving the nanometer-scale structure of biomolecules in natural conditions still remains a challenging task.

We report the first distance measurement in nucleic acid at room temperature using EPR. The model 10-mer DNA duplex has been labeled with advanced triarylmethyl radicals, then immobilized on a sorbent in water solution and investigated by DQC EPR [1]. We succeeded in development of optimal triarylmethyl-based labels, approach for site-directed spin labeling (SDSL) and efficient immobilization procedure that, working together, allowed us to measure as long distances as ~4.5 nm with high accuracy at 300 K. Another current challenge in pulsed dipolar EPR spectroscopy is a design of spin labels and SDSL strategies for distance measurements in nucleic acids at room/physiological temperature. For this purpose, relaxation properties of trityl radicals represent a significant advantage. Although DQC distance measurement in immobilized trityl-labeled protein in liquid solution (at 4 °C) has been recently reported [2], to the best of our knowledge, this has not yet been achieved for nucleic acids. Further studies in this direction are currently underway.

One of these challenges is SDSL of long (exceeding 50–70 base pairs) natural nucleic acids that is not possible using common solid-phase synthesis. In this work, we propose novel SDSL approach suitable for long natural RNAs, which is based on the attachment of linker containing aliphatic amino group to the target nucleotide residue and following selective coupling of spin label to this amino group [3]. Such linker can be attached to the desired RNA residue via sequence-specific reaction with the derivatives of oligodeoxyribonucleotides. To verify this approach, we applied it to model RNA duplex with known structure and expected distance between corresponding residues. A new 2,5-bis(spirocyclohexane)-substituted spin label with advanced stability and re-

laxation properties has been used, and the distance distribution measured using Q-band (34 GHz) pulse DEER corresponds well to the expected one. We have additionally validated the obtained results by studying similar RNA duplex, where the linker with aliphatic amino group was introduced via a solid-phase synthesis. The applicability of novel SDSL approach to long RNAs is a crucial benefit for the future structural studies using pulse EPR.

This work was supported by RFBR (No. 12-04-01435) and Russian Scientific Fund (No 14-14-00922).

1. Shevelev G.Yu., Krumkacheva O.A., Kuzhelev A.A., Lomzov A.A., Rogozhnikova O.Yu., Trukhin D.V., Troitskaya T.I., Tormyshev V.M., Fedin M.V., Pyshnyi D.V., Bagryanskaya E.G.: J. Am. Chem. Soc. **136**(**28**), 9874–9877 (2014)
2. Yang Z., Liu Y., Borbat P., Zweier J., Freed J.H., Hubbell W.L. *et al.*: J. Amer. Chem. Soc. **134**, 9950–9952 (2012)
3. Babaylova E.S., Ivanov A.V., Malygin A.A., Vorobjeva M.A., Venyaminova A.G., Polienko Yu.F., Kirilyuk I.A., Krumkacheva O.A., Fedin M.V., Karpova G.G., Bagryanskaya E.G.: Org. Biomol. Chem. **12**(**19**), 3129–3136 (2014)

Solid State NMR Studies of Heterogeneous Catalysts

G. Buntkowsky, T. Gutmann, and **H. Breitzke**

Institute of Physical Chemistry, Technical University Darmstadt, Darmstadt D-64287, Germany, gerd.buntkowsky@chemie.tu-darmstadt.de

In recent years, solid-state NMR spectroscopy has evolved into an important characterization tool for the study of solid catalysts and chemical processes on their surface. This interest is mainly triggered by the need of environmentally benign organic transformations. The result of this need is a large number of new catalytically active hybrid materials, which are organized on the meso- and nanoscale. Typical examples of these catalysts are supported homogeneous transition metal catalysts, transition metal nanoparticles (MNPs) or polymer based supported core shell structures. Solid-state NMR spectroscopy is able to characterize both the structures of these materials and the chemical processes on the catalytic surface. The main part of the contribution presents examples of the solid-state NMR spectroscopy characterization of Rhodium and Ruthenium containing catalysts [1–5]. Finally, first results of DNP enhanced solid state NMR spectroscopy of these systems are presented.

1. Gutmann T., Ratajczyk T., Dillenberger S., Xu Y.P., Gruenberg A., Breitzke H., Bommerich U., Trantzschel T., Bernarding J., Buntkowsky G.: Solid State Nucl. Mag. **40**, 88–90 (2011)
2. Gruenberg A., Gutmann T., Rothermel N., Xu Y., Breitzke H., Buntkowsky G.: Z. Phys. Chem. **227**, 901–915 (2013)
3. Gutmann T., Rosal I., Chaudret B., Poteau R., Limbach H.-H., Buntkowsky G.: Chem. Phys. Chem. **14**, 3026–3033 (2013)
4. Rafter E., Gutmann T., Löw F., Buntkowsky G., Philippot K., Chaudret B., van Leeuwen P.W.N.M.: Catalysis Science & Technology **3**, 595–599 (2013)
5. Abdulhussain S., Breitzke H., Ratajczyk T., Grünberg A., Srour M., Arnaut D., Weidler H., Kunz U., Kleebe H.J., Bommerich U., Bernarding J., Gutmann T., Buntkowsky G.: Chem. Eur. J. **20**, 1159–1166 (2014)

Spin Relaxation in Disordered Media

F. S. Dzheparov

Institute for Theoretical and Experimental Physics, Moscow 117218, Russian Federation, dzheparov@itep.ru

Theoretical grounds and typical experimental appearances of spin dynamics and relaxation in solids containing randomly distributed nuclear and/or electronic spins are considered. Brief content of the report is as follows.

- General outlines of the spin transport theory. Interrelation of longitudinal and transversal relaxation related to dynamics of occupancies and phases.
- Basic master equations for delocalization of polarization in disordered spin systems. Long-range transitions *vs* percolation theory. Propagator and its singular point. Dynamical and kin-ematical memory. Inapplicability of moment expansion for observables. Concentration expansion as a general constructive basis for analytical methods. Ways of regrouping of concentration expansions, semi-phenomenology, coherent medium approximation. Numerical simulations.
- Disordered nuclear spin systems: impurity nuclei in a dense spin crystal (model example: ^{8}Li-^{6}Li in LiF) and in diamagnetic solid (example: magnetically diluted ^{29}Si in silicon).
- Magnetically diluted electronic spin systems. Master equations for low Zeeman temperatures. Cluster expansions and regularization of spin-spin interactions. Saturation on the wing of the dipolar broadened line.
- Nuclear spins and NMR free induction decay in paramagnetic media.
- Nuclear relaxation via paramagnetic impurities.

Electrons Localization in Ge/Si Nanoheterostructures Studied by ESR

A. V. Dvurechenskii[1,2], **A. F. Zinovieva**[1], and **A. V. Nenashev**[1,2]

[1] Institute of Semiconductor Physics, Siberian Branch of Russian Academy of Science, Novosibirsk 630090, Russian Federation
[2] Novosibirsk State University, Novosibirsk 630090, Russian Federation, dvurech@isp.nsc.ru

Electron spins in quantum dots are a promising object for the implementation of quantum computation ideas and spintronics devices. One of the main requirements to select materials for quantum computation is the spin coherence time. For information exchange in quantum calculations the electronic states should be coupled usually by exchange interaction. Quantum calculations need selective access to individual qubits for implementation of one-qubit and two-qubit operations. There are many ideas to realize access to individual qubits based on magnetic field, coherent light, and electric field. One of the ability is to distinguish electrons by *g*-factor value. And qubit array should be large enough for parallel computing. Many these requirements hold true in silicon based quantum dot nanoheterostructure grown by molecular beam epitaxy. The strain-induced potential wells in Si around Ge dots provide electron localization. The weak spin orbit coupling in Si and existence of developed technology to reduce none zero magnetic moment isotopes make provision for long decoherence time of electron spin in Si. The present report aimed to review results on spin dynamics in array of Ge/Si quantum dot nanoheterostructure. The main items of the talk are following:

- Electronic and atomic configuration of Ge quantum dot in Si.
- Electron localization in double quantum dot molecules grown with effect of vertical alignment of nanocrystal nucleation. *g*-factor engineering.
- Spin relaxation in ordered quantum dot array Ge/Si structures by growth on strained heterophase and pit-patterned substrates.

The work was funded by Russian Scientific Foundation (grant 14-12-00931).

1. Zinovieva A.F., Nikiforov A.I., Timofeev V.A., Nenashev A.V., Dvurechenskii A.V., Kulik L.V.: Phys. Rev. B. **88**, 235308 (2013)
2. Zinovyev V.A., Dvurechenskii A.V., Kuchinskaya P.A., Armbrister V.A.: Phys. Rev. Lett. **111**(26), 265501(5) (2013)

Molecular Motions in Frozen Phospholipid Bilayers in Presence of Cryoprotectors: Spin Label EPR Study

K. B. Konov[1], N. P. Isaev[2], D. V. Leonov[2,3], and **S. A. Dzuba[2,3]**

[1] Zavoisky Physical-Technical Institute, Russian Academy of Sciences, Kazan 420029, Russian Federation
[2] Voevodsky Institute of Chemical Kinetics and Combustion, Russian Academy of Sciences, Novosibirsk 630090, Russian Federation
[3] Novosibirsk State University, Novosibirsk, 630090 Russian Federation, dzuba@kinetics.nsc.ru

The cryoprotectors such as glycerol, sugars and sugar alcohols can stabilize biological systems under extreme conditions of desiccation and freezing. Electron spin echo (ESE) spectroscopy was applied to study phospholipid bilayers solvated by aqueous solutions of glycerol, sucrose, trehalose and sorbitol and containing incorporated spin-labeled lipids or stearic acids. The ratio of the echo time traces for the two field positions in the EPR spectrum possessing the largest and smallest anisotropies gave the anisotropic contribution to the echo decay, which obeys exponential time dependence with good accuracy. At low temperatures, the anisotropic contribution is induced by stochastic (or diffusive) orientational vibrations of the molecule as a whole (i.e., stochastic molecular librations), with the exponential decay rate W_{anis} proportional to $\langle\alpha^2\rangle\tau_c$, where $\langle\alpha^2\rangle$ is the mean angular amplitude of the motion and τ_c is the correlation time. In all cases, it was found that W_{anis} begins to increase sharply above 170–200 K, which was ascribed to the dynamical transition known for biological systems at these temperatures. For hydration by the sucrose and trehalose solutions, W_{anis} increased noticeably also above ~120 K, which was explained by bilayer expanding due to direct bonding of sugar molecules to the bilayer surface. Glycerol solution was found to increase the dynamical transition temperature by ~30 K. The profiles of penetration into the bilayer of deuterated glycerol and sucrose were measured by electron spin echo envelope modulation spectroscopy (ESEEM). The molecular mechanisms of the cryoprotective action of these substances are discussed.

Time-Resolved and Field Dependent CIDNP of Biologically Important Molecules

A. V. Yurkovskaya and **O. B. Morozova**

International Tomography Center, Novosibirsk 630090, Russian Federation,
yurk@tomo.nsc.ru

Long-range charge transfer in proteins provokes undiminishing interest over decades. Not only are reactions involving paramagnetic intermediates of these particles ubiquitous in chemistry and biochemistry, but these reactions also present challenges to understand the time scales of motion, the coupling of charges to the surrounding environment, and the scale of interaction energies. Chemically Induced Dynamic Nuclear Polarization (CIDNP) is a useful tool for studying elusive radical pairs (RPs) which are often beyond the reach of EPR spectroscopy because of their short lifetimes and low stationary concentration. Nonetheless, spin dynamics in transient RPs can produce significant CIDNP effects which are stored in the diamagnetic reaction products for the time periods of the order of nuclear T_1-relaxation times and can be studied by NMR spectroscopy. In many cases CIDNP formed after geminate recombination of RPs is directly proportional to hyperfine coupling constants (HFCCs) [1]. This enables determination of relative HFCCs in RPs. However, when one of the RP partners is a radical with precisely known HFCCs, this method allows one to obtain the absolute values of HFCCs of the second partner radical. Thus, CIDNP gives an NMR way to obtain EPR parameters and enables investigating kinetics of radical reactions in solutions at room temperature. At the same time, the analysis of CIDNP is often more complicated than that of EPR and requires modeling of spin evolution in RPs. A way to obtain the EPR parameters is measuring CIDNP dependence on the external magnetic field strength; theoretical modeling of such field dependences potentially allows one to obtain EPR parameters, in particular, HFCCs in RPs, electronic exchange interaction, and the difference, Δg in the electronic g-factors of the RP partners. However, coherent polarization re-distribution among scalar coupled spins leads to the distortion of CIDNP intensities [2] that could create problems in interpreting CIDNP at low fields.

1. Morozova O.B., Ivanov K.L., Kiryutin A.S., Sagdeev R.Z., Köchling T., Vieth H.-M., Yurkovskaya A.V.: Phys. Chem. Chem. Phys. **13**, 6619 (2011)
2. Ivanov K.L., Pravdivtsev A.N., Yurkovskaya A.V., Vieth H.-M., Kaptein R.: Progress in Nuclear Magnetic Resonance Spectroscopy **81**, 1 (2014)

Electronic Structure and Magnetic Anisotropy in 3d-Transition Metal Single Ion Magnets from the First Principles

E. A. Suturina[1,2], **M. Atanasov**[1], and **F. Neese**[1]

[1] Max Planck Institute for Chemical Energy Conversion, Mülheim an der Ruhr D-45470, Germany, Elizaveta.Suturina@cec.mpg.de
[2] Novosibirsk State University, Novosibirsk 630090, Russian Federation

The field of molecular magnetism has developed quite fast over last decades. Among various methods employed, theoretical analysis of magnetic properties on a molecular scale plays an important role in this progress. Recently, a new theoretical approach to magnetism of metal complexes from the first principles has been introduced and applied to a series of single transition metal ion complexes [1]. Systems with quenched orbital momentum, as well as their counterparts with unquenched orbital angular momentum were scrutinized. The highly anisotropic magnetic properties exhibited by the latter systems render them promising single-molecular magnets. [2]

The proposed approach is based on *ab initio* multi-reference calculations (CASSCF/NEVPT2) with further account of spin-orbit coupling via the quasi-degenerate perturbation theory. The electronic structure calculations revealed that the magnetic properties of the complexes considered are determined by an interplay of the ligand field and spin-orbit coupling effects. Moreover, the changes of magnetic properties due to dynamical vibronic coupling can also be taken into account.

It was shown that trigonal and linear iron (II) complexes (viz., $Fe[N(SiMe_3)(Dipp)]_2$, $Fe[C(SiMe_3)_3]_2$, $Fe[N(H)Ar^*]_2$, $Fe[O(Ar^0)]_2$, and $[tpa^RFe]$) have unquenched orbital momenta, therefore, the simple spin-Hamiltonian formalism cannot be applied in this case. The distortion of the ligand field out of three-fold symmetry destroys the axial anisotropy of the effective magnetic moment. This distortion causes the splitting of magnetic doublets of non-Kramers' systems, which, in turn, opens the channel for the fast temperature independent magnetic relaxation. In contrast to the iron(II), iron(I) (as in $Fe^I[C(SiMe_3)_3]_2$) is a Kramers' system, and the geometry distortion does not lead to splitting of the magnetic doublet. This renders the linear complex $Fe^I[C(SiMe_3)_3]_2$ the best single ion magnet based on a transition metal [2].

1. Aravena D., Suturina E.A. *et al.*: Coord. Chem. Rev. (2014)
2. Layfield R.A.: Organometallics **33**, 1084 (2014)

Spin Labeling: 50 Years of History

G. I. Likhtenshtein

Department of Chemistry, Ben-Gurion University of the Negev, Beer-Sheva, Israel, gertz@bgu.ac.il

It is known that there are delicate links and fine parallels between an art and science. Both these spheres of human endeavor involve a unique combination of professional skill and creative search. Sometimes an intuitive line of a great poet or philosopher may be likened to the opening of a new horizon in science. Thus, the composer Maurice Ravel in his famous "Bolero" allegorically depicts the process of birth and development of an epochal discovery that gives rise to many advantages. At first, a musical tune arises whose sound is so weak, so feeble, that it can be easily drowned out by the surroundings. In the second movement, the music is repeated with the same melody, but now with an additional hue. The process repeats itself, again and again, until eventually the most powerful strains of bold, majestic music are then performed by the symphonic orchestra. Like that opening musical movement, the initial publications on the chemistry of a novel class of stable radicals, nitroxides, and its application as spin labels were first met with skepticism, and even strong criticism, from qualified and very professional members of the scientific community. But, later, more and more young enthusiasts joined the ranks of scientists applying this new tool in their research, and ever increasing reports of nitroxides were published in the various fields of chemistry, physics, biology, material science, and biomedicine. The theoretical and experimental data presented in this review clearly demonstrate both history and the current progress within the nitroxide spin labeling. The review described concisely the main periods of the spin labeling history: prehistory, golden decade, further development, new era and outlook.

SECTION 1

CHEMICAL AND BIOLOGICAL SYSTEMS

What Iron Electron Configuration – d^7 or d^9 is Characteristic of Electronic Structure of Dinitrosyl Iron Complexes with Thiolate Ligands in the Solutions

A. F. Vanin

Semenov Institute of Chemical Physics Russian Academy of Sciences, Moscow, Russian Federation, vanin.dnic@gmail.com

Mononuclear and binuclear dinitrosyl iron complexes (M- and B- DNIC) with thiolate ligands {formulas $[(RS_2)Fe(NO)_2]$ and $[(RS_2)Fe_2(NO)_4]$} as NO and NO^+ donors hold considerable promise as a base in the design of a radically new generation of drugs with a broad spectrum of therapeutic activities. The properties of electronic structures of the complexes in the dissolved state underlying their ability to act as NO and NO^+ donors will be considered in the report. From our point of view this ability can be explained only from the paradigm of the model of the $[Fe^+(NO^+)_2]$ core ($[Fe(NO)_2]^7$ according to the Enemark-Feltham classification). Similarly, the $\{[RS^-_2)Fe^+(NO^+)_2]^+\}$ structure describing the distribution of unpaired electron density in M-DNIC corresponds to the low-spin (S = 1/2) state with a d^7 electron configuration of the iron atom and predominant localization of the unpaired electron on $MO(d_z^2)$ and the square-plane structure of M-DNIC. The chemical equilibrium characteristic of $Fe^+(NO^+)_2$ fragment and its constituents $\{(Fe^+(NO^+)_2 \Leftrightarrow Fe^{2+} + NO + NO^+)\}$ ensures NO and NO^+ generation by the complexes. The proposed mechanism of M- and B-DNIC formation in the solutions as well as the results of EPR and optical studies of M- and B-DNIC demonstrating NO and NO^+ release from the complexes will be presented in the report. Our opponents who studied M- and B-DNIC in crystalline state proposed that the distribution of unpaired electron density in M-DNIC is described as $\{[RS^-_2)Fe^{3+}(NO^-)_2]^-\}$. Spin-pairing of electron density on iron (Fe^{3+}, S = 5/2) and two nitroxyl ligands (NO^-, S = 1) resulted in the sum spin of the complexes S = 1/2 with a d^9 electron configuration of the iron atom ($[Fe(NO)_2]^9$ according to the Enemark-Feltham classification). The complex in the crystalline state is characterized with tetrahedron structure. The investigators propose that electronic and spatial structures of the complexes do not change during the process of complex dissolving. In the frame of this model, it is hardly to explain the ability of DNICs with thiolate ligands to act as NO and NO^+ donors.

Nitroxide Biradicals with Acetylene Groups in the Bridge: Structure, Internal Mobility, EPR, and DFT Calculations

O. I. Gromov[1], E. N. Golubeva[1], and **A. I. Kokorin[2]**

[1] Chemistry Department, Lomonosov Moscow State University, Moscow 119991, Russian Federation
[2] N. Semenov Institute of Chemical Physics RAS, Moscow 119991, Russian Federation

Nitroxide biradicals with bridges containing one or several acetylene and other groups in the bridge are of particular interest: they are assumed to be rather conformationally rigid and convenient for theoretical studying of direct and indirect electron spin exchange [1]. A series of R_6-$(C{\equiv}C)_n$-R_6 biradicals, n = 0–3, with a wide range of $r_{NO\text{-}NO}$ distances between N-O groups is available [2, 3]. Here R_6 is 1-oxyl-2,2,6,6-tetramethylpiperidine-3,4-ene nitroxide ring. The X-ray structural and EPR data along with DFT calculations of structural and EPR parameters for these biradicals and for R_6-$(C{\equiv}C)_m$-p-C_6H_4-$C{\equiv}C$-R_6 (m = 1, 2) are compared.

DFT calculations on UDFT/B3LYP/cc-pVDZ level yield structural and EPR parameters well agreed with experimental data. The comparison of calculated and experimental zero field splitting constants allows a conclusion that R_6-$(C{\equiv}C)_n$-R_6 biradicals, indeed, have fixed $r_{NO\text{-}NO}$ distances. On the other hand, DFT calculations predict rather low potential barriers of the internal rotation of nitroxide rings around the main molecular axis in the biradical. This barrier decreases in R_6-$(C{\equiv}C)_n$-R_6 row with increasing of the number of -C≡C- groups n in the bridge. This implies an almost free internal rotation around the -$(C{\equiv}C)_n$- bridge at room temperature instead of a limited number of rigid conformations. This means also that a value of the exchange integral $|J|$ measured in liquid solutions characterizes not a certain conformer, but is a parameter averaged by the rotation.

This work was supported by RFBR Grant 12-03-00623-a. Calculations were performed using resources of the Supercomputing Center of Lomonosov Moscow State University [4]. We are thankful to Dr. V. N. Khrustalev (A. N. Nesmeyanov Institut of Organoelement Compounds RAS, Moscow), provided us the X-ray data of the biradicals.

1. Umanskiy S.Ya., Golubeva E.N., Plakhutin B.N.: Russ. Chem. Bull. **62**(7), 1511 (2013)
2. Kokorin A.I.: Appl. Magn. Reson. **26**, 253 (2004)
3. Kokorin A.I., Golubeva E.N., Mladenova B. *et al.*: Appl. Magn.Reson. **44**, 1041 (2013)
4. Sadovnichy V., TikhonravovA., Voevodin Vl., Opanasenko V. in: Contemporary High Performance Computing: From Petascale toward Exascale (Chapman & Hall/CRC Computational Science), pp. 283–307. USA, Boca Raton, CRC Press, 2013.

EPR Study of Tetranitroxide Derivatives of C60

R. B. Zaripov[1], **G. R. Nureeva**[1,2], **L. I. Savostina**[1,2], **V. K. Voronkova**[1], **K. M. Salikhov**[1], **V. P. Gubskaya**[3], and **I. A. Nuretdinov**[3]

[1] Zavoisky Physical-Technical Institute, Russian Academy of Sciences, Kazan 420029, Russian Federation, Zaripov.ruslan@gmail.com
[2] Kazan Federal University, Kazan 420008, Russian Federation
[3] Arbuzov Institute of Organic and Physical Chemistry, Kazan 420088, Russian Federation

Fulleren molecules since opening have attracted widespread attention. For the moment the interest to the derivatives of fullerene is increased. Due to sphere-like structure it is possible to link some molecules by targeted manner [1]. Moreover it is possible to insert atom or simple molecule into the fullerene cage [2]. The main idea of synthesise a new kind of fullerene derivative is obtaining a new properties and application fields of such molecule. Recently it was shown that nitroxide derivative of fullerene can be used as efficient compounds in a treatment of serious diseases [3].

In this work we study a new kind of fullerenes adducts with two nitroxide biradicals. Tetraradical derivatives of methano[60]fullerene were investigated in the X-, Q-, W-bands at different temperatures in toluene solution form.

At Fig. 1 it is denoted two isomers of tetraradical adducts of methano[60] fullerene: equatorial (R1) and trans-3 (R2) (by Hirsh classification). Experimental data shows that EPR spectrum of R2 coincides with the nitroxide malonate methano[C60]fullerene one. Nitroxide malonate methano[C60]fullerene contains only one biradical group and was investigated previously in [3, 4]. EPR spectrum of R1 is more complex. The EPR spectrum at room temperature gives raise additional lines between main nitroxide lines (by compared with monoradical).

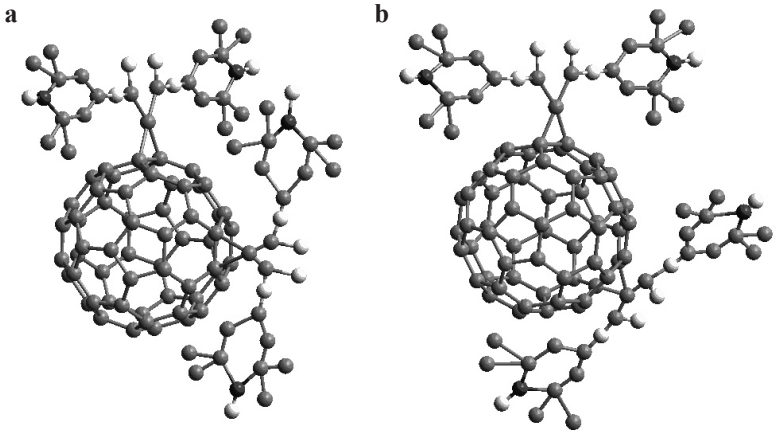

Fig. 1. a Trans-3 isomer (R2), **b** equatorial isomer (R1).

These facts indicate that R2 reveals only intrabiradical exchange interaction and R1 reveals both intra- and interbiradical couplings.

To compare experimental results the quantum chemical calculations for nitroxide malonate methano[C60]fullerene was performed. Quantum chemical calculations of structure and hyperfine coupling constants (HFC) of biradical molecules were performed by ORCA [5] with functional PBE and basis sets (SVP, TZVP). Exchange integral J_{AB} was calculated by use broken symmetry model [6].

Authors are grateful to the Russian Foundation for Basic Research (grant No. 12-03-97078) and Government of Tatarstan Republic and President Grant for Government Support of Young Russian Scientists (grant No. 14.120.14.4957-MK) for partial financial support.

1. Taojun Zhuang *et al.*: Appl. Phys. Lett. **103**, 203301 (2013)
2. Plant S.R. *et al.*: Chem. Sci. **4**, 2971 (2013)
3. Gubskaya V. *et al.*: Org. Biomol. Chem. **5**, 976 (2007)
4. Franco L. *et al.*: Mol. Phys. **104**, 1543 (2006)
5. Neese F.: Comp. Mol. Science **2**, 73 (2012)
6. Soda T. *et al.*: Chem. Phys. Lett. **319**, 223 (2000)

SECTION 2

MODERN METHODS OF MAGNETIC RESONANCE

Solid-State NMR in Heterogeneous Catalysis

O. B. Lapina[1,2], **A. A. Shubin**[1,2], and **V. V. Terskikh**[3]

[1] Boreskov Institute of Catalysis, Novosibirsk 630090, Russian Federation, olga@catalysis.ru
[2] Physics Department, Novosibirsk State University, Novosibirsk 630090, Russian Federation, A.A.Shubin@catalysis.ru
[3] Department of Chemistry, University of Ottawa, Ottawa K1N6N5, Ontario, Canada, Victor.Terskikh@nrc-cnrc.gc.ca

Detailed knowledge of the catalyst structure is important for understanding a variety of factors which may affect its catalytic activity and selectivity. Among other techniques that can be used for catalysts characterization, a nuclear magnetic resonance (NMR) spectroscopy is unique in its ability to provide molecular-level information about structure and dynamics. Modern solid-state NMR in combination with *ab initio* DFT quantum chemical calculations makes it possible to distinguish different active sites in solid catalysts, to determine the local structure of each site and to monitor their connectivities, correlations and dynamics.

In this presentation we will use an example of supported oxide catalysts to demonstrate capabilities of advanced solid-state NMR in combination with modern computational methods. Supported binary M_1O_x/M_2O_x and multilayered $M_3O_x/M_1O_x/M_2O_x$ catalysts ($M_{1\text{-}3}$ = Si, Al, Ti, V, Nb) will be described and analyzed via multinuclear ^{1}H, ^{27}Al, ^{29}Si, ^{51}V, and ^{93}Nb NMR spectroscopy to determine the molecular-level structure of catalytically active nanodomains. Special attention will be given to applications of modern solid-state NMR methods, including very high magnetic fields (up to 21 Tesla), very fast magic angle spinning (MAS) up to 70 kHz speed of rotation, and specialized pulse techniques such as SATRAS, MASSA, MQMAS, and CPMAS. Based on NMR data, several types of supported surface domains have been identified, with their structural characteristics found depending on a number of factors. Among these factors are (i) the surface concentration of the active component, (ii) the nature of catalyst support and its surface structure, (iii) the nature of layers and the structure of multilayered materials, (iv) the deposition sequence used in synthesis, (v) treatment conditions. While it is very difficult or even impossible to determine experimentally all different types of active surface sites, this problem may be simplified by using complementary quantum chemical calculations. Combining cluster and periodic GIPAW DFT calculations, we suggest several plausible models of the surface active sites in the multilayered catalysts under investigation.

This work has been supported in part by RFBR (13-03-00482) and by MES. The Siberian Supercomputer Centre (Novosirirsk, Russia, http://www2.sscc.ru) is acknowledged for granting access to its computational facilities (integration grant no. 130).

Nuclear Spin Isomers of Molecules for Signal Enhancement in NMR and MRI

I. V. Koptyug[1,2], V. V. Zhivonitko[1], K. V. Kovtunov[1], I. V. Skovpin[1], D. A. Barskiy[1,2], and **O. G. Salnikov[1,2]**

[1] Laboratory of Magnetic Resonance Microimaging, International Tomography Center, SB RAS, Novosibirsk 630090, Russian Federation, koptyug@tomo.nsc.ru
[2] Department of Natural Sciences, Novosibirsk State University, Novosibirsk 630090, Russian Federation

The correlated spin states of the nuclear spin isomers of molecules (NSIM) make them highly attractive for NMR. In particular, when parahydrogen is used in catalytic hydrogenations, it can enhance NMR signals of reaction products and intermediates by several orders of magnitude owing to the phenomenon of parahydrogen-induced polarization (PHIP). This technique has been recently extended from homogeneous catalytic processes in solution to heterogeneous catalytic reactions [1]. This development makes it possible to produce hyperpolarized gases and to separate easily the hyperpolarized fluids from the catalyst. The latter advantage is very important for in vivo spectroscopic and imaging applications of NMR. In addition, PHIP can become a useful hypersensitive NMR-based tool for studying mechanisms of heterogeneous catalytic processes and for in situ studies of operating catalytic reactors.

Nevertheless, the use of parahydrogen has certain disadvantages and limitations. The rupture of the H-H chemical bond upon H_2 activation subsequently leads to the relatively rapid loss of the correlation of nuclear spins. In particular, heterogeneous hydrogenations catalyzed by metals proceed via the dissociative chemisorption of H_2 on metal surfaces which limits the achievable signal enhancements. The potential solution of this problem is the use of nuclear spin isomers of molecules other than H_2. The enrichment of ethylene NSIM by means of a chemical synthesis has been demonstrated recently [2]. In the context of "long-lived spin states" addressed extensively in the last few years, NSIM of ethylene are second only to parahydrogen in terms of the T_{LLSS}/T_1 ratio. In addition, it was demonstrated that hyperpolarization can be produced without subjecting NSIM of ethylene to a chemical reaction.

1. Kovtunov K.V., Zhivonitko V.V., Skovpin I.V., Barskiy D.A., Koptyug I.V.: Top. Curr. Chem. **338**, 123 (2013)
2. Zhivonitko V.V., Kovtunov K.V., Chapovsky P.L., Koptyug I.V.: Angew. Chem. Int. Ed. **52**, 13251 (2013)

Detecting a New Source for Photochemically Induced Dynamic Nuclear Polarization

G. Kothe[1], M. Lukaschek[1], G. Link[1], S. Kacprzak[1], B. Illarionov[2], M. Fischer[2], W. Eisenreich[3], A. Bacher[3], and **S. Weber[1]**

[1] Institut für Physikalische Chemie, Universität Freiburg, Freiburg 79104, Germany
gerd.kothe@physchem.uni-freiburg.de
[2] Institut für Lebensmittelchemie, Universität Hamburg, Hamburg 20146, Germany
[3] Lehrstuhl für Biochemie, Technische Universität München, Garching 85748, Germany

Recently, nuclear quantum oscillations have been observed in an organic triplet state subject to an external magnetic field [1]. Analysis reveals that the nuclear spins can participate in the intersystem crossing process. As a consequence, a correlation is formed between the moments of the electron and nuclear spin subsystems giving rise to light-induced nuclear spin magnetization in the presence of a magnetic field [2]. A similar mechanism has been proposed on the basis of quantum coherence experiments [1]. The novel mechanism opens new perspectives for the analysis of photo-CIDNP in mechanistic studies of photoactive proteins. Here, we report magnetic field dependent ^{13}C NMR studies of a LOV2-mutant of phototropin reconstituted with ^{13}C-labeled flavin cofactors.

From the cyclic reaction scheme of this protein, two potential sources for photo-CIDNP can be identified: Triplet flavin, ^{13}F, generated in high quantum yield by photoexcitation of the flavin cofactor and the triplet radical pair $^3(F^{-\bullet}W^{+\bullet})$, formed by electron abstraction of ^3F from tryptophan W491 in the apo-protein [3]. Study shows that at fields of $B_0 < 9$ T, both $^3(F^{-\bullet}W^{+\bullet})$ and ^3F contribute to photo-CIDNP formation. However, due to the steep decrease of the "radical pair polarization" after the polarization maximum, at fields of $B_0 > 11$ T, ^3F provides the dominant contribution. Thus, we have for the first time detected that a triplet state is the major source for photo-CIDNP in a photoactive protein [4].

1. Kothe G., Yago T., Weidner J.-U., Link G., Lukaschek M., Lin T.-S.: J. Phys. Chem. B **114**, 14755 (2010)
2. Kandrashkin Yu. E., unpubl.
3. Eisenreich W., Joshi M., Weber S., Bacher A., Fischer M.: J. Am. Chem. Soc. **130**, 13544 (2008)
4. Kothe G., Lukaschek M., Link G., Kacprzak S., Illarionov B., Fischer M., Eisenreich W., Bacher A., Weber S., unpubl.

The Influence of the Magnetic Nuclei in Intersystem Crossing of Pentacene

Yu. E. Kandrashkin

Zavoisky Physical-Technical Institute, Russian Academy of Sciences, Kazan 420029, Russian Federation, SpinAlgebra@gmail.com

The initial nuclear spin coherency observed in electron spin echo (ESE) experiment [1] increases the interest to the photoexcited pentacene in p-terphenyl crystals and requires the revision of the mechanism of the intermolecular processes initiated by light irradiation. This phenomenon is rather difficult to explain unless the hypothesis that the nuclear spins are involved into the intersystem crossing (ISC) is proposed. To elucidate the nuclear spin coherency formed directly the laser flash Gerd Kothe with coauthors [1] assumed that the non-equilibrium state of the nuclear spin is transferred by the second order perturbation term of the hyperfine interaction (HFI) from the initial electron spin polarization formed during the mediated by spin-orbit coupling ISC.

We present an alternative model that is based on the mechanism of ISC promoted by the HFI. It predicts the generation of the additional terms to the initial density matrix including the electron-nuclear ordering that is responsible for the initial coherency between the nuclear sublevels. The proposed model explains most of the observed properties of the ESE signal formed by the MW irradiation of the electronic states T_0 and T_- in pentacene:

- the strong intensity of the out-of-phase ESE signal, comparable with in-phase signal;
- the observation of the coherency between the nuclear sublevels of the T_- state while no oscillations between the nuclear sublevels of the state T_0 are detected;
- the inversed ratio of the amplitude of the nuclear coherencies of the protons at positions 12 and 13.

The work was supported by a grant of the Russian Foundation for Basic Research (project 12-03-97078).

1. Kothe G., Yago T., Weidner J.-U., Link G., Lukaschek M., Lin T.-S.: J. Phys. Chem. B **114**, 14755–14762 (2010)

SECTION 3

THEORY OF MAGNETIC RESONANCE

Proton Spin Dynamics in Polymer Melts: New Perspectives for Experimental Investigations of Polymer Dynamics

N. Fatkullin[1], **S. Stapf**[2], **M. Hofmann**[3], **R. Meier**[3], and **E. A. Rössler**[3]

[1] Institute of Physics, Kazan Federal University, Kazan 420008, Russian Federation, Nail.Fatkullin@kpfu.ru
[2] Dept. Technical Physics II/Polymer Physics, TU Ilmenau, Ilmenau D-98684, Germany, siegfried.stapf@tu-ilmenau.de
[3] Universität Bayreuth, Experimentalphysik II, Bayreuth D-95440, Germany, ernst.roessler@uni-bayreuth.de

The proton spin dynamics in polymer melts is determined by intramolecular and intermolecular magnetic dipole-dipole contributions of proton spins. During many decades it was postulated that the main contribution is a result of intramolecular magnetic dipole-dipole interactions of protons belonging to the same polymer segment. This postulate is far from reality. The relative weights of intra- and intermolecular contributions are time (or frequency) dependent and sensitive to details of polymer chain dynamics. It is shown that for isotropic models of polymer dynamics, in which already at short times the segmental displacements are not correlated with the polymer chain's initial conformation, the influence of the intermolecular dipole-dipole interactions becomes stronger with increasing evolution time (i.e. decreasing frequency) than the corresponding influence of the intramolecular counterpart. On the other hand, an inverted situation is predicted by the tube-reptation model: here the influence of the intramolecular dipole-dipole interactions increases faster with time than the contribution from intermolecular interactions. This opens a new perspective for experimental investigations of polymer dynamics by proton NMR, and first results are reported.

Financial support from Deutsche Forschungsgemeinschaft (DFG) through grants STA 511/13-1 and RO 907/15 and 907/16 is gratefully acknowledged.

1. Kehr M., Fatkullin N., Kimmich R.: J. Chem. Phys. **126**, 094903 (2007)
2. Fatkullin N., Gubaidullin A., Stapf S.: J. Chem. Phys. **132**, 094903 (2010)
3. Herrmann, Kresse B., Gmeiner J., Privalov A.F., Kruk D., Fatkullin N., Fujara F., Rössler E.: Macromolecules **45**, 6516–6526 (2012)
4. Fatkullin N., Gubaidullin A., Mattea C., Stapf S.: J. Chem. Phys. **137**, 224907 (2012)
5. Rössler E.A., Stapf S., Fatkullin N.: Curr. Op. Colloid Interface Sci. **18**, 173–182 (2013)
6. Fatkullin N., Mattea C., Stapf S.: J. Chem. Phys. **139**, 194905 (2013)

Entanglement and Quantum Discord in NMR Experiments

E. B. Fel'dman

Theoretical Department, Institute of Problems of Chemical Physics of RAS,
Chernogolovka 142432, Russian Federation, efeldman@icp.ac.ru

Entanglement and quantum discord are important characteristics of quantum nonlocality and are responsible for the advantages of quantum devices over their classical counterparts. NMR methods give advanced tools for the realization of quantum algorithms [1]. NMR methods for quantum information processing are based on so called pseudo-pure states [2] in the high-temperature approximation. In that picture, the density matrix contribution, proportional to the unit operator, is thrown out. The theory, based on the truncated density matrix, predicts entangled states even at the room temperature. We have considered a two-spin system in the conditions of the multiple quantum (MQ) NMR experiment beyond the high-temperature approximation hypothesis and have found that entangled states are possible in the milli-kelvin region [3]. Entangled states are absent at the room temperature. The same limitation applies to all other NMR experiments. Thus, the perspectives of the NMR methods of quantum information processing had not being clear.

The situation has changed after quantum discord was introduced as a measure of quantum correlations [4, 5]. It turned out that quantum correlations can exist for mixed states even at zero entanglement. In particular, NMR experiments are described by mixed states at the room temperature. Quantum discord can be sufficiently large when entanglement is zero. We have considered entanglement and quantum discord in MQ NMR experiments. Experimental investigations of quantum discord in NMR experiments at the room temperature are also discussed.

The work is supported by the Russian Foundation for Basic Research (grants No. 13-03-00017, 13-03-12418) and Program No. 8 of the Presidium of RAS.

1. Nielsen M.A., Chuang I.L.: Computation and Quantum Information. Cambridge: University Press, 2000.
2. Cory D.G., Fahmy A.F., Havel T.F.: Proceedings of the National Academy of Sciences of the USA **94**, 1634 (1997)
3. Fel'dman E.B., Pyrkov A.N.: JETP Lett. **88**, 398 (2008)
4. Olliever H., Zurek W.H.: Phys. Rev. Lett. **88**, 017901 (2001)
5. Henderson L., Vedral V.: J. Phys. A: Math. Gen. **343**, 6899 (2001)

SECTION 4

STRONGLY CORRELATED ELECTRON SYSTEMS

Order-by-Disorder in the Frustrated Quantum Spin Magnet $CoAl_2O_4$

V. Kataev[1,2], S. Zimmermann[1,3], A. Alfonsov[1], E. Vavilova[2], M. Iakovleva[2], H.-J. Grafe[1], H. Luetkens[4], H.-H. Klauss[3], A. Maljuk[1], T. Dey[1], S. Wurmehl[1], and **B. Büchner[1,3]**

[1] Leibniz Institute for Solid State and Materials Research IFW Dresden, Dresden D-01069, Germany, v.kataev@ifw-dresden.de
[2] Zavoisky Physical-Technical Institute, Russian Academy of Sciences, Kazan 420029, Russian Federation
[3] Technical University of Dresden, Dresden D-01069, Germany
[4] Paul Scherrer Institute, Villigen 5232, Switzerland

Frustration of magnetic interactions in quantum spin magnets on the basis of transition metal (TM) oxides can yield unconventional magnetic ground states such as a spin-liquid state or complex spin-spiral structures. A large ground state degeneracy arising due to frustrated geometry of the spin lattice or competing magnetic exchange is accidental and can be lifted by small perturbations such as magnetic anisotropy, impurities or structural disorder. Here, a stabilization of a specific ordered state can be driven by a paradoxical mechanism refereed as "order-by-disorder". Such interesting phenomena are realized, for example, in spinels AB_2X_4 where the tetrahedral A site is occupied by a magnetic TM ion and the octahedral B site is nonmagnetic.

In this talk, our recent experimental investigation of the A-site spinel material $CoAl_2O_4$ will be presented. The magnetic properties of single crystals of $CoAl_2O_4$ have been addressed by thermodynamic methods (specific heat and magnetization) and by a number of local probe techniques, such as high-field sub-THz ESR, NMR and muon spin relaxation spectroscopies. We find that frustration gives rise to an extended spin fluctuation regime before a static spin order sets in at $T_N \approx 10$ K. Furthermore, at low temperatures there are clear experimental indications in favor of the scenario of a competition between a collinear type antiferromagnetic order and noncollinear spin spiral state. In line with recent theories of the "order-by-disorder" mechanism we discuss possible implication of structural disorder present in the studied single crystals on the spin ground state of $CoAl_2O_4$.

Effects of Disorder in Doped Honeycomb Iridates

E. Vavilova[1], V. Kataev[1,2], G. Prando[2], A. Alfonsov[2], H.-J. Grafe[2], B. Büchner[2], H. Wu[3], Q. Huang[3], K. Baroudi[4], C. Yim[4], and **R. J. Cava[4]**

[1] Zavoisky Physical-Technical Institute, Russian Academy of Sciences, Kazan 420029, Russian Federation, jenia.vavilova@gmail.com
[2] Leibniz-Institut für Festkörper- und Werkstoffforschung, Dresden, Deutschland
[3] National Institute of Standards and Technology, Gaithersburg, USA
[4] Department of Chemistry, Princeton University, USA

5d transition metal oxides, particularly Iridates, exhibit a striking example of the effects of spin-orbit coupling on the properties of the correlated electron materials. That can lead to a lot of novel electronic states: spin-orbital ordered states, spin liquids, topological order and so on.

Our study deals with a chemical modification of honeycomb lattice of Na_2IrO_3 [1]. In particular, we investigated the impact of different kinds of doping on the overall magnetic properties using magnetometry, NMR and MuSR technique. We found total or partial suppression of antiferromagnetic order when doping by Zn, Cu and Ni ions and developing of the glassy-like behavior of magnetic subsystem. No evidences for spin-liquid phases was observed in all doped samples.

1. Baroudi K. *et al.*: J. Sol. St. Chem. **210**, 195 (2014)

Investigation of the Heterostructure $YbMnO_3/SrTiO_3$ by ESR Method

R. M. Eremina[1,2], I. V. Yatsyk[1,2], D. V. Mamedov[1], T. P. Gavrilova[1], I. I. Fazlizhanov[1], V. I. Chichkov[3], and **N. V. Andreev[3]**

[1] Zavoisky Physical-Technical Institute, Russian Academy of Sciences, Kazan 420029, Russian Federation, tatyana.gavrilova@gmail.com
[2] Kazan Federal University, Kazan 420008, Russian Federation, REremina@yandex.ru
[3] National University of Science and Technology MISiS, Moscow 119049, Russia

The thin film of the multiferroic $YbMnO_3$ of thickness about 100 nm was deposited onto ferroelectric material $SrTiO_3$ ($YbMnO_3/SrTiO_3$). $YbMnO_3/SrTiO_3$ was investigated using electron spin resonance (ESR) in the wide temperature range. The most interesting result was observed in the temperature range from 50 K to 80 K where in ESR spectrum except the exchange-narrowed line from $YbMnO_3$ we observed the oscillations of the absorption power. The same features of the ESR spectrum was observed in heterostructure $GdMnO_3/SrTiO_3$ in the temperature range from 40 K to 100 K.

The reported study was partially supported by RFBR, research projects No. 12-02-00717_a and 13-02-97120.

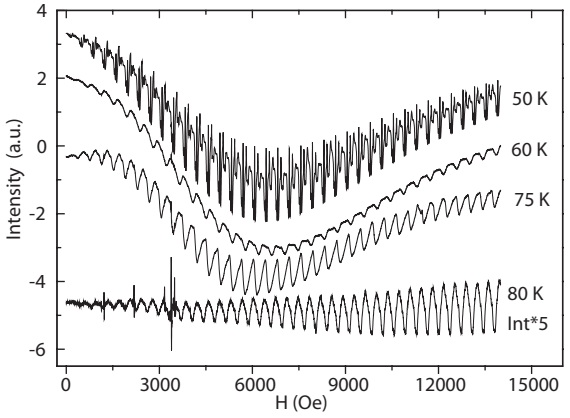

Fig. 1. Temperature evaluation of the ESR spectra in heterostructure $YbMnO_3/SrTiO_3$ in X-band.

SECTION 5

LOW-DIMENSIONAL SYSTEMS AND NANO-SYSTEMS

Spin Splitting of Edge π-Electronic States of Nanographites at their Interaction with Acceptor Molecules: ESR, CESR and MS Studies

A. M. Ziatdinov and **N. S. Saenko**

Institute of Chemistry, Far Eastern Branch of the RAS, Vladivostok 690022, Russian Federation
ziatdinov@ich.dvo.ru

The electronic structure and magnetic properties of nanographene and stack of nanographenes (nanographite) may differ significantly from those of bulk graphite due to the presence of edge π-electronic states near the peripheral regions of zigzag form [1]. In this work the results of ESR, conduction ESR (CESR) and magnetic susceptibility (MS) investigations of changes in these states at the interaction of graphite with some acceptor molecules are presented

With the set of complementary physical methods it has been found that studied PAN-based activated carbon fibers (ACFs) consist of three-dimensional disordered networks of nanographite domains, divided from each other by micropores and amorphous phase of carbon. Each nanographite consists of 2–4 nanographene layers. The in-plane size of nanographite is ≈1–3 nm (Fig. 1).

The ESR and MS data show that there are two types of spin carriers in studied ACFs: conduction electrons and localized centers, which are characterized with the same values of *g*-factor and ESR lineshape asymmetry parameter A/B (Fig. 2). Basing on the data of these methods, it was shown that the density of states near the Fermi level of nanographites is several orders higher than that of the bulk graphite. This result suggests the existence of edge π-electronic states in nanographites.

The energy of the peak of density of the edge π-electronic states of honeycomb carbon networks is slightly less than Fermi energy [2]. Therefore, the expected

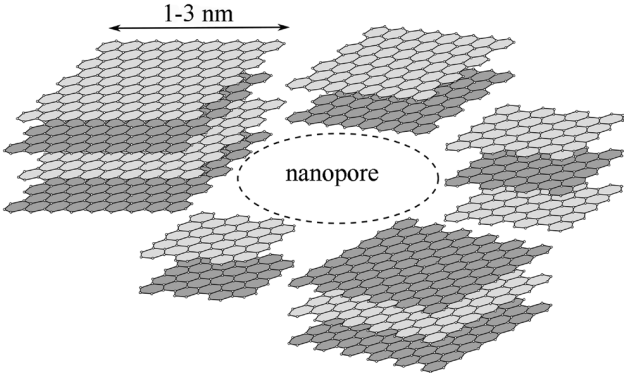

Fig. 1. The schematic representation of the PAN-based ACFs.

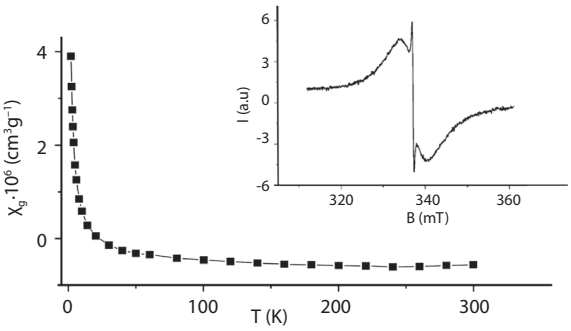

Fig. 2. The magnetic susceptibility of ACFs *vs.* temperature. Dots and solid line are the experimental and theoretical values, respectively. Inset presents the ESR spectrum at 120 K.

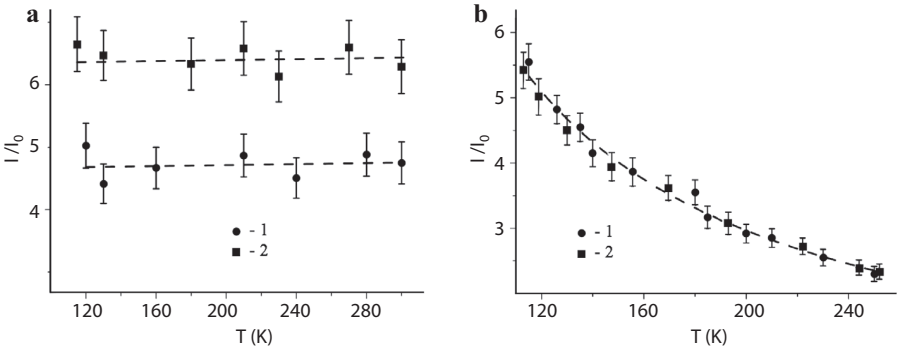

Fig. 3. The intensities of wide (**a**) and narrow (**b**) components of ACF ESR spectrum *vs.* temperature. 1 – initial sample, 2 – sample after high-vacuum pumping. I_0 – the intensity of reference CESR signal of LiF:Li.

result of their interactions with acceptor molecules is the increasing density of state at the Fermi level. However, we have observed the decreasing intensity of the signal of spin resonance on the delocalized electrons (density of states at the Fermi level) of nanographites both in the cases of ACF interactions with chlorine and oxygen. We suggest that the reasons for this are electron-electron interactions of edge π-electrons, which initiate spin splitting of the edge states as density of states at the Fermi level reaches some critical value. It has been shown that mentioned point of view on the nature of considered phenomenon does not contradict the results of other physical methods of investigations of edge π-electronic states, including scanning probe microscopy [3, 4].

1. Fujita M. *et al.*: J. Phys. Soc. Jpn. **65**, 1920 (1996)
2. Kobayashi Y. *et al.*: Phys. Rev. B. **71**, no. 193406 (2005)
3. Ziatdinov M.A. *et al.*: Phys. Rev. B. **87**, no. 115427 (2013)
4. Ohtsuka M. *et al.*: ACSNano **7**, 6868 (2013)

Peculiarities of Magnetic Properties of New 2D Honeycomb Lattice Tellurates $A_2Ni_2TeO_6$ (A = Li, Na)

E. A. Zvereva[1], **V. Y. Kudryashov**[1], **V. B. Nalbandyan**[2], **I. L. Shukaev**[2], and **A. N. Vasiliev**[1]

[1] Physics Faculty, Moscow State University, Moscow, 119991, Russian Federation
zvereva@mig.phys.msu.ru
[2] Chemistry Faculty, Southern Federal University, Rostov-on-Don 344090, Russian Federation

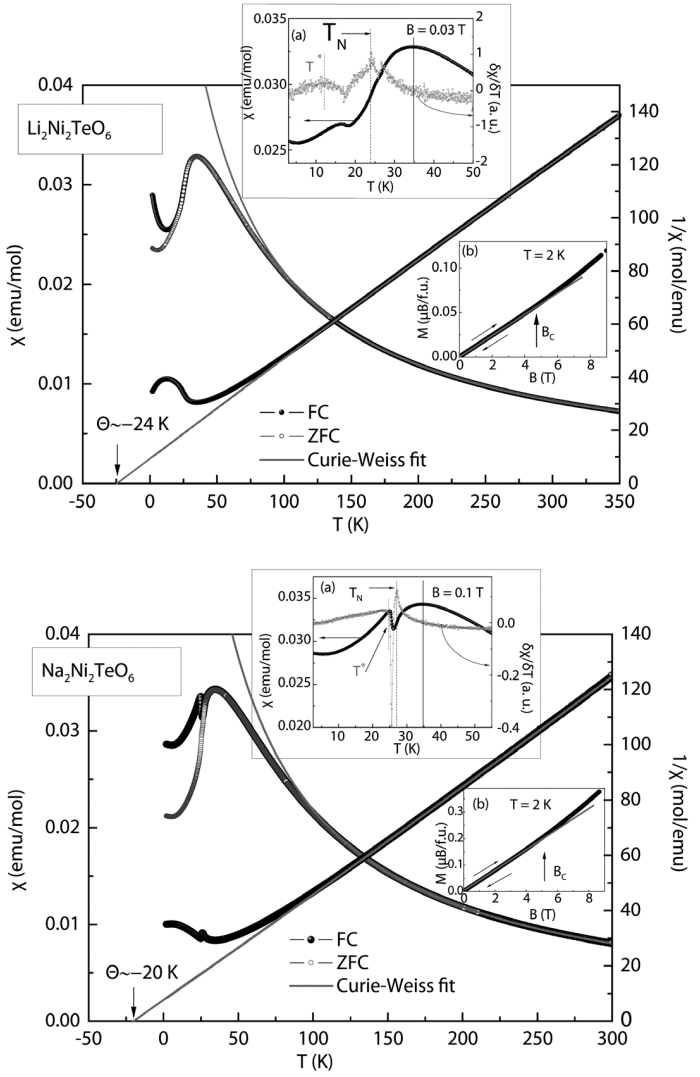

Fig. 1. Temperature dependence of magnetic susceptibility $\chi(T)$ at B = 0.1 T. Insets: **a** enlarged low-T part of $\chi(T)$ and $d\chi/dT(T)$; **b** magnetization isotherm at T = 2 K.

The static and dynamic magnetic properties of new layered honeycomb lattice oxides $A_2Ni_2TeO_6$ (A = Li, Na) were investigated. The magnetic susceptibility $\chi(T)$ passes through a maximum for both compounds indicating antiferromagnetic (AFM) order at low temperature. In addition one more unusual anomaly at $T^* < T_N$ was revealed on $\chi(T)$ in weak magnetic fields ($B < 0.1$ T for Li and $B < 1$ T for Na samples respectively). At high temperatures, $\chi(T)$ follows the Curie-Weiss law with the Weiss temperature ~–24 K and ~–20 K respectively. T_N was estimated from the maximum of $d\chi/dT(T)$ and is ~25 and 27 K for Li sample and Na sample respectively. The effective magnetic moment is ~4.5 μ_B/f.u. and agrees with theoretical estimations using determined effective g-value ~2.19 and assuming high-spin configuration of Ni^{2+} ($S = 1$). Applied magnetic field suppresses the T^* anomaly and shifts T_N to low-T side. At the same time the magnetization curves demonstrate an upward curvature suggesting the possible presence of a magnetic field induced spin-flop transition at $B_C \sim 5$ T.

The financial support of the Foundation for Basic Research (grants 14-02-00245, 14-03-01122) is gratefully acknowledged.

Tunnel Magnetoresistance of Magnetic Point Contacts

N. Useinov and **L. Tagirov**

Institute of Physics, Kazan Federal University, Kazan 420008, Russian Federation,
Niazbeck.Useinov@kpfu.ru

The quantum and macroscopic performances of point contacts (PC's) have been intensively studied both experimentally and theoretically (see, for example, Refs. [1–3]). The tunneling magnetoresistance (TMR) effect in magnetic nanostructures, where various ferromagnetic layers are separated by insulators, has attracted considerable interest due to its important applications at room temperatures [2]. Our research is devoted to building of a consecutive theory of TMR adapted to magnetic PC, which have the structure $FM^L/I/FM^R$, where FM^L are left and FM^R right ferromagnetic metals, I is an insulator. In the present work, a model of PC between two ferromagnetic metals with different conduction properties of the spin sub-bands is considered. The PC is simulated by a nanosized circular insulating disk of the radius a = 60 Å made in a membrane, which divides the space on two half-spaces, occupied by single-domain ferromagnetic metals. A model of tunnel barrier has been used to account for the finite contact length. The electron motion on the both sides of the contact can be described by transport equations for quasi-classical Green functions (GF's) [4]. These GF's are symmetric and antisymmetric with respect to z-projection of the quasiparticle momentum, and satisfy Boltzmann equations in the τ approximation. We develop a theory of electric transport through magnetic PC's taking into account gradient terms in the series expansion of GF's. The theory covers ballistic $l > a$ and diffusive $l < a$ regimes (l is the mean free path) to explain the variety of

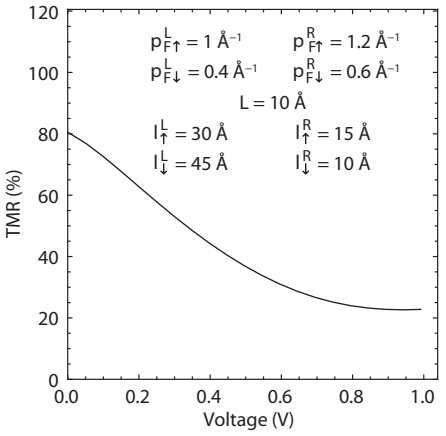

Fig. 1. The TMR dependence on the voltage applied to PC with antiparallel alignment the magnetization of the left and right ferromagnetic layers at room temperature.

observed experimental data. The basic mathematical background and calculation details can be found in article [5].

Results of the TMR calculations for different ferromagnetic metals are shown in Fig. 1. The tunnel barrier thickness between the magnetic domains is assumed to be equal L = 10 Å. The height of the energy potential above the Fermi energy is U_b = 1.2 eV. The values of Fermi wave vectors $p_{F,\alpha}^{L(R)}$ and spin-polarized mean-free paths $l_\alpha^{L(R)}$ for electrons of spin sub-bands of the ferromagnetic layers are shown in the Fig. 1 (where $\alpha = (\uparrow,\downarrow)$ is the spin index). The effective mass of the electrons in the ferromagnetic layers correspond to the free electron mass m_e. The curve is calculated without gradient terms in the series expansion of GF's. Calculation of TMR considering the gradient terms in the expansion of the GF's will be the subject of further research. In the present work, we investigated mean-free path effects on TMR. In some cases the TMR monotonously decreases as the PC cross-section increases. For some cases with large difference in spin sub-band mean-free paths, the calculated TMR shows non-monotonous behavior in the region where the radius of the contact becomes comparable with the mean-free path of electrons. We attribute this effect to the gradual change of conduction regimes ballistic↔diffusive in vicinity of the PC upon changing the contact cross-section size. The theoretical dependence of TMR on the contact size can be used in interpreting the experimental data on tunnel structures like of CoFeB/MgO/CoFe.

The financial support of the RFBR (research project No.14-02-00348 a) is gratefully acknowledged.

1. Doudin B., Viret M.: J. Phys.: Condens. Matter **20**, 083201 (2008)
2. Lee H.-M., Lee Y.-C., Chen H.-H. *et al.*: Spin **2**, 1230002 (2012)
3. Wang C., Seinige H., Tsoi M.: J. Phys. D: Appl. Phys. **46**, 285001 (2013)
4. Tagirov L.R., Vodopyanov B.P., Efetov K.B.: Phys. Rev. B **63**, 104428 (2001)
5. Useinov A.N., Deminov R.G., Tagirov L.R., Pan G.: J. Phys.: Condens. Matter **19**, 196215 (2007)

Potentials of NMR for Transport and Structural Characterization of Nanoporous Solids

R. Valiullin

Institute of Experimental Physics, Leipzig University, Leipzig 04103, Germany,
valiullin@uni-leipzig.de

Recent progress in chemical synthesis of nanoporous solids has boosted the area of their potential applications both in technological processes and fundamental research. Transport of molecular species confined to such materials plays a decisive role in many physicochemical processes, including mass separation and catalysis, and is, therefore, a key quantity for modeling and predicting the process efficiency. Our current understanding of many features of dynamics of confined fluids is, however, far from complete. This is caused, in particular, by a very rich phase behavior of nano-confined fluids and by the lack of systematic experimental studies covering broad conditions under which porous solids are exploited.

In this contribution, the results of the experimental exploration of equilibrium mass transfer in mesoporous solids using a combination of NMR methods are overviewed. In nanoporous host systems, the underlying transport mechanisms are excessively complicated by the complexity of the phenomena occurring in the pore spaces. In this respect, particular benefits of using NMR to explore the fluid dynamics in nanopores are: (i) the pulsed field gradient NMR diffusion experiments [1] can be performed in broad ranges of pressures and temperatures, allowing to trace diffusivity patterns under varying phase-state conditions and, in this way, to identify and to explore different transport mechanisms [2]; (ii) in parallel to transport properties, NMR can simultaneously yield information on the phase state under one and the same conditions [3]; (iii) by applying different tracer molecules, selective diffusion measurement in different subspaces of hierarchically organized porous solids is possible [4]. Selected examples will be used to demonstrate the versatility of NMR for the most comprehensive characterization of nano-structured materials.

1. Kärger J., Valiullin R: Diffusion in Porous Media, in: Encyclopedia of Magnetic Resonance. Chichester: John Wiley, 2011.
2. Valiullin R.: Annual Reports on NMR Spectroscopy **79**, 23 (2013)
3. Valiullin R., Kärger J., Gläser R.: Phys. Chem. Chem. Phys. **11**, 2833 (2009)
4. Kärger J., Valiullin R.: Chem. Soc. Rev. **42**, 4172 (2013)

SECTION 6

OTHER APPLICATIONS OF MAGNETIC RESONANCE. RELATED PHENOMENA

Goethite (α-FeOOH) Magnetic Transition by ESR and Auxiliary Techniques

D. F. Valezi[1], M. T. Piccinato[1], P. W. C. Sarvezuk[2], F. F. Ivashita[2], A. Paesano Jr.[2], J. Varalda[3], D. H. Mosca[3], C. L. B. Guedes[1], and **E. Di Mauro[1]**

[1] Laboratório de Fluorescência e Ressonância Paramagnética Eletrônica (LAFLUPE)-CCE, Universidade Estadual de Londrina, Londrina-PR 86051-990, Brazil, dimauro@uel.br
[2] Departamento de Física-CCE, Universidade Estadual de Maringá, Maringá-PR 87020-900, Brazil, andrea.paesano@pq.cnpq.br
[3] Departamento de Física, Universidade Federal Paraná, Curitiba-PR 81531-990, Brazil, mosca@fisica.ufpr.br

Natural and synthetic samples of the mineral goethite were characterized by Electron Spin Resonance (ESR), vibrating sample magnetometry and Mössbauer spectroscopy techniques, with the main objective of studying the magnetic transition from antiferromagnetic to the paramagnetic state that this mineral undergoes upon reaching a certain critical temperature (Néel temperature). Although it was not expected ESR signal in goethite samples at room temperature, due to its antiferromagnetic arrangement [1], a resonance line was observed in all spectra. This behavior was attributed to the existence of vacancies in the mineral structure [2–4]. Increasing the temperature from 352 K the goethite spectrum showed an additional ESR line, which intensity grows up until it stabilizes around 444 K. The appearance of this resonance line was attributed to the tendency of the magnetic moments align with the applied magnetic field, due to the thermal energy overcoming local exchange interactions and thereafter the transition to the paramagnetic state at Néel temperature T_N = 372 K. Magnetometry and Mössbauer measurements corroborate such assumption with the transition temperature identified as T_N = 370 K (in magnetometry case). Simulations of the goethite ESR spectra in paramagnetic state were performed, for the first time, by deconvolution of the resonance lines into two contributions, one from species with vacancies in their vicinity, and other ones with complete vicinity. Thereby, it was possible to identify the magnetic transition of goethite using the ESR technique and confirm the results with auxiliary techniques.

1. Cornell R.M., Schwertmann U.: The Iron Oxides: Structure, Properties, Reactions, Occurrences and Uses. 2nd edn. Darmstadt: Wiley-VCH, 2003.
2. Banerjee S.K.: Earth and Planetary Science Lett. **8**, 197 (1970)
3. Özdemir Ö., Dulonp D.J.: Geophysical Research Lett. **23**, 921 (1996)
4. Liu Q., Yu Y., Torrent J., Roberts A., Pan Y., Zhu R.: Journal of Geophysical Research **111**, B12S34 (2006)

Formation of the Train of Short Pulses from a Single Photon Field

R. N. Shakhmuratov

Zavoisky Physical-Technical Institute, Russian Academy of Sciences, Kazan 420029, Russian Federation, shakhmuratov@kfti.knc.ru

Filtering of a single-photon field by an optically thick vibrating absorber is capable to trans-form significantly the shape of a single-photon wave packet. Interference of the incident ra-diation field with coherently scattering field alters from constructive to destructive one with a period of the absorber vibration producing a train of short pulses from a smooth envelope of a single-photon wave packet.

Pulse EPR Study of Photo-Induced States of Systems on the Basis of Zinc Porphyrin

A. Sukhanov[1], **V. Voronkova**[1], **E. Mikhalitsyna**[2], **V. Tyurin**[2], and **K. Salikhov**[2]

[1] Zavoisky Physical-Technical Institute, Russian Academy of Sciences, Kazan 420029, Russian Federation, ansukhanov@mail.ru
[2] A. N. Frumkin Institute of Physical Chemistry and Electrochemistry, Russian Academy of Science, Moscow, Russian Federation

Systems on the basis of metal porphyrins and their derivatives attract increased attention during the last years because of the perspectives they open in constructing nanoscale devices and nanostructured materials. The study of the photoexcited states of such molecules can provide information about the intramolecular processes. It is well known that spin sublevels of porphyrin photoexcited triplet are populated selectively during photoexcitation, and time-resolved electron paramagnetic resonance (TREPR) is a powerful tool to study the spin-involved processes initiated by the light irradiation. However, the interpretation of the TREPR spectra of photoexcited states for the complicated porphyrin systems can be difficult and using pulsed EPR techniques together TREPR makes it possible to obtain additional information about photo-induced states [1].

In this work the advantages of using time-resolved and pulse EPR simultaneously are demonstrated by the example of the study of two new zinc porphyrin systems study. System I is built up of a zinc porphyrin macrocycle with a covalently bonded copper ion complex. System II is built up of three conjugated molecules of zinc porphyrin. Three zinc porphyrin molecules are located in one plane and two extreme molecules differ from the center molecule.

Time-resolved, echo-detected EPR and nutation spectroscopy data made it possible to establish a partial transfer of the electron spin polarization from the triplet state of the photo-excited Zn-porphyrin macrocycle to spin states of the copper complex. Echo-detected EPR data in X- and Q- bands showed the existence of two triplet states with different values of zero field splitting parameters for complex II. The observed continuous-wave TREPR spectrum was described by a sum of the spectra of three triplet states.

We are grateful to the Russian Foundation for Basic Research (project no. 12-03-97078-p) and the Government of the Republic of Tatarstan for partial financial support.

1. Maretti L., Islam S.S.M., Ohba Y. *et al.*: Inorganic Chemistry **44**, 9125 (2005)

Mechanism of Photoreaction in Aqueous Solutions Involving Radicals of S-Methylcysteine and S-Methylglutathione Studied by Time Resolved and Magnetic Field Dependence CIDNP

M. S. Panov[1,2], **O. B. Morozova**[1], and **A. V. Yurkovskaya**[1,2]

[1] International Tomography Center, Novosibirsk 630090, Russian Federation
[2] Novosibirsk State University, Novosibirsk 630090, Russian Federation,vasnik89@gmail.com

Sulfur-centered radicals are expected to play a key role in the migration of unpaired electrons over long distances through the peptide and protein matrix [1]. Considering all the information gathered so far, the oxidation mechanism of sulfur-containing amino acids and peptides has revealed a very important irreversible route, namely, decarboxylation. The immediate chemical consequence of decarboxylation is the formation of α-aminoalkyl radicals, which are known to be strongly reducing species. This may result in a change of the redox properties of the system and/or in the loss of enzymatic activity accompanied by a change of the native conformation of the protein. It is question of interest, how electron transfer from sulfur atom can cause decarboxylation reaction.

In present study we have investigated photoreactions between 3,3′,4,4′-benzophenone tetracarboxylic acid (TCBP) and S-methyl-L-cysteine (Cys(Me)), and photo oxidation of S-methylglutathione (GSMe) by exited triplets of 4-benzophenone carboxylic acid (4-CBP). From pH dependence of CIDNP kinetics pK_a = 3.2 ± 0.5 and pK_a = 9.7 ± 0.5 were determined for amino groups of Cys(Me)$^{\bullet}$ and GSMe$^{\bullet}$ radicals, respectively. At pH above these values fast decarboxylation reaction was revealed. To determine the structure of the intermediate radicals, magnetic field dependence of CIDNP signal intensities was measured. From comparison of experimental data with model calculations, the *g*-factors of radicals *g*(Cys(Me)$^{\bullet}$) = 2.0077 ± 2 and *g*(GSMe$^{\bullet}$) = 2.0082 ± 3 were extracted. These *g*-factors are significantly lower than typical values of S-centered radicals, which indicate that spin density delocalization incorporates light atoms such as oxygen or nitrogen. Based on this fact, confirmed by results of quantum-chemical calculations and CIDNP pattern we suggest five-membered ring structure with [S∴O] bond for the Cys(Me)$^{\bullet}$ radical. Close *g*-factor value, influence of charge of the amino group on proceeding of decarboxylation reaction and CIDNP pattern proves ten-membered cyclic structure to GSMe$^{\bullet}$ with [S∴O] bond between thioether group and carboxylic group of glutamic acid residue, in contrast to what has expected on the basis of analysis of transient absorption spectra [2].

Financial support by the program of RFBR (Projects No. 13-03-00437, No. 14-03-31563, No. 14-03-00453, No. 14-03-00397), Grant No. MD-3279.2014.2 of the President of the Russian Federation is gratefully acknowledged.

1. Schöneich C.: Biochim. Biophys. Acta **1703**, 111−119 (2005)
2. Filipiak P., Hug G.L., Bobrowski K. *et al.*: J. Phys. Chem. B **117**, no. 8, 2359−2368 (2013)

Pulsed Electron-Electron Double Resonance Spectroscopy on a High-Spin Mn^{2+} Ion Non-Covalently Attached to a Nitroxide Radical

D. Akhmetzyanov, J. Plackmeyer, B. Endeward, V. Denysenkov, A. Marko, and **T. F. Prisner**

Institute of Physical and Theoretical Chemistry and Center for Biomolecular Magnetic Resonance, Goethe University, Frankfurt am Main 60438, Germany, dmitry@prisner.de

The pulsed electron-electron double resonance method (PELDOR) [1] is valuable for the precise determination of distances between paramagnetic species in the range of 2–8 nm. Determination of such distances in biomacromolecules elucidates the conformational dynamics and intermolecular interactions of complexes. Since most biomolecules are diamagnetic, site-specific spin labelling with nitroxide spin species [2] is used for such type of experiments. Recently, Gd^{3+} and Mn^{2+} chelate complexes have been introduced as spin markers for proteins and nucleic acids [3, 4]. These spin species are beneficial for EPR studies at high magnetic fields.

Mn^{2+} ions are especially interesting for biological applications, since some biological macromolecules initially contain manganese as a catalytic active center. In addition, Mn^{2+} ion can replace Mg^{2+} ion which is important for the tertiary structural fold of nucleic acid molecules.

The purpose of the current work is a systematic study on a model compound containing a Mn^{2+} ion and a nitroxide spin label to understand the influence of the high-spin multiplicity of Mn^{2+} ion to the PELDOR performance. The model compound was synthesized and PELDOR experiments were performed at a conventional Q-band setup and a home-built G-band (180 GHz, 6.422 T) spectrometer. Analysis of the PELDOR data revealed distances which are in agreement with predictions based on the crystal structures of similar compounds, which is promising for further applications to biological systems.

1. Milov A., Ponomarev A., Tsvetkov Yu.: Chem. Phys. Lett. **110**, 67 (1984)
2. Hubbell W., Gross A., Langen R., Lietzow M.: Curr. Opin. Struct. Biol. **8**, 649 (1998)
3. Potapov A., Yagi H., Huber T., Jergic S., Dixon N., Otting G., Goldfarb D.: J. Am. Chem. Soc. **132**, 9040 (2010)
4. Banerjee D., Yagi H., Huber T., Otting G., Goldfarb D.: J. Phys. Chem. Lett. **3**, 157 (2012)

Transceiver System for New Specialized Medical Magnet-Resonance Tomographs

A. A. Bayazitov, Ya. V. Fattakhov, A. R. Fakhrutdinov, V. N. Anashkin, V. A. Shagalov, and **P. Chumarov**

Zavoisky Physical-Technical Institute, Russian Academy of Sciences, Kazan 420029, Russian Federation, bajazitv.alf@rambler.ru

In the world are actively created, developed and perfected various methods of diagnosing diseases. One of which is a method of NMR imaging. The specialized medical magnetic resonance tomograph with induction of magnet field 0.4 T is developed. This device can be used for diagnostics of joints pathology.

The device has following general technical and operating characteristics: magnetic field induction is 0.4 T; spatial resolution is no more than 1 mm; investigation layer's minimum thickness is 1 mm; maximum number of simultaneously obtained sections is 32.

Earlier in Zavoisky Physical-Technical Institute "whole body" model with magnetic field induction of 0.06 T with resistive magnets was developed. This tomograph successfully passed technical and medical acceptance tests that where carried out by leading specialists of Russian Ministry of Health. Members of inspection board decided that the magnetic resonance tomograph "TMR-0.06-KFTI" can be recommended for medical applications. It was confirmed that the technical and diagnostics characteristics of this device correspond to standard characteristics accepted in the world for low-field tomographs.

For new MRI-system new transmitter and transceiver systems were developed.

There are several types of NMR scanners. On the basis of: resistive, permanent or superconducting magnet. In the basis of small-size trauma NMR tomography lies permanent magnet. Magnet of this type of application has the following features: a medical of human (upper and lower limbs), research (small animals, plants, various archaeological artifacts, samples of liquids or solids, etc.). Small Workspace imposes constraints on the application. The advantage

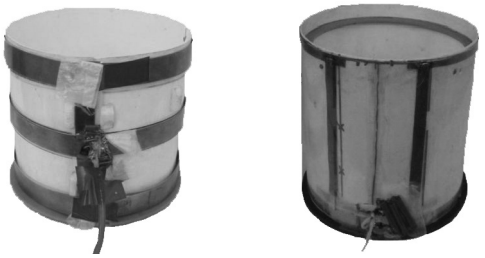

Fig. 1. Sensor "joint" of the cylindrical type, the receiving system to the left, to the right of the transmission system.

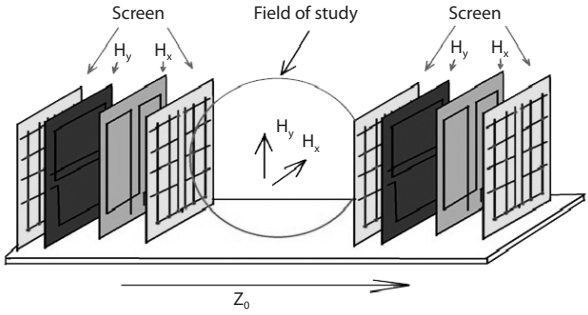

Fig. 2. Scheme sensor "joint" open type.

of these scanners is that they are more compact, lower cost compared to their overall more variations with the induction of the magnetic field of 0.4 Tesla.

In small trauma scanners RF transmission system is in close proximity to the reception, or even receiving and transmitting system may be a single circuit. Reducing the size of the transmission system, we increase the fill factor. Thus increasing the signal/noise ratio.

– In the course of research conducted:
– Sensor technology for creating "joint" of the cylindrical type.
– Sensor technology for creating "joint" open.
– On the subject of the application of different types of screens.
– Operating frequency f = 17 MGts sensor.

In the course of doing research on the possibility of using different types of screens: a cylindrical continuous ribbon of cylindrical copper circuit (consisting of closed rings centered along one axis), flat screen electrical type (consists of unclosed contours). Also conducted a study on ways to incorporate screens (with connection to the receiving circuit to zero).

When using electric screens observed no effect of frequency rebuilding circuit. This effect arises as a result of variation of the capacitance in the field of view. When using this screen is the compensation of this indicator.

In addition, studies conducted regarding the use of the screen limits the spread of the signal beyond the useful area.

Aggregation of Antimicrobial Peptide Alamethicin in Bacteria Cell Observed by EPR

N. P. Isaev[1], **R. I. Samoilova**[1], **M. De Zotti**[2], **F. Formaggio**[2], **C. Toniolo**[2], and **J. Raap**[3]

[1] Institute of Chemical Kinetics and Combustion, Novosibirsk 630090, Russian Federation, isaev@kinetics.nsc.ru
[2] University of Padova, Padova 35131, Italy
[3] Leiden Institute of Chemistry, Gorlaeus Laboratories, the Netherlands

The development of antibiotics may be the greatest scientific invention that saved millions of lives and significantly increased life expectancy. However its excessive usage formed bacterial resistance that grows faster than new drugs are designed.

Antimicrobial peptides which are the part of organism defense system may be a possible alternative to classical antibiotics. Its mechanism of action is under hard investigation. The most common approaches use model membrane systems and it was shown that some peptides may form membrane pores at high peptide/lipid concentration (around 1/20) via barrel stave or toroidal pore mechanisms. Pores formation leads to increased membrane permeability and cell death. Bacterial membrane morphology and composition differs a lot from model ones, but to our very best knowledge so far there are only three works that attempt to investigate peptides mechanism of action directly in bacteria cells [1–3].

In this work we investigated pore formation mechanism of spin-labeled peptide alamethicin in Bifidobacterium cells using CW EPR and PELDOR. Alamethicin is water insoluble, so we also studied efficiency of its delivery to bacteria by unilamellar liposomes and SDS micelles.

1. Milov A.D., Samoilova R.I., Tsvetkov Yu.D., Gusev V.A., Formaggio F., Crisma M., Toniolo C., Raap J.: Appl. Magn. Reson. **23**, 81–95 (2002)
2. Gee M.L., Burton M., Grevis-James A., Hossain M.A., McArthur S., Palombo E.A., Wade J.D., Clayton A.H.: Sci. Rep. **3**, 1557 (2013)
3. Avitabile C., D'Andrea L.D., Romanelli A.: Sci. Rep. **4**, 4293 (2014)

Management of Relative Phases of Excited Dipoles with Pulse of Weak Magnetic Field and Photon Echo Measurement of *g*-factors both Ground and Excited States Er^{3+} in $LuLiF_4$

V. N. Lisin and **A. M. Shegeda**

Zavoisky Physical-Technical Institute, Russian Academy of Sciences, Kazan 420029, Russian Federation, valerylisin@gmail.com

Accumulated phases of two groups of Er^{3+} ions with spin projection in ground state $S_z = \pm 1/2$ are shifted by pulse magnetic field on the different values $\delta\varphi = \pm 1/2\varphi$. Relative phase of two groups of radiators is not equal to zero as result. When magnetic pulse overlaps in time with echo-pulse then phase becomes time-dependent: $\varphi(t) = \int_{t_0}^{t} Z(t')\,dt'$. Expressions for dipole moment and intensity of echo formally do not vary (because perturbation is diagonal). Echo time form is modulated [1, 2]: $I(t) = I_0(t)[1 + \cos(\varphi(t))]/2$. Here $I_0(t)$ is echo intensity without magnetic pulse, $Z(t') = (g_{e\|} - g_{g\|})\beta Ht'/\hbar$ is Zeeman splitting of optical line, $H(t')$ is magnetic pulse amplitude, t_0 is the time of the beginning of pulse action, β is the Bohr magneton, $\hbar$ is the Planck constant, the plus and minus signs correspond to the σ and π laser polarizations, $g_{g\|}$ and $g_{e\|}$ is *g*-factors of the ground $^4I_{15/2}$ and excited $^4F_{9/2}$ states of Er^{3+} ion in $LuLiF_4$. The pulse magnetic field is directed along the crystal axis *C*.

If magnetic and echo pulses had a flat top, then modulation period *T* is not dependent from time and inverse modulation periods $1/T$ well enough approximates Zeeman splitting:

$$\varphi(t + T) - \varphi(t) = 2\pi \approx TZ, \qquad Z/(2\pi) \approx 1/T.$$

We were forced to significantly increase the echo duration and flat top of magnetic pulses as compared to those used in our earlier papers [1, 2]. Now in our experiment laser duration half max is 20 ns, duration echo half max is 28 ns, duration of the magnetic pulse flat part is 25 ns. Experimental dependences

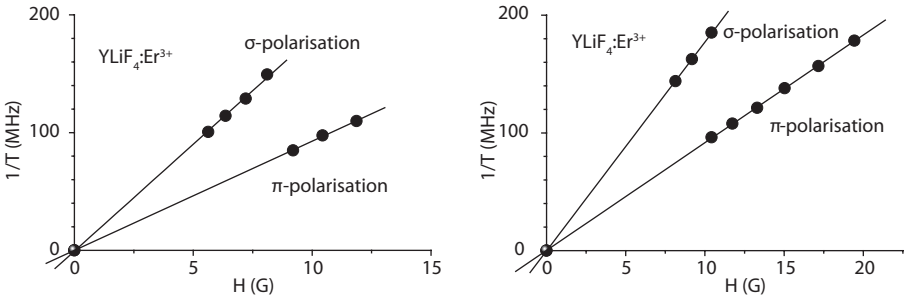

Fig. 1. Experimental dependences.

inverse modulation periods $1/T$ *vs* H are shown (Fig. 1) for σ and π-polarizations versus magnetic field amplitude for Er^{3+} in $YLiF_4$ and $LuLiF_4$. H is magnetic pulse amplitude in flat top.

The results are $g_{g\|} = 3.14$, $g_{e\|} = 9.77$ for Er^{3+} in $YLiF_4$ and $g_{g\|} = 3.06$, $g_{e\|} = 9.6$ for Er^{3+} in $LuLiF_4$. The values of ground and exctited state g-factors in $YLiF_4$ are well coincide with obtained from EPR ($g_{g\|} = 3.14$ (Sattler 1971)) and optical absorbtion ($g_{e\|} = 9.84$ (Kulpa 1975)). The value of ground state g-factor in $LuLiF_4$ is well coincide with obtained from EPR ($g_{g\|} = 3.14$ (Abdulsabirov 1988)).

1. Lisin V.N., Shegeda A.M., Gerasimov K.I.: JETP Lett. **95**, 61 (2012)
2. Lisin V.N., Shegeda A.M.: JETP Lett. **96**, 298 (2012)

POSTERS

EPR and NMR Investigations of the Thermal Annealing Effect on the Structure of MACG

M. M. Akhmetov[1], **V. Yu. Petukhov**[1], **G. G. Gumarov**[1], **G. N. Konygin**[2], **D. S. Rybin**[2], **M. M. Bakirov**[1], and **A. B. Konov**[1]

[1] Zavoisky Physical-Technical Institute, Russian Academy of Sciences, Kazan 420029, Russian Federation, mansik86@mail.ru
[2] Physical-Technical Institute Ural Branch of RAS, Izhevsk, Russian Federation, dsrybin@mail.ru

Calcium gluconate (CG) is one of the most common drugs for treatment of diseases associated with hypocalcaemia. We have previously shown that the mechanical activation of calcium gluconate leads to the significant increase in its therapeutic efficacy [1]. In this case the mechanical impact can lead to numerous structural transformations [2]. In order to assess the effect of heating during the mechanical treatment on the destruction of molecules of mechanically activated calcium gluconate (MACG) [3] the thermal annealing (TA) of the sample was performed.

Samples were annealed in a quartz tube in a stream of dry nitrogen. Changes in the structure were investigated using EPR and NMR methods. EPR spectra were recorded on an EMX Plus Bruker spectrometer at the frequency of 9.73 GHz at T = 295 K with DPPH as the reference. NMR spectra were recorded on spectrometer an AVANCE 400 Bruker. For solid-state measurements the cross-polarization mode at the magic angle spinning was applied, and for the liquid-state measurements the insets with known chemical shifts were used.

Figure 1 shows the EPR spectra for two MACG samples consisting of a single absorption line with different g-factors. For a sample without additional processing the g-factor was 2.0051 with the line width ΔH = 8 Oe [4], while for a sample subjected to subsequent annealing at 185 °C for 20 min g = 2.0043

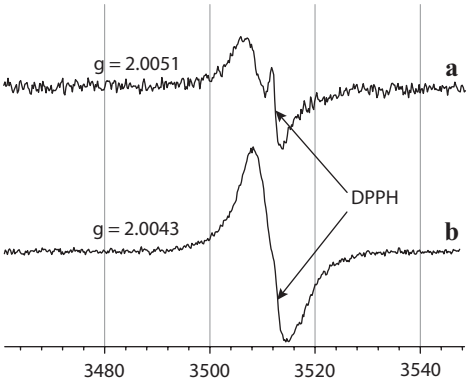

Fig. 1. EPR spectra of samples: **a** MACG, **b** MACG+TA (185 °C).

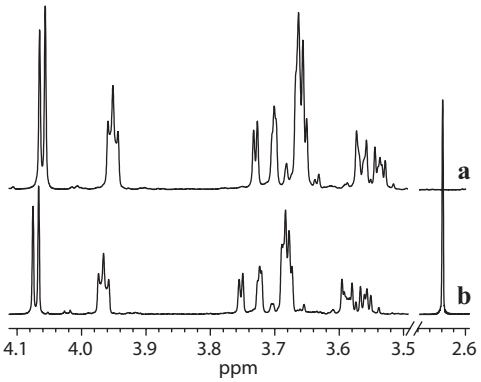

Fig. 2. ^{1}H NMR spectra of samples: **a** MACG, **b** MACG+TA (115 °C).

with the line width ΔH = 8 Oe under processing. This may indicate the change in the structure of the paramagnetic center.

Solid-state ^{13}C NMR spectra differed slightly. However, the NMR spectra for solutions of these samples manifested noticeable changes. In the ^{1}H NMR spectrum of the MACG sample after thermal annealing at 115 °C an additional line at the 2.638 ppm and the displacement of all lines were observed (Fig. 2). This fact clearly indicates the availability of an additional proton in the structure of the molecule.

Thus EPR and NMR studies make it possible to conclude that annealing at temperatures up to 185 °C does not lead the disruption of the carbon chain of the CG molecules. At the same time there are significant changes in the proton environment of CG molecules as indicated the appearance of additional lines in the NMR spectra and the change in the *g*-factor of the paramagnetic center. Detailed changes in the structure of the MACG molecule at thermal heating are the subject of our further studies.

The work was supported by the Russian Foundation for Basic Research, project no. 12-02-01316-a.

1. Konygin G.N., Gilmutdinov F.Z., Dorofeev G.A. *et al.*: Materials of conference "Topical issues of Pediatric Surgery", **56** (2003)
2. Gumarov G.G., Petukhov V.Yu., Konygin G.N. *et al.*: Almanac of clinical medicine **17**, 47 (2008)
3. Boldyrev V.V.: Bulletin SB RAMS **143** (2000).
4. Gumarov G.G., Petukhov V.Yu., Konygin G.N. *et al.*: Journal of Physical Chemistry **87**, 1 (2013)

EPR Investigations of Disprosium Dimer with the Field-Induced Slow Magnetic Relaxation

A. Baniodeh[1], R. Galeev[2], A. Sukhanov[2], R. Eremina[2], V. Voronkova[2], Ch. E. Anson[1], A. Mondal[1], and **A. K. Powell[1]**

[1] Karlsruhe Institute of Technology, University of Karlsruhe, Karlsruhe D-76131, Germany
[2] Zavoisky Physical-Technical Institute, Russian Academy of Sciences, Kazan 420029, Russian Federation

The magnetic properties of rare-earth ions attract increasing interest in the studies of molecular magnetism. This is particularly applicable to the highly anisotropic Dy^{3+} and Tb^{3+} ions.

In this work we present the results of studing the magnetic properties of the compound $[Dy_2(Htea)_2(O_2CPh)_4] \cdot MeOH$ (**1**) built up of Dy-Dy dimers. The nearest environment of the Dy^{3+} ion in the dimer is similar to that in Fe_2Dy_2 cluster [1].

The EPR, direct current (dc) and alternating current (ac) magnetic susceptibility studies were carried out on the sample **1**. An ac signal was observed in the in-phase (χ' *vs.* T plot) below 10 K but no out-of-phase signal (χ'') was observed at zero dc field, indicating the absence of the single-molecule magnet behavior. The ac susceptibility measurements under a static dc field indicated that the applied dc field slows down the relaxation time by reducing or suppressing quantum tunneling of the magnetization.

The EPR spectra of polycrystalline samples were measured at X- and Q-bands in the tem-perature range of 50–4 K. The low-temperature spectra were described in the model taking into account the anisotropic Zeeman and dipole-dipole and exchange interactions between two Dy^{3+} ions. Fitting the simulated and experimental spectra of **1** at X- and Q-bands made it possible to determine the principal values of the $\{g\}$-tensor: $g_x = 11$, $g_y = 8.2$, $g_z = 1$ which differ strongly from those in Fe_2Dy_2. This anisotropy of the $\{g\}$-tensor indicates on the mixed spin states of the ground doublet that may favor the quantum tunneling of the magnetization.

This research is supported in part by the Russian Foundation for Basic Research (project no. 13-02-01157).

1. Baniodeh A. *et al.*: Dalton Trans. **42**, 8926–8938 (2013)

Self-Organization Features of the Copper(II) Bromide Compound with 3-Amino-4-Ethoxycarbonylpyrazole

A. S. Berezin[1,2], **V. A. Nadolinny**[1], and **L. G. Lavrenova**[1,2]

[1] Nikolaev Institute of Inorganic Chemistry, Novosibirsk 630090, Russian Federation, berezin-1991@ngs.ru
[2] Novosibirsk State University, Novosibirsk 630090, Russian Federation

Synthesis and study of compounds with the magnetically active structure are both of the fundamental and practical interest in the electronics, medicine, etc [1]. The main goal of this paper is to investigate the self-organization features of the copper(II) bromide compound with 3-amino-4-ethoxycarbonylpyrazole (CuL_2Br_2) by EPR, XRD, SQUID and Raman scattering.

The CuL_2Br_2 crystal structure is a triclinic system and it is a polymeric chains along **a**. The CuL_2Br_2 coordination core is CuN_2Br_4 forming a distorted octahedron. The EPR spectrum of the initial powder sample is a single line with the temperature-independent g = 2.155, the line width equals 830 G at 300 K. By lowering the temperature of the sample to T = 77 K the line half width is reduced to 720 G. Simultaneously the sample changes the color reversibly. After the heat treatment of the sample (77 → 300 K) the new absorption line appears in the zero magnetic fields in the EPR spectrum. The heat treatment reiteration leads to increase of the new line intensity and decrease of the intensity of the line with g = 2.155 in the EPR spectra. The XRD data indicate, after the heat treatment the phase change occurs in the sample, presumably, with the formation of the strained structures. In Raman spectra, the disappearance of the pyrazole rings vibrations is observed in the treated sample [2]. Stabilization of the pyrazole

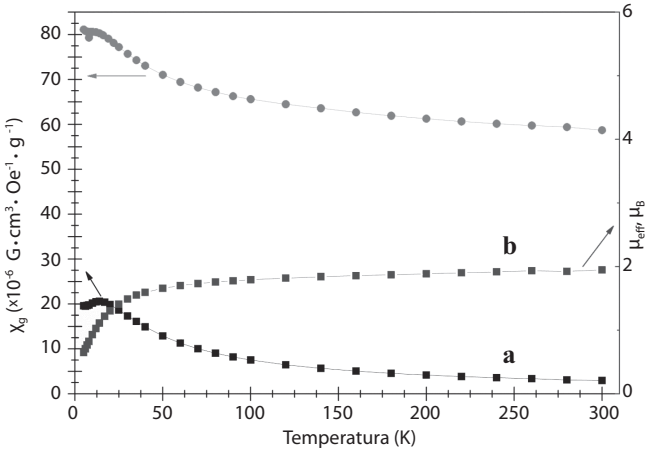

Fig. 1. Temperature dependences of the magnetic susceptibility (**a**) and the effective magnetic moment (**b**) of the initial and the magnetic susceptibility (●) of the trained CuL_2Br_2 samples.

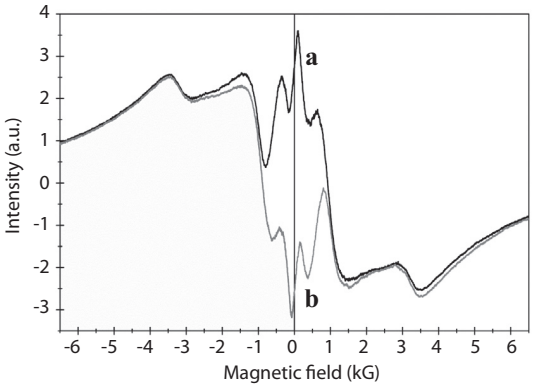

Fig. 2. EPR spectrum of compacted polycrystalline sample where magnetic field changes from –6 to +6 kG (**a**) and back-wards (**b**).

ring is expected due to the bromide forks. However, the dispersion or dissolution of the trained sample leads to the return to its original state.

The temperature dependence of the μ_{eff} of the initial CuL_2Br_2 sample indicates the antiferromagnetic type of interaction between the copper ions with the spin-spin interaction constant equals –16 cm^{-1} and the Néel temperature equals 26 K (Fig. 1). After sample training the temperature dependence of the magnetic susceptibility has the anomalously large values in the entire investigated range indicating the appearance of the ferromagnetic interactions in antiferromagnetic system (no impurities according to the chemical analysis). In the EPR spectra of the sample with new absorption line, the hysteresis loop is observed, the maximum value of which is reduced with increasing the temperature. All of these indicate the formation of the magnetic domain structure in the sample. Moreover, this sample immediately is attracted to a magnet. So, the trained compound exhibits ferromagnetic properties and ability to nonresonantly absorb the high frequency energy. But the new absorption line intensity and line width increases with increasing temperature. Such behavior is characteristic for the spin glass [3].

Based on the data, the two models of self-organization are proposed. First, polymer chains of the sample are moved towards to each other such that the bromide forks stabilize pyrazole rings, whereupon the additional exchange interaction channels arise between the copper atoms. Second model, angles between the ligands and the Cu plane change, as stated above the bromide forks stabilize pyrazole rings, thereby the interaction between the copper atoms in the chain is changed.

After self-organization, the CuL_2Br_2 has a residual magnetization. Moreover, the self-organization occurs both in the polycrystalline form and in the film structures during thermal or pressure training (Fig. 2).

This work was supported by the project No.66 on the Programme of the Presidium of RAS No.24.

1. Wienk M.M., Janssen R.A.J.: J. Am. Chem. Soc. **119**, 4492 (1997)
2. Troitskaya V.S. *et al.*: Chemistry of Heterocyclic Compounds **10**, no. 4, 471–476 (1974)
3. Zaritsky I. M. *et al.*: JETP Lett. **55**, 516 (1992)

Phase Separation in $La_{0.75}Gd_{0.25}MnO_3$ Detected by ESR

R. M. Eremina[1,2], I. V. Yatsyk[1,2], D. V. Mamedov[1], T. P. Gavrilova[1], and A. G. Badelin[3]

[1] Zavoisky Physical-Technical Institute, Russian Academy of Sciences, Kazan 420029, Russian Federation, tatyana.gavrilova@gmail.com
[2] Kazan Federal University, Kazan 420008, Russian Federation, REremina@yandex.ru
[3] Astrakhan State University, Astrakhan 414056, Russian Federation

ESR spectra of $La_{0.75}Gd_{0.25}MnO_3$ ceramic samples were investigated in the temperature range from 100 to 300 K. ESR spectrum of $La_{0.75}Gd_{0.25}MnO_3$ consists of one exchange narrowed line at room temperature (see top inset in Fig. 1a). The additional line (bottom inset in Fig. 1a) appears at $T \sim 260$ K and disap-

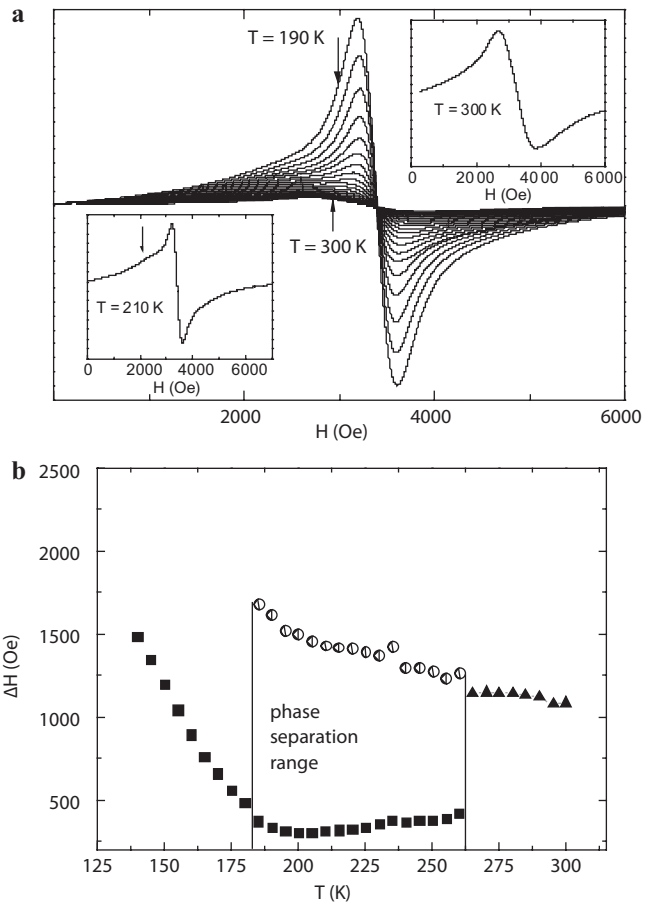

Fig. 1. Temperature dependence: **a** ESR spectra, **b** ESR linewidth in $La_{0.75}Gd_{0.25}MnO_3$ in X-band.

pears at $T \sim 180$ K in the ESR spectrum of $La_{0.75}Gd_{0.25}MnO_3$. All temperature evaluation of the ESR spectra in $La_{0.75}Gd_{0.25}MnO_3$ is presented in Fig. 1a. The presence of two lines in ESR spectrum of $La_{0.75}Gd_{0.25}MnO_3$ can be explained by the phase separation in the sample. The temperature dependencies of linewidth are presented in Fig. 1b. The temperature range of the phase separation state is higher than the magnetic phase transition temperatures in pure $LaMnO_3$ (~140 K) and $GdMnO_3$ (~42 K).

ESR of Nd^{3+} and Dy^{3+} Ions in $CsCaF_3$ Single Crystals

M. L. Falin[1], V. A. Latypov[1], and **S. L. Korableva[2]**

[1] Zavoisky Physical-Technical Institute, Russian Academy of Sciences, Kazan 420029, Russian Federation, vlad@kfti.knc.ru
[2] Kazan Federal University, Kazan 420008, Russian Federation

Double fluoride crystals with perovskite structure ABF_3 are very interesting because they are convenient model systems for studying the magneto-optical properties of impurity dopant ions. In these matrices it is possible to substitute two various cations being inequivalent positions. This enables one to carry out investigations of impurity dopant ions in sixfold or uncommon twelvefold coordinations. The physical properties of rare-earth ions in last coordination are not sufficiently studied. The introduction of three-charge rare-earth ions is hampered because of heterovalent substitution and the essential difference in the ionic radii of rare-earth ions and lattice cations. This report is concerned with investigation of impurity paramagnetic centers formed by Nd^{3+} and Dy^{3+} ions in $CsCaF_3$ single crystals.

The crystals were grown using the Bridgman-Stockbarger method. The concentration of the impurity ions was 0.1–1.0 w%. EPR experiments was carried out using an X-band spectrometer ERS-231 (Germany) at T = 4–15 K.

The parameters of the corresponding spin Hamiltonians, the ground states and their wave functions were determined. Structural models of the observed complexes were proposed. The analysis of the obtained results as compared to those obtained for the same paramagnetic ions in other hosts [1–5] was carried out.

This study was supported by the grant NSh-4653.2014.2 and the Russian Foundation for Basic Research (project no.13-02-97031r_Volga region_a).

1. Bespalov V.F., Falin M.L., Kazakov B.N. *et al.*: Appl. Magn. Reson. **11**, 125 (1996)
2. Falin M.L., Bill H., Lovy D., Latypov V.A.: Appl. Magn. Reson. **14**, 427 (1998)
3. Falin M.L., Latypov V.A., Kazakov B.N. *et al.*: Phys. Rev. B **61**, 9441 (2000)
4. Falin M.L., Anikeenok O.A., Latypov V.A. *et al.*: Phys. Rev. B **80**, 174110 (2009)
5. Falin M.L., Gerasimov K.I., Latypov V.A. *et al.*: Phys. Rev. B **87**, 115145 (2013)

ESR of Er^{3+} Ions at Cubic Sites in $CsCaF_3$ and Cs_2NaYF_6 Single Crystals

M. L. Falin[1], **V. A. Latypov**[1], **A. V. Lovchev**[2], and **N. M. Khaidukov**[3]

[1] Zavoisky Physical-Technical Institute, Russian Academy of Sciences, Kazan 420029, Russian Federation, falin@kfti.knc.ru
[2] Kazan Federal University, Kazan 420008, Russian Federation
[3] Institute of General and Inorganic Chemistry, Moscow 119991, Russian Federation

The fundamental level of rare earth ions diluted in crystals of cubic symmetry may belong to the Γ_8 representation of the cubic group. Bleaney [1] showed that in the presence of a magnetic field such a level gives rise to a system of four sublevels unequally spaced presenting a linear Zeeman effect. The transition probabilities between non-adjacent levels may be different from zero. Most of the rare earth ions have been studied in fluorite single crystals (MeF_2) which have cubic symmetry and ground doublet states (Γ_6 and Γ_7). This work presents the first results of the EPR investigation of Er^{3+} ions in $CsCaF_3$ and Cs_2NaYF_6 single crystals. It is found that the relevant parameters for the two studied matrices differ, in spite of the fact that the nearest environment of the impurity rare earth ion is nearly identical.

Fluoroelpasolities $A_2^+B^+C^{3+}F_6^-$ (A = Cs, B = Na, C = Y, Sc) having the cubic structure in the wide temperature interval are perfect model systems in which the isomorphous substitution of cations by trivalent rare-earth ions provides an

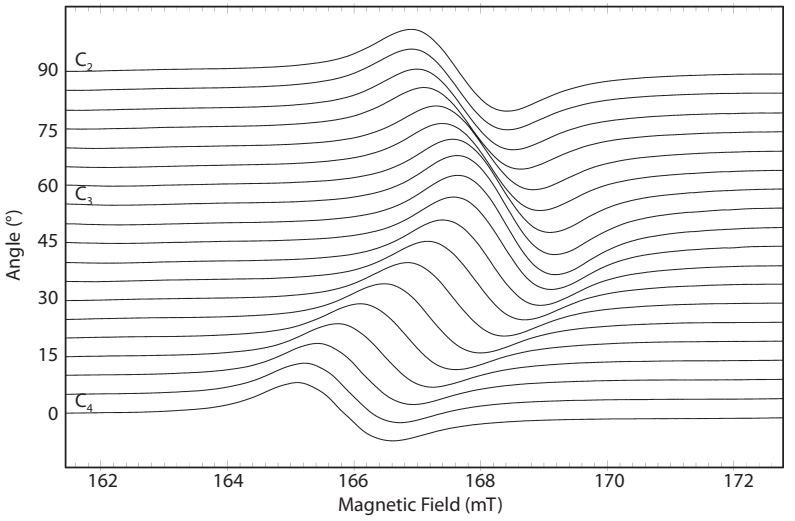

Fig. 1. Angular dependence of the EPR spectra Er^{3+} in Cs_2NaYF_6 (transition $1/2 \leftrightarrow -1/2$) in (110) plane. T = 4.2 K, ν = 9330 MHz.

opportunity to study optical and magnetic properties of dopants in a wide concentration range. Double fluoride crystals with perovskite structure $A^{+}B^{2+}F_3^{-}$ (A = Cs, B = Ca) are very interesting because, on the one hand, they find extensive application in practice, and, on the other hand, they are convenient model systems for studying magneto-optical properties of impurity dopant ions. In principle, it is possible to substitute two various cations in inequivalent positions in these matrices. This enables one to carry out investigations of impurity dopant ions in sixfold or uncommon twelvefold coordination.

Crystals of cubic elpasolites A_2BCF_6 doped with rare-earth ions were grown under hydrothermal conditions. Under these conditions, spontaneously nucleated crystals of up to 0.5 cm^3 were grown in the upper crystallization zone of the autoclave for 200 h. The crystals $CsCaF_3$ were grown using the Bridgman-Stockbarger method. The concentration of the impurity ion was 1 w%.

EPR experiments was carried out using an X-band spectrometer ERS-231 (Germany) at $T = 4$ K (see Fig. 1).

The parameters of the corresponding spin Hamiltonians, the ground states and their wave functions were determined. Structural models of the observed complexes were proposed. The experimental results were analyzed in comparison with those for the same paramagnetic ion in other hosts [4–6].

This study was supported by the grant NSh-4653.2014.2 and the Russian Foundation for Basic Research (project no.13-02-97031r_Volga region_a).

1. Bleaney B.: Proc. Phys. Soc. B **73**, 939 (1959)
2. Abraham M.M., Finch C.B., Kolopus J.L., Lewis J.T.: Phys. Rev. B **3**, 2855 (1971)
3. Antipin A.A., Klimachev A.F., Korableva S.L., Livanova L.D., Fedii A.A.: Fiz. Tverd. Tela **17**, 1042 (1975)
4. Falin M.L., Zaripov M.M., Leushin A.M., Ibragimov I.R.: Fiz. Tverd. Tela **29**, 2814 (1987)
5. Korableva S.L.: Fiz. Tverd. Tela **20**, 3701 (1978)
6. Falin M.L., Eremin M.V., Zaripov M.M., Ibragimov I.R., Leushin A.M., Abdulsabirov R.Yu., Korableva S.L.: J. Phys.: Condens. Matter **1**, 2331 (1989)

EPR Study of Nitric Oxide Production in Spinal Cord of Rats after Spinal Cord Injury in Acute and Chronic Periods

Kh. L. Gainutdinov[1,2], G. G. Iafarova[1,2], V. V. Andrianov[1,2], T. V. Baltina[2], and **V. S. Iyudin[1]**

[1] Zavoisky Physical-Technical Institute, Russian Academy of Sciences, Kazan 420029, Russian Federation, kh_gainutdinov@mail.ru
[2] Kazan Federal University, Kazan 420008, Russian Federation

The role of nitric oxide (NO) in the functioning of nervous and cardiac systems is very important [1]. The literature provides evidence of two opposing modes of NO influence on the physiology of various tissues: (1) positive, stimulatory, versus (2) toxic, damaging action that may lead to cell death. Hence it can be asserted that the "sign" of effect depends on the amount of NO, yet it is not clear what amounts should be regarded as low, normal, or elevated. *t* is shown that the change of the NO production in the tissues can result in various pathologies [2]. Early by method of EPR spectroscopy we studied the changes of intensity of NO production after modeling of hypokinesia to rats (the limitation of moving activity) through analyses of quality of NO containing paramagnetic complexes in tissues of heart and liver. It was establishment that after 30- and 60- days hypokinesia take place the 2-3 fold increase of NO quality as in heart and in liver tissues. [3]. One of the problems arise under a spinal pathology is the limitation of moving activity. Rehabilitation after spinal cord injury is one of the actual questions of modern medicine. High frequency of spine-spinal cord injury combined with the complexity of the pathogenesis of traumatic disease of spinal cord and insufficient effectiveness of treatment methods. In present no clear opinion about the role of NO in pathogenesis of traumatic disease of the spinal cord: it is able to mediate regulatory and cytotoxic effects. Therefore, we carried out a study of the dynamics of changes in the levels of NO in the tissues of spinal cord of rats in acute and chronic periods of traumatic disease of spinal cord using EPR spectroscopy.

This series of experiments were performed on rats of Wistar population weighing an average of 200 g. Animals were kept in conditions of vivarium with adjustable light regime 12 hours a day, 12 hours a night, with free access to food and water. Standard open spine-spinal cord injury inflicted on the level of the first lumbar vertebra (L1). Operations were performed in a sterile operating room, with the use of neurosurgical instruments. For anesthesia was used ketamine. We studied the content of NO in the tissues of spinal cord. During EPR samples preparation the spin traps method has been used (prof. Vanin A.F.) [4]. As a spin traps were applied the complex of Fe^{2+} with diethyldithiocarbamate (DETC)-$(DETC)_2$-Fe^{2+}-NO.

It was shown that in the acute period (in 3 days after injury) of spinal cord injury the level of NO production in tissues of spinal cord were on average 3

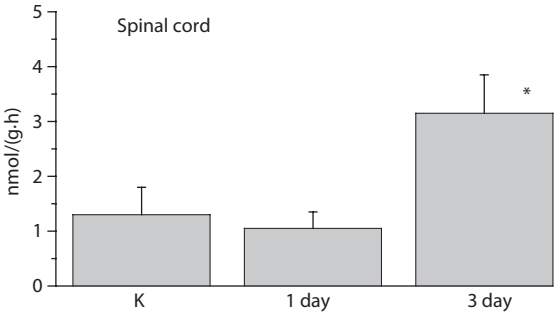

Fig. 1. Intensity of EPR signal of spin trap $(DETC)_2$-Fe^{2+}-NO from spinal cord of control and rats in 1 and 3 days after spinal cord injury.

times higher than in intact animals (Fig. 1) in the future, there is some decrease, but NO production remains above the test values in average 2 times. Thus, the acute spinal cord injuries accompanied by a significant increase of production of NO, which is maintained in chronic period of a disease.

The financial support of the Foundation for Basic Research (grant 12-04-97035_r_Povolj'e_a) is gratefully acknowledged.

1. Boehning D., Snyder S.H.: Annu. Rev. Neurosci. **26**, 105 (2003)
2. Li H., Wallerath T., Forstermann U.: Nitric Oxide **6**, 132–147 (2002)
3. Gainutdinov Kh.L., Andrianov V.V., Iyudin V.S. *et al.*: Biophysics **58**, no. 2, 203–205 (2013)
4. Mikoyan V.D., Kubrina L.N., Serezhenkov V.A. *et al.*: Biochim. Biophys. Acta: **1336**, no. 2, 225–234 (1997)

Separation of the Contribution of Exchange Interaction to the Shape of EPR Spectra of Nitroxide Radicals in Solutions

R. T. Galeev, M. M. Bakirov, and **K. M. Salikhov**

Zavoisky Physical-Technical Institute, Russian Academy of Sciences, Kazan 420029, Russian Federation, galeev@kfti.knc.ru

In the paper [1] the method separation of the contributions of dipol-dipol and exchange interactions to the shape of EPR spectra was supposed. However, this method does not take to account unsolved superfine structure of the EPR lines of radicals. We propose some modificated algorithm for separation which takes to consideration the superfine structure.

This research is supported in part by the Russian Foundation for Basic Research (project no. 12-03-97071) and the President of the Russian Federation (grant no. NSh-5602.2012).

1. Salikhov K.: Appl. Magn. Reson. **38**, 237 (2010)

Evaluation of Serum Blood Cytochrome *c* Oxidase in Sportsmen by Low Temperature EPR

M. I. Ibragimova[1], A. I. Chushnikov[1], G. V. Cherepnev[2], V. Yu. Petukhov[1], and **I. V. Yatsyk[1]**

[1] Zavoisky Physical-Technical Institute, Russian Academy of Sciences, Kazan 420029, Russian Federation ibragimova@kfti.knc.ru
[2] Tatarstan Republic Clinical Hospital No.2, Kazan 420043, Russian Federation, rkb2_rt@mail.ru

Additional abnormal absorption lines have been detected in some EPR spectra (X-band, 77 K) of serum samples collected from professional sportsmen (hockey teams of CHL) [1]. Significant portion of new signals may be caused by cytochromes, namely by cytochrome *c* oxidase. EPR studies of cytochromes are mainly carried out at helium temperatures (for review see [2]). Therefore in this study we aimed to run low temperature EPR (from 5 to 80 K) of serum blood collected from professional sportsmen. X-band EPR spectra of equal amounts of serum placed in quartz ampoules were recorded on the "Bruker EMXplus" spectrometer.

The majority of EPR spectra measured at 80 K had only the absorption lines corresponding to plasma proteins Fe^{3+}-transferrin (g = 4.21) and Cu^{2+}-ceruloplasmin (g = 2.058). In the temperature range of 5–40 K in 6 (out of 7) spectra the new signals with rather high intensities and g-factors of 11; 8.6 and 5.85 were detected. The signal intensities depend on temperature and display interindividual variation. Most likely, signals are caused by cytochrome *c* oxidase present in serum. We believe the signal with g = 5.85 comes from high-spin Fe(III) heme *a*. Broad unusual line with $g \sim 11$ can arise from magnetic exchange coupling in binuclear center between the five unpaired electrons of high spin Fe(III) heme a_3 and from the single unpaired electron of Cu_B. The nature of the signal with g = 8.6 is not completely clear. D. Hunter *et al*. [2] observed this line in spectra of mitochondrial membranes containing cytochrome *c* oxidase treated with sodium fluoride.

In conclusion, low temperature EPR may be potentially useful for serum cytochrome *c* oxidase monitoring. Noteworthy, none of the current laboratory routine clinical tests allows for serum cytochrome *c* oxidase quantification.

The work is supported by RFFR Grant No. 13-02-97065.

1. Ibragimova M.I. *et al*.: Biofisika **59**, 520 (2014)
2. Hunter D.J.B. *et al*.: Biophys. J. **78**, 439 (2000)

Lability of the Spin State of Fe(III) Complexes with Tetradentate N_2O_2 Schiff Base Ligands

T. A. Ivanova[1], L. V. Mingalieva[1], I. V. Ovchinnikov[1], I. F. Gilmutdinov[2], O. A. Turanova[1], G. I. Ivanova[1], and **V. A. Shustov[1]**

[1] Zavoisky Physical-Technical Institute, Russian Academy of Sciences, Kazan 420029, Russian Federation
[2] Kazan Federal University, Kazan 420008, Russian Federation

The compounds of Fe(III) ions ($3d^5$ electron configuration) with near electron terms of different spin multiplicity $^6A_1(S = 5/2)$ and $^2T_2(S = 1/2)$ can change the spin state (spin-crossover phenomenon) under the temperature, pressure or light irradiation influence. The multidentate Schiff base-type systems are used extensively for creating spin-crossover materials. Method of electron paramagnetic resonance (EPR) in combination with other research methods allows to study in detail the features of the intramolecular and intermolecular interactions and spin transitions between high-spin (HS) and low-spin (LS) states in this class of compounds with FeN_4O_2 coordination unit. A number complexes Fe(III) with tetradentante Schiff base-type ligands $[FeLX_2]Y$, where L = acen, salen, vanen; X = Him, CH_3Him; Y = BF_4, BPh_4, ClO_4, synthesized and studied by EPR and magnetic susceptibility in the temperature range 5–340 K in the present work.

Fe (III) ions in the compounds $[Fe(acen)X_2]BPh_4$ with X = Him are in the LS state in the temperature range 5–340 K. But the replacement of X = Him on CH_3Him in the compound leads to a temperature induced spin transition in the temperature range 190–340 K. Moreover, the compounds with other counterions Y = BF_4, ClO_4 in complexes of $[Fe(acen)(CH_3Him)_2]Y$ have the LS state in whole temperature range.

The compounds $[Fe(salen)(CH_3Him)_2]Y$ with Y = BF_4, ClO_4, BPh_4 formed HS complexes. Replacing the counter-anion does not lead to significant changes in the properties of paramagnetic centers. Spin transition in the temperature range 100–300 K occurs in compound with unsubstituted axial ligand X-$[Fe(salen)(Him)_2]BPh_4$ unlike the compound with L = acen. With other ligand L1 = vanen = CH_3Osalen compound $[FeL1(CH_3Him)_2]ClO_4$ have LS state.

The relationship between the spin-variable, structural, and chemical properties of complexes $[FeLX_2]Y$, and also the changing of nature of intermolecular interactions between them in the series of studied compounds discussed.

The work was supported by RFBR (grant No. 12-03-97090-r)

Investigation of Posphorus-Related Centers in Synthetic Diamonds Grown at HPHT Conditions in P-C Medium

A. Komarovskikh[1], **V. Nadolinny**[1], **Yu. Palyanov**[2], and **I. Kupriyanov**[2]

[1] Nikolaev Institute of Inorganic Chemistry SB RAS, Novosibirsk 630090, Russian Federation, komarrr@ngs.ru

[2] Sobolev Institute of Geology and Mineralogy SB RAS, Novosibirsk 630090, Russian Federation

Doping of diamond with phosphorus leads to the creation of n-type conductivity. But most of the works on this topic are empirical, so the description of phosphorus incorporation into the diamond is incomplete.

In this presentation information is given on EPR studies of synthetic microdiamonds grown at HPHT conditions in the P-C medium. In diamonds with low concentration of phosphorus (~100 ppm) series of nitrogen-phosphorus defects has been revealed. In the crystals grown at 1600 °C and 7 GPa isolated substitutional nitrogen (P1) and phosphorus (MA1) atoms are observed by EPR. First heat treatment at 1700 °C and 7 GPa results in the formation of NP1 center containing nitrogen and phosphorous atoms separated by two carbon atoms. If the annealing temperature is increased to 1800 °C NP1 center transforms into a pair of nitrogen-phosphorus atoms separated by one carbon atom (NP2

Table 1. EPR parameters of the phosphorus-containing centers in synthetic diamonds [1].

Center	*S*, *g*-values	Spin Hamiltonian parameters (Gs)
MA1	$S = 1/2$, $g = 2.0025$	$A(P)_{\parallel} = 23.2$, $A(P)_{\perp} = 19.6$ $A(C_1)_{\parallel} = 181.3$, $A(C_1)_{\perp} = 139.2$
NIRIM8 (NP1)	$S = 1/2$, $g_1 = 2.00243$, $g_2 = 2.0028$, $g_3 = 2.0026$	$A(P)_1 = 20.8$, $A(P)_2 = 20.2$, $A(P)_3 = 21.8$ $A(N)_1 = 40.8$, $A(N)_2 = 31.0$, $A(N)_3 = 30.0$
NP2	$S = 1/2$, $g = 2.0025$	$A(P)_{\parallel} = 23.4$, $A(P)_{\perp} = 20.9$ $A(N)_{\parallel} = 64.2$, $A(N)_{\perp} = 30.9$
NP3	$S = 1/2$, $g = 2.0025$	$A(P)_{\parallel} = 174.8$, $A(P)_{\perp} = 182.3$ $A(N)_{\parallel} = 1.0$, $A(N)_{\perp} = 3.3$
NP4	$S = 1/2$, $g_1 = 2.0009$, $g_2 = 2.0012$, $g_3 = 2.00047$	$A(P)_1 = 54.56$, $A(P)_2 = 38.38$, $A(P)_3 = 38.0$
NP5	$S = 1/2$, $g_{\parallel} = 2.00087$, $g_{\perp} = 2.0009$	$A(P)_{\parallel} = 65.22$, $A(P)_{\perp} = 10.24$
NP6	$S = 1/2$, $g_1 = 2.00085$, $g_2 = g_3 = 2.00083$	$A(P)_1 = 75.85$, $A(P)_2 = 29.42$, $A(P)_3 = 23.28$
NP7	$S = 1$, $g = 2.0012$	$D = 19.7$, $E = 0$, $A(P) = 3.6$
NP8	$S = 1/2$, $g_{\parallel} = 2.0044$, $g_{\perp} = 2.0011$	$A(P)_{\parallel} = 56.3$, $A(P)_{\perp} = 31.5$
NP9	$S = 1/2$, $g_1 = 2.0026$, $g_2 = 2.0057$, $g_3 = 2.0026$	$A(P_1)_1 = 96$, $A(P_1)_2 = 91$, $A(P_1)_3 = 134$ $A(P_2)_1 = 20$, $A(P_2)_2 = 20$, $A(P_2)_3 = 16$

center) and then into a close pair of nitrogen-phosphorus atoms (NP3 center). Further annealing at a temperature of 2300 °C leads to the lattice relaxation of the structures of nitrogen-phosphorus centers NP1-NP3, paramagnetic centers NP4-NP6 with semivacancy structures formed. NP4-NP6 have HFS of only one phosphorus atom. These centers differ in different position of nitrogen atom in the structure of the defect [1].

Experiments on electron irradiation (3.5 MeV, $5 \cdot 10^{17}$ e cm^{-2}) and subsequent annealings of diamonds containing MA1, NP1-NP3 centers do not result in the formation of new centers. But irradiation leads to the decrease of the spectra intensities of phosphorus containing centers and the little increase of the spectra intensity of substitutional nitrogen P1. This is caused by the electron redistribution in the sample since electron irradiation always gives vacancies in the lattice, negatively charged vacancy commonly observed by EPR after irradiation. 700 °C annealing restores relative intensities of the impurity centers, negatively charged vacancy disappearing. Experiments on electron irradiation of the 2300 °C annealed sample with subsequent 700 °C annealing gives new center NP7, it proposed to have the structure of eight-vacancy chain with a phosphorus atom in the center. NP7 is thought to be formed by attachment of vacancies to phosphorus-containing defect with a semivacancy structure [1].

In the sample grown in the medium with higher concentration of phosphorus microcrystals with different impurity concentration are formed during spontaneous crystallization. In some microcrystals nitrogen-phosphorus defect NP3 is still observed. In other microcrystals pure phosphorus paramagnetic centers NP8 and NP9 have been detected. NP8 demonstrates HFS of one phosphorus atom, NP9 demonstrates HFS of two phosphorus atoms. The latter one is supposed to be phosphorus pair in adjacent carbon positions. Structure of the NP8 is discussed. Also in some microcrystals there is so high concentration of phosphorus impurity that conductivity electrons are observed.

1. Nadolinny V., Komarovskikh A., Pal'yanov Y., Kupriyanov I.: Phys. Status Solidi A **210**, 2078 (2013)

The Influence of Sucrose and Trehalose on a Mobility of Lipid Membrane

K. B. Konov[1], **N. P. Isaev**[2], and **S. A. Dzuba**[2,3]

[1] Zavoisky Physical-Technical Institute, Russian Academy of Sciences, Kazan 420029, Russian Federation, kostyakonov@gmail.com
[2] Institute of Chemical Kinetics and Combustion, Novosibirsk 630090, Russian Federation
[3] Novosibirsk State University, Novosibirsk 630090, Russian Federation

It is well known that sucrose and trehalose can protect cell and its interior from damaging action of freezing and desiccation. The water replacement hypothesis asserts the sugars might replace the water around polar heads in cell membranes, thus stabilizing its structure in the absence of water. In addition, it is considered that the cryoprotective action of sugars associates with the affect on mobility of lipid bilayer.

The electron spin echo technique fits well to study the effect of sugars presence on the mobility of cell membrane. This technique allows to obtain information about anisotropic transverse relaxation, which depends on molecular motions. This method provides information about the mobility of different parts of lipid bilayer below a temperature of 250 K. At higher temperatures continuous-wave EPR can give some information about molecular motions.The aim of this work is to study the influence of sugars on the mobility of cell membrane. The stearic

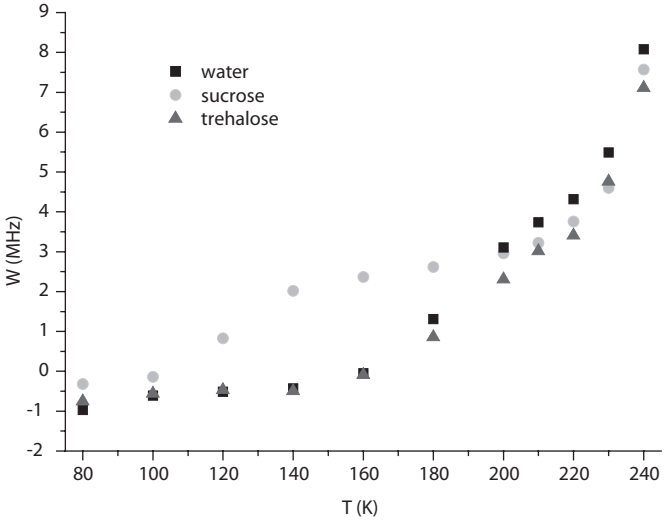

Fig. 1. Anisotropic relaxation rate of stearic acid spin-labeled at 5th position hydrated in water, water-trehalose and water-sucrose mixtures.

acids spin labeled at 5th and 16th carbon position along aliphatic chain with nitroxide radical were mixed with 1,2-dipalmitoylsn-glycero-3-phosphocholine (DPPC) and hydrated in water-sugar solution (concentration 1 and 0.2 mol).

1. Crowe J.H., Crowe L.M. *et al.*: Biochimica et Biophysica Acta **947**(2), 367–84 (1988)
2. Golovina E.A., Golovin A.V. *et al.*: Biophysical Journal **97**, 490–499 (2009)
3. Geert van den Bogaart, Hermans N. *et al.*: Biophysical Journal **92**, 1598–1605 (2007)

PELDOR Theory for Overlapping EPR Spectra

K. M. Salikhov, I. T. Khairuzhdinov, and **R. B. Zaripov**

Zavoisky Physical-Technical Institute, Russian Academy of Sciences, Kazan 420029, Russian Federation, semak-olic@mail.ru

The current theory of pulse electron double resonance (PELDOR) has been generalized to the case, when paramagnetic particles (spin labels) in pairs or groups have the electron paramagnetic resonance (EPR) spectra, which overlap essentially or coincide. The three-pulse PELDOR signal modulation (oscillations) induced by the dipole-dipole interaction between paramagnetic spin ½ particles in pairs embedded in disordered systems has been analyzed comprehensively. It has been shown that the PELDOR signal contains additional terms in contrast to the situation considered in the current theory, when the EPR spectra of the spin labels in the pairs do not overlap. In disordered systems the pairs of spin labels have the characteristic dipolar interaction frequency. For pairs of spin labels the oscillations of the PELDOR signal reveal this characteristic frequency. The oscillation amplitude of the PELDOR signal depends on the overlapping of the EPR spectra of spin labels. The consistent approach to treating the PELDOR data for the groups containing three or more spin labels has been outlined on the basis of the results for the pairs of spin labels. It has been also analyzed how the spin flips and molecular motion or molecular isomerization can affect the manifestation of the interaction between the spin labels in the PELDOR experiments. PELDOR experiments for the stable biradicals (biradicals I containing 1-oxyl-2,2,5,5-tetramethylpyrroline-3-yl spin labels and biradicals II containing 3-imidazoline spin labels) have been performed. The results have been interpreted within the theory developed in this work.

Spin Exchange between Charged Paramagnetic Particles in Diluted Solutions

K. M. Salikhov[1,2], A. E. Mambetov[1], M. M. Bakirov[1], I. T. Hairuzhdinov[1], R. T. Galeev[1], R. B. Zaripov[1], and **B. Bales[3]**

[1] Zavoisky Physical-Technical Institute, Russian Academy of Sciences, Kazan 420029, Russian Federation, pinas1@yandex.ru
[2] Kazan Federal University, Kazan 420008, Russian Federation
[3] Western Institute of Nanoelectronics, University of California, Los Angeles 18111, USA

Kinetic equations for the spin density matrix which take into account the binary collisions and a method of calculating the spin exchange effective radius have been generalized to the case of diluted solutions of charged paramagnetic particles. The effective radius of the spin exchange and constant of the bimolecular spin exchange rate between charged paramagnetic particles in solutions have been calculated numerically. Calculations have been performed under the assumption that the exchange interaction is isotropic and decays exponentially with the increase in the distance between radicals, and the solution has the given dielectric permittivity and Debye screening radius. Dependences of the spin exchange rate constant on the mutual diffusion coefficient, exchange and electrostatic interactions parameters have been found numerically.

Transformations of the EPR spectrum for water solutions of the 3-carboxy-2,2,5,5-tetramethyl-1-pyrrolidinyloxy (3-Carboxy-Proxyl, $C_9H_{16}NO_3$) (3CP) radical have been studied experimentally as a function of the concentration of paramagnetic particles, temperature and ionic strength of the solution. The concentration broadening of the EPR spectrum lines has been found from experimental data.

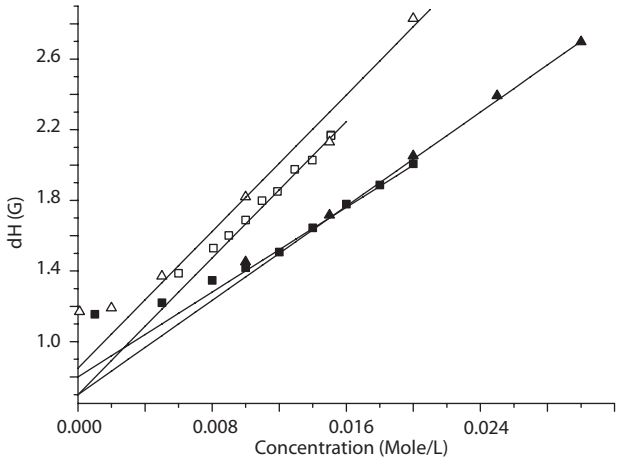

Fig. 1.

The spin exchange rate for charged radicals is less than that for neutral ones (Fig. 1). It has been shown that in the studied system the spin exchange gives the main contribution to the concentration broadening of the EPR spectrum lines. It has been also shown that for the studied system the case of the weak spin exchange is implemented. The constant of the spin exchange rate between oppositely charged radicals found from the experiment and calculated within the developed theory are in good agreement (Fig. 1).

1. Molin Yu.N., Salikhov K.M., Zamaraev K.I.: Spin exchange. Springer Verlag, Berlin Heidelberg New York, 1980.
2. Мамbetov A.E., Salikhov K.M.: ZhETP **128**, 1013–1024 (2005)
3. Salikhov K.M.: Appl. Magn. Reson. **38**, 237–256 (2010)

High-Frequency EPR Spectroscopy of Iron in Beryl

G. S. Shakurov[1], **V. G. Thomas**[2], **D. A. Fursenko**[2], **E. S. Zhukova**[3], and **B. P. Gorshunov**[3]

[1] Zavoisky Physical-Technical Institute, Russian Academy of Sciences, Kazan 420029, Russian Federation, shakurov@kfti.knc.ru
[2] Institute of Geology and Mineralogy SB of RAS, Novosibirsk, Russian Federation
[3] Institute of General Physics, Moscow 119991, Russian Federation

Beryl ($Al_2Be_3Si_6O_{18}$) belongs to the cyclosilicates and has a hexagonal crystal structure with space group P6/*mcc*. The nearest neighbors of each aluminum ion are six oxygen ions. The beryllium and the silicon ions are surrounded by tetrahedra of oxygen ions. The transition metal ions can substitute both octahedral and tetrahedral sites. Besides in the crystal structure along *c*-axis there are channels, which serve accommodate water molecules and impurity ions. The samples that are obtained by hydrothermal synthesis can contain up to three weight percent of water. Recently spectroscopic properties of beryl in the terahertz region were investigated [1]. It was established that transmission through the crystal depends strongly from direction of the polarization relative to c-axis and these peculiarities are connected with vibration of water molecules. Since some of non-Kramers ions (Cr^{2+}, Fe^{2+}, Mn^{3+} et al.) have excited levels in the tera- and subterahertz region, the high-frequency EPR spectroscopy of these impurities is difficult. Nevertheless we undertook the study of synthetic beryl doped with Fe by high-frequency (65–850 GHz) tunable EPR spectroscopy method. We observed resonance transitions in the synthetic beryl that contained iron (0.036 formula units). The sample of the blue color had dimension 4×8×14 mm. The dependence of the frequency transitions from the magnetic field allow to make the conclusion that singlet↔doublet transitions takes place. The EPR lines had highly asymmetric shape. One of the wings had structure. After annealing in vacuum at the temperature 1000 °C during 24 hrs crystal was milky white. The intensity of EPR line decreased and structure disappeared. From early optical measurements are known that Fe^{2+} ions can substitute the aluminum in the octahedral site and the beryllium in the tetrahedral one. The existence of pair Fe^{2+}-Fe^{3+} in the neighboring octahedra also was proved. In the report various options for explaining the observed results are discussed.

The work was supported by Foundation for Basic Research (project 14-02-00255-a).

1. Gorshunov B.P. *et al.*: J. Phys. Chem. Lett. **4**, 2015 (2013)

EPR and Group-Theoretical Studies of the Transition to Incommensurate Phase of $MgGeF_6 \cdot 6H_2O$ Crystals

P. G. Skrylnik and **A. M. Ziatdinov**

Institute of Chemistry of the Far Eastern Branch of the Russian Academy of Sciences, Vladivostok 690022, Russian Federation, ziatdinov@ich.dvo.ru

The group-theoretical investigations of the structural phase transition to incommensurate state of $MgGeF_6 \cdot 6H_2O$ crystals, revealed by the electron paramagnetic resonance (EPR) method [1], as well as analysis of the EPR results, are reported. The consideration of temperature dependences of Mn^{2+} admixture ion EPR spectrum symmetry and parameters leads to the conclusion that at T_{i1} = 403 ± 0.3 K they undergo second order structural phase transition to incommensurately modulated state, the order parameter of this transition may be the angle of $[Mg(H_2O)_6]^{2+}$ octahedra rotation around crystal $\mathbf{C}_3$ axis (theoretical calculations confirm the quadratic dependence of the fine structure parameter D on the angle of rotation ϕ (Fig. 1)). At temperature decreasing below first order phase transition T_{i2} = 380 ± 0.3 K the gradual transformation of plane-wave modulation of lattice displacements into soliton mode occurs. At T_c = 311 ± 0.3 K the first order improper ferroelastic phase transition into monoclinic phase occurs. The group-theoretical analysis of the phase transition at T_{i1} in the $MgGeF_6 \cdot 6H_2O$ crystals, carried out for the first time, has shown that the existence of the incommensurately modulated phase is conditioned by the fundamental reasons (presence of Lifshitz invariant). Basing on the available structural data, the set of groups promising for the analysis as high-temperature praphase contains $R\bar{3}$, $R\bar{3}m$, $P\bar{3}$ and $P\bar{3}m1$. Corresponding irreducible

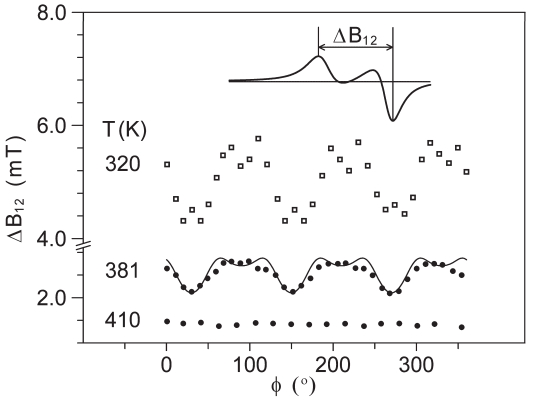

Fig. 1. Angular dependences of the value of Mn^{2+} EPR low field hyperfine structure line ΔB_{12} parameter for $MgGeF_6 \cdot 6H_2O$:Mn^{2+} crystals at rotating the sample around the $\mathbf{C}_3$ axis (along the ϕ angle), which makes the angle θ = 50° with B_0, at different temperatures (the X-band). Dots correspond to experimental values. Solid line corresponds to the theoretical angular dependence (describing the experimental one for T = 381 K). Inset presents the definition of ΔB_{12} lineshape parameter.

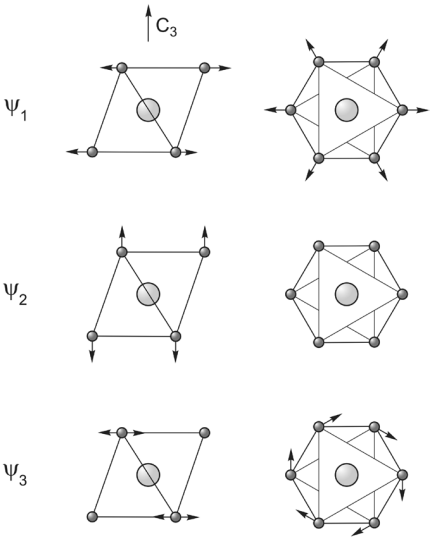

Fig. 2. The scheme of atomic dis-placements corresponding to the components of basis functions of IRs: ψ_1 – radial displacements, ψ_2 – axial displacements along $\mathbf{C}_3$, ψ_3 – rotation of octahedron around $\mathbf{C}_3$. Large circles correspond to the Mg (Ge) atoms, small ones to the O (F) atoms, respectively.

representations (IRs) designated with Brillouin zone points Λ_i and Δ_i (i = 1–3), have been tested on the existence of Lifshitz invariants with using the tables by Stokes *et al.* [2]. It follows from analysis that the primary order parameter of the phase transition at T_{i1} is determined (as magnitude of atom displacements of water and/or fluorine octahedra with respect to the high-temperature phase above T_{i1}):

1. Λ_2 ($R\bar{3}m$) and Δ_2 ($P\bar{3}m1$) – the angle of octahedra rotation around trigonal axis (case ψ_3, Fig. 2).
2. Λ_1 ($R\bar{3}m$) and Δ_1 ($P\bar{3}m1$) – the magnitude of axial distortions of octahedra relative to trigonal axis (case of combination of ψ_1 and ψ_2 distortions, Fig. 2).
3. Λ_1 ($R\bar{3}$) and Δ_1 ($P\bar{3}$) – the combination of axial distortions and rotations of octahedra around trigonal axis. The ratio between those components is determined with the parameters of interatomic interactions in studied crystals (case of combination of ψ_1, ψ_2 and ψ_3 distortions, Fig. 2).

From these options only the first choice is in agreement with experimental data indicating that in the ferroelastic phase of $MgGeF_6 \cdot 6H_2O$ crystals there are water molecule octahedra with two different orientations around trigonal axis of complexes but with equal axial distortions. Therefore, the description of the phase transition at T_{i1} with the Λ_2 ($R\bar{3}m$) or Δ_2 ($P\bar{3}m1$) representations and with using the concept of praphase ($R\bar{3}m$ or $P\bar{3}m1$, respectively) is the most preferable variant. The conclusions of this analysis on the nature of order parameter, the structural motifs of incommensurate phase and the possible character of temperature evolution of the structure are in agreement with the EPR investigation data.

1. Ziatdinov A.M., Kuryavyi V.G., Davidovich R.L.: Sov. Phys. Solid State **29**, 215 (1987)
2. Stokes H.T., Hatch D.M., Nelson H.M.: Phys. Rev. B **47**, 9080 (1993)

Combined Magneto-Electric Spin Resonance of Impurity Ions in Synthetic Forsterite

V. Tarasov, N. Solovarov, A. Sukhanov, and **R. Zaripov**

Zavoisky Physical-Technical Institute, Russian Academy of Sciences, Kazan 420029, Russian Federation, tarasov@kfti.knc.ru

The conventional line shape of resonance transitions in continuous-wave electron paramagnetic resonance (EPR) spectra recorded at the magnetic field modulation has is the derivative of the absorption contour of the spectral line. EPR lines with the absorption shape instead of the derivative of the absorption contour were observed in the continuous-wave EPR spectra of holmium impurity ions in synthetic forsterite recorded on an ELEXSYS E 580 EPR spectrometer [1]. These experimental data were interpreted as a result of the simultaneous excitation of the magnetic dipole and electric quadrupole transitions by magnetic and electric components of the resonance microwave field. Here we present additional experimental data obtained for chromium and holmium impurity ions in forsterite that support this interpretation of the origin of the EPR lines of the anomalous shape. Measurements were carried out on an ELEXYS E580 X-band EPR spectrometer supplied with a cylindrical dielectric resonator ER4118MD5-W1 of the Flexline series and on an EMXplus EPR spectrometer supplied with a cylindrical cavity resonator ER4122SHQ operating at the TE011 mode. The temperature of the sample was varied between 5 and 40 K.

In particular, it was found that at the same value of the microwave magnetic field in both resonators the probability of resonance transitions in the dielectric resonator of the ELEXSYS spectrometer is significantly higher than that in the metal resonator of the EMX spectrometer. It could be explained by the assumption that the resonance transitions in the dielectric resonator of the ELEXSYS spectrometer are excited not only by the magnetic component B_1 of the microwave field but also by the gradient of its electric component E_1.

This work was partially supported by RFBR, research project No. 12-02-00535 a.

1. Tarasov V.F., Zaripov R.B., Solovarov N.K., Sukhanov A.A., Zharikov E.V.: JETP Lett. **93**, 753 (2011)

NMR Characterization of Gasoline-Ethanol Blends

A. Turanov[1] and **A. K. Khitrin**[2]

[1] Zavoisky Physical-Technical Institute, Russian Academy of Sciences, Kazan 420029, Russian Federation, sasha_turanov@rambler.ru
[2] Department of Chemistry, Kent State University, OH 44242, USA, akhitrin@kent.edu

Today, gasoline-ethanol blends are widely used motor fuels. E10, the blend with 10% ethanol, is a common fuel in the US and several other countries. Addition of ethanol increases the fuel octane number [1], decreases oil consumption and carbon footprint. Disadvantages mostly come from the presence of water: shorter shelf life, risk of phase separation, especially at low temperatures, and corrosive aggressiveness [2]. Only 0.5% of water in E10 blend causes fast phase separation.

There are several available techniques to measure water content in gasoline blends based on Karl Fischer titration, extraction, or measuring impedance. All the methods are indirect and have their own limitations. NMR can provide the most direct, fast and accurate method of measuring both the water and ethanol concentrations in a fuel.

Table 1. Mass percentage of water in ethanol, ethanol in the blend, and water in the blend.

Sample	Water in ethanol (%)	Ethanol in gasoline (%)	Water in gasoline (%)
1	0.92	10.9	0.101
2	1.18	10.7	0.128
3	0.78	10.7	0.084

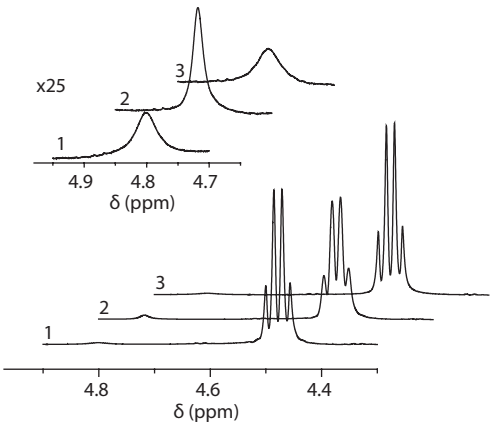

Fig. 1. Expanded region of the spectra including water and CH_2 ethanol peaks for the three samples. The spectra are shifted both horizontally and vertically for better view.

Three samples of regular gasoline have been purchased on the same day near Kent, Ohio, from thee different gas stations (BP, Shell, and Sheetz). Since a comparison of the quality of different brands was not our goal, we assigned random numbers to the samples, and used only these numbers in the text. For the concentration measurements, it is crucial to record high resolution proton spectra without sample dilution. We used very efficient NORD (NO Radiation Damping) pulse sequence [3] to accomplish this task. Quantitative high-resolution spectra are obtained with a single transient, so no lock is needed. Coefficients of self-diffusion of different molecules have been measured using a standard Stejskal-Tanner pulse sequence [4] with pulsed field gradients.

High resolution ^{1}H NMR spectra can be used for fast and accurate measurement of water content in gasoline-ethanol fuel blends. The spectra also contain information on proton exchange rates, which can be used as an indirect indicator of chemical stability. Pulsed-field-gradient NMR diffusion measurements provide information on sizes of ethanol-water clusters and also on viscosity of fuel blends.

We acknowledge a support from NSF CHE-1048645 (AK) and the Fulbright Foundation (AT).

1. Foong T.M., Morganti K.J., Brear M.J., da Silva G., Yang Y., Dryer F.L.: Fuel. **115**, 727 (2014)
2. Baena L.M., Gomez M., Calderon J.A.: Fuel. **95**, 320 (2012)
3. Khitrin A.K., Jerschow A.: J. Magn. Reson. **225**, 14 (2012)
4. Stejskal E.O., Tanner J.E.: J. Chem. Phys. **42**, 288 (1965)

EPR Study of Molecular Structure of Exchange Coupled (Mn^{2+}-Ag^{2+}) Pairs Formed in the BaF_2 Crystals

V. A. Ulanov[1,2], **R. R. Zainullin**[2], **E. R. Zhiteitsev**[1], and **M. M. Zaripov**[1]

[1] Zavoisky Physical-Technical Institute, Russian Academy of Sciences, Kazan 420029, Russian Federation, ulvlad@inbox.ru
[2] Kazan State Power Engineering University, Kazan 420066, Russian Federation

It is known that the crystals of alkaline-earth fluorides with fluorite structure can accommodate large molar fractions of trivalent rare-earth impurities which form the hexameric clusters [Me_6F_{36}] in the host crystal lattice [1]. Our earlier investigations of the solid-state reactions between defects of impurity d-ions at high temperatures revealed a possibility to synthesize paramagnetic impurity clusters of two [2, 3] or three [4] similar d-ions in the bodies of the fluorite type crystals. In particular, these clusters could be formed due to diffusion of the impurity ions in the body of host lattice at temperatures near to melting point. It was found that each of these ions initially substitutes for a lattice cation and find itself in the center of an anionic cube formed by eight fluorine ions. If the ion is Jahn-Teller type its anionic neighbors relax to new equilibrium positions. The ground state of Jahn-Teller ion becomes an orbital singlet, and a field of Jahn-Teller deformations appears around the ion. When the distances between impurity ions become short enough they can form a cluster due to interaction via the fields of Jahn-Teller deformations. Another mechanism of cluster formation is an electronic exchange between the impurity ions.

The present work was devoted to experimental investigation of products of physical-chemical reactions between point defects of dissimilar impurity d-ions (Mn^{2+} and Ag^{2+}). The samples BaF_2:(Mn+Ag) were grown by the Bridgman technique in a helium atmosphere containing some quantity of fluorine gas. A graphite of high chemical purity was used as a material for crucibles. Iron and silver were introduced in the BaF_2 single crystals by diffusion from a crystal surface at temperatures T = 1200–1300 K. The EPR measurements were performed at X-and Q-band. The EPR spectra were recorded at liquid helium temperature (T = 4.2 K), and the anisotropic spectra with well resolved fine, hyperfine and superhyperfine structures were revealed in the samples under investigation. It was found that the magnetic symmetry of the Mn-Ag pairs was tetragonal (fourfold axis C_4 was parallel to a crystallographic ⟨001⟩ axis). Spin momentum of Mn-Ag pair centre was S = 3, and this fact speaks about ferromagnetic exchange between Mn^{2+} and Ag^{2+} ions forming a pair centre. Zero field splitting of electronic states of the centers was rather large and most EPR data on the ground spin multiplet of the centers were got at Q-band.

Angular dependencies in the EPR spectra were described using spin-Hamiltonian ($S = 3$):

$$
\begin{aligned}
H_S = {} & \beta_e \left[g_{\parallel} H_z S_z + g_{\perp} (H_x S_x + H_y S_y) \right] + B_2^0 O_2^0 + B_4^0 O_4^0 + B_4^4 O_4^4 + \\
& + \left[A_{\parallel}^{\mathrm{Mn}} S_z I_z^{\mathrm{Mn}} + A_{\perp}^{\mathrm{Mn}} (S_x I_x^{\mathrm{Mn}} + S_y I_y^{\mathrm{Mn}}) - g_N^{\mathrm{Mn}} \beta_N (H_x I_x^{\mathrm{Mn}} + H_y I_y^{\mathrm{Mn}} + H_z I_z^{\mathrm{Mn}}) \right] + \\
& + \left[A_{\parallel}^{\mathrm{Ag}} S_z I_z^{\mathrm{Ag}} + A_{\perp}^{\mathrm{Ag}} (S_x I_x^{\mathrm{Ag}} + S_y I_y^{\mathrm{Ag}}) - g_N^{\mathrm{Ag}} \beta_N (H_x I_x^{\mathrm{Ag}} + H_y I_y^{\mathrm{Ag}} + H_z I_z^{\mathrm{Ag}}) \right] + \\
& + \sum_n^4 \left[S \cdot A^{\mathrm{F(I},n)} \cdot I^{\mathrm{F(I},n)} - g_N^{\mathrm{F}} \beta_N H \cdot I^{\mathrm{F(I},n)} \right] + \\
& + \sum_k^4 \left[S \cdot A^{\mathrm{F(II},k)} \cdot I^{\mathrm{F(II},k)} - g_N^{\mathrm{F}} \beta_N H \cdot I^{\mathrm{F(II},k)} \right], \qquad (1)
\end{aligned}
$$

where the superhyperfine interaction tensors, $A^{\mathrm{F(I},\,n)}$ and $A^{\mathrm{F(II},\,k)}$, are of monoclinic symmetry and correspond to two groups of four equivalent ligands (^{19}F) numbered by I and II. Elements of the $A^{\mathrm{F(I},\,n)}$ and $A^{\mathrm{F(II},\,k)}$ were determined from angular dependencies of the superhyperfine splittings in the EPR spectra.

To get quantitative information on structure of the (Mn-Ag) pairs, matrix elements of the spin-Hamiltonian (1) were compared with corresponding elements of spin-Hamiltonian

$$\mathscr{H} = \mathscr{H}_{S1} + \mathscr{H}_{S2} + JS_1S_2, \qquad (2)$$

where $\mathscr{H}_{S1}$ and $\mathscr{H}_{S2}$ are spin-Hamiltonians of single ion fragments of the (Mn-Ag) pair and J is isotropic exchange parameter. Thus, superhyperfine interaction parameters A_S and A_P were evaluated for all eight ligand fluorine nuclei. Theoretical analysis of single ion superhyperfine tensor elements and parameters A_S and A_P gave us approximate values of the ion-ligand distances and approximate directions of the ion-ligand vectors.

1. Kazanskii S.A., Ryskin A.I., Nikiforov A.E., Zaharov A.Yu., Ougrumov M.Yu., Shakurov G.S.: Phys. Rev. B **72**, 014127 (2005)
2. Zhiteitsev E.R., Zaripov M.M., Ulanov V.A.: Fizika Tverdogo Tela **47**, 1212 (2005)
3. Fazlizhanov I.I., Ulanov V.A., Zaripov M.M.: Fizika Tverdogo Tela **44**, 1483 (2002)
4. Ulanov V.A., Zaripov M.M., Fazlizhanov I.I.: Fizika Tverdogo Tela **47**, 1596 (2005)

Paramagnetic Resonance and Structural Phase Transition in $Pb_5Ge_3O_{11}$

V. A. Vazhenin, E. L. Rumyantsev, M. Yu. Artyomov, and **A. P. Potapov**

Institute of Physics and Applied Mathematics, Ural Federal University,
Yekaterinburg 620000, Russian Federation, vladimir.vazhenin@urfu.ru

The authors of [1, 2] have obtained the temperature dependence (including the critical region) of spontaneous polarization P_s in $Pb_5Ge_3O_{11}$ as a result of EPR investigations of resonance positions and abnormal (in the vicinity of T_C) line-width of trigonal Gd^{3+} centers. The authors have arrived at the conclusion that behavior of the local order parameter did not contradict the results of phenomenological theory for uniaxial ferroelectrics and fluctuation effects and logarithmic corrections could be observed only in the range of several Kelvin degrees in the vicinity of T_C.

In this work we present results of our investigation of temperature behavior of Gd^{3+} spectrum in $Pb_5Ge_3O_{11}$.

Contrary to [1, 2], according to our data, the square of the spin Hamiltonian parameter b_{43}, which linearly depend on the order parameter and is responsible for domain splitting of the spectrum, demonstrates essentially non-linear dependence on temperature. The similar non-linear dependence of $P_s^2(T)$ follows from temperature behavior of that part of fine structure parameter $\Delta b_{20}(P) \sim P_s^2$, which depends on polarization.

Detail investigation of orientation behavior of anomalous line width carried by us revealed that broadening is not caused by the fluctuations of $b_{43} \sim P_s$ as has been assumed in [1, 2] but is due to scatter in the spin Hamiltonian parameters b_{21} and c_{21}. These parameters are absent in the averaged spin-Hamiltonian but appear in local one [3] due to the products $p_z p_x$ and $p_z p_y$, where p_i are components of the local polarization induced by charged defects.

1. Trubitsyn M.P., Volnianskii M.D., Ermakov A.S., Linnik V.G.: Condens. Matter Phys. **2**, 677 (1999)
2. Trubitsyn M.P., Waplak S., Krokhmal Yu.D.: Phase Transitions **80**, 155 (2007)
3. Vazhenin V.A., Rumyantsev E.L., Artyomov M.Yu., Starichenko K.M.: Phys. Solid State **40**, 293 (1998)

A Spin Crossover Dendrimeric Iron(III) Complex with Magnetic Ordering

V. Vorobyeva[1], **N. Domracheva**[2], and **A. V. Pyataev**[3]

[1] Zavoisky Physical-Technical Institute, Russian Academy of Sciences, Kazan 420029, Russian Federation, vvalerika@gmail.com, domracheva@mail.knc.ru
[2] Kazan Federal University, Kazan 420008, Russian Federation, 151eu@mail.ru

The coexistence of magnetic ordering and spin crossover in the Fe(III) dendrimeric complex shown in Fig. 1 was found by EPR and Mössbauer spectroscopy. EPR spectra demonstrated the presence of three types of iron(III) centers in the system: one low spin (LS) (S = 1/2) and two high spin (HS) (S = 5/2) centers with strong low-symmetry and weak distorted octahedral crystal fields. Analysis of the magnetic behavior reflected by I versus T (where I is the EPR lines integrated intensity of the whole spectrum) shown that dendrimeric Fe(III) complex has sufficiently different behavior in two temperature intervals. The first (4.2–75 K) interval corresponds to antiferromagnetic exchange interactions between iron centers, whereas a gradual spin transition process between LS and HS centers occurs in the second temperature (75–300 K) interval. Mössbauer spectroscopy and magnetic susceptibility data completely confirm the EPR results.

This work was supported by FANO Presidium program No. 24.

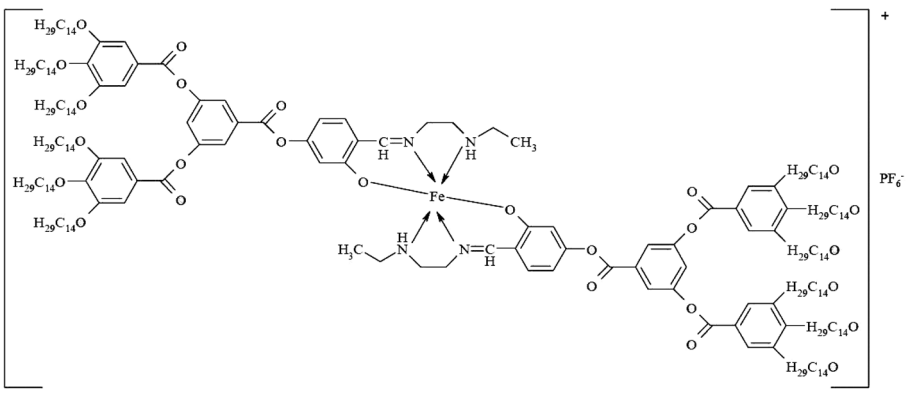

Fig. 1. Schematic model of the compound.

The Formation of Epsilon-Fe_2O_3/SiO_2 Nanoparticles: Investigation via FMR *in situ*

S. S. Yakushkin, G. A. Bukhtiyarova, and **O. N. Martyanov**

Boreskov Institute of Catalysis SB RAS, Novosibirsk State University, Novosibirsk 630090, Russian Federation, stas-yk@catalysis.ru

The iron-oxide based systems are one of the most available, cheap and nontoxic magnetic materials, which can be used in various applications, e.g. magnetic memory, controlled drug delivery, catalysis etc. The systems based on ε-Fe_2O_3 nanoparticles among those materials attract particular and growing attention during the last decades. The ε-Fe_2O_3 phase, is the intermediate between α- and γ-Fe_2O_3, it was characterized just recently, e.g. in 1998 [1]. Thanks to the low surface energy ε-Fe_2O_3 can be synthesized in nanoparticle form only [2]. According to the literature, up to the present time no one was successful to obtain ε-Fe_2O_3 nanoparticles without admixture of other iron oxide polymorphs. The main problem here is the lack of information about the initial stages of nanoparticles formation.

Ferromagnetic resonance (FMR) method is the powerful tool for magnetic nanoparticles research. FMR has very high sensitivity (>10^7 μ_B) while dealing with superparamagnetic particles. In the Boreskov Institute of Catalysis the ε-Fe_2O_3/SiO_2 nanoparticle system was created for the first time that has no other detectable iron-oxide polymorphs with narrow size distribution of ε-Fe_2O_3 supported nanoparticles [3].

It was shown that the system displays superparamagnetic behavior at room temperature [4]. FMR method *in situ* in comparison with HR TEM, XRD, Mossbauer spectroscopy, and magnetization measurements data were applied to investigate the initial stages of the ε-Fe_2O_3/SiO_2 nanoparticles formation. It was shown that the stabilization of the nanoparticles precursor on the silica support is the key factor to obtain the monophase system.

The work was supported by RAS Presidium (program no. 27, project no. 46) and Skolkovo Foundation (Grant Agreement for Russian educational organization no. 1 on 28.11.2013).

1. Tronc E., Chaneac C., Jolivet J.P.: J. Sol. Stat. Chem. **139**, 93 (1998)
2. Gich M., Roig A. *et al.*: Faraday Discuss. **136**, 345 (2007)
3. Bukhtiyarova G.A., Shuvaeva M.A., Bujukov O.A., Yakishkin S.S., Martyanov O.N.: J. Nanoparticle Res. **13**, 5527 (2011)
4. Yakushkin S.S., Dubrovskiy A.A., Balaev D.A., Shaykhutdinov K.A., Bukhtiyarova G.A., Martyanov O.N.: J. Appl. Phys. **111**, 044312 (2012)

EPR of Tetragonal and Monoclinic Nickel Centers in BaF_2 Crystals

R. R. Zainullin[2,1], **G. S. Shakurov**[1], and **V. A. Ulanov**[2,1]

[1] Zavoisky Physical-Technical Institute, Russian Academy of Sciences, Kazan 420029, Russian Federation, rrza7@yandex.ru
[2] Kazan State Power Engineering University, Kazan 420066, Russian Federation

Nickel impurity centers in the fluorite group crystals (CdF_2, CaF_2, SrF_2 and BaF_2) were the objects of number EPR investigations. Ni^{2+} centers of a trigonal symmetry were revealed in the CdF_2:Ni and CaF_2:Ni crystals [1]. Authors of the work [1] proposed that the trigonal symmetry of the Ni^{2+} centers was realized due to a strong Jahn-Teller effect in the ground triplet orbital state. Impurity centers of the Ni^+ ions were got by X-ray irradiation of the CaF_2:Ni, SrF_2:Ni and BaF_2:Ni samples [2, 3]. Magnetic properties of these centers had a tetragonal symmetry, and the impurity Ni^+ ions were found in off-center positions of a tetragonal type. The off-center shift of Ni^+ was found about 1 A. It was proposed that this off-center shift was realized due to a pseudo-Jahn-Teller effect. In the X-ray irradiated CaF_2:Ni crystals the Ni^{3+} centers of cubic symmetry were observed too [3].

Our interest to the BaF_2 crystals activated by paramagnetic ions is associated with the fact that these crystals are often used as substrates in various semiconducting devices. It seems to us the paramagnetic centers in such substrate can allow an operation the charge transport processes in semiconducting layers by optical irradiation of the substrate.

In the present work the BaF_2 crystals activated by nickel were investigated by EPR method. The BaF_2:Ni crystals were grown by the vertical Bridgman method in a graphite crucible. A helium and fluorine gas mixture was used as an atmosphere for a crystal growth process. Nickel was introduced into the melt as a metallic powder. Using the X-band, Q-band, and tunable submillimeter EPR spectrometers three type paramagnetic centers were revealed in the BaF_2:Ni samples at $T = 4.2$ K. First and second of them had tetragonal symmetries and third a monoclinic one.

At Q- and X-band the first type tetragonal centers gave rise electronic transitions between $M_S = +1$ and $M_S = -1$ levels of $S = 2$. Using the tunable submillimeter EPR spectrometer, the zero field splitting Δ between $M_S = \pm 1$ and $M_S = 0$ of the first type centers was found to be 100.5 ± 0.5 GHz. It was found too that second type tetragonal centers could be characterized by $\Delta = 127.4 \pm 0.5$. The g-tensor components for the first and second type centers were found to be $g_{\parallel} = 2.14 \pm 0.01$ and $g_{\perp} = 2.01 \pm 0.01$.

EPR spectra of the third type centers which had a monoclinic symmetry were described by spin-Hamiltonian

$$H_S = B_2^0 O_2^0(S) + B_2^2 O_2^2(S) + \beta_e [g_x B_x S_x + g_y B_y S_y + g_z B_z S_z] \qquad (1)$$

which was represented in a local coordinate system $X'Y'Z'$ with X' and Z' being parallel to a (011) crystallographic plane. The angle between Z' and ⟨001⟩ crystallographic axis was equal to 27 ± 3 degrees. The spin-Hamiltonian (1) could be characterized by $S = 1$, $B_{20} = 12.3$ GHz, $B_{22} = -0.5$ GHz, $g_x = 3.32$, $g_y = 3.24$, $g_z = 2.45$.

The observed centers of tetragonal symmetry were ascribed to (Ni^{3+}-Ni^{+}) pairs in a ferromagnetic state. Relatively high concentration of these centers could be explained by that the formation of such defect associates was profitable.

The monoclinic centers were accounted for the associates of substitutional Ni^{2+} and interstitial F-defects. Experimental facts on monoclinic centers can be understood if one proposes that a Ni^{2+} ion substitutes host cation and finds itself in a cubic crystal field. In such situation the ground orbital term (^{3}F) is splitted by this crystal field and ^{3}T crystal field orbital multi-plet becomes the ground one. If an interstitial fluorine ion arises near to Ni^{2+} in a tetragonal site then the ground ^{3}T orbital triplet of the Ni^{2+} will be splitted into orbital singlet and orbital doublet. Obviously, in the case under consideration, (Ni^{2+}-F^{-}_{int}) associate finds itself in the ground doublet orbital state and the vibration interaction with trigonal modes can be realized. Simultaneous action of the Jahn-Teller trigonal distortion and tetragonal distortion induced by interstitial fluorine ion can lead to monoclinic symmetry of the (Ni^{2+}-F^{-}_{int}) associates.

The above mentioned hypothesis was confirmed by our latest EPR investigations of BaF_2:Ni samples at $T = 77$ K. Additional spectra of tetragonal symmetry characterized with $S = 1$ were observed. These spectra demonstrated the well resolved superhyperfine structures (SHFS). Analysis of the SHFS showed the molecular structure with nine fluorine ions in the nearest environment of the Ni^{2+} ion.

1. Gehlhoff W., Ulrici W.: Phys. Stat. Sol. (b) **102**, 11 (1980)
2. Alonso P.J., Casas Gonzalez J., den Hartog H.W.: Phys. Stat. Sol. (b) **102**, 721 (1980)
3. Alonso P.J., Casas Gonzalez J., den Hartog H.W., Alcala R.A.: J. Phys. C: Solid State Phys. **16**, 3593 (1983)

Temperature Dependence of the Electron Paramagnetic Resonance Parameters of Semiconducting Compound

A. M. Zuzin, V. V. Radaykin, M. A. Bakulin, and **S. A. Savostina**

Ogarev Mordovia State University, Saransk 430000, Russian Federation,
radajkinvv@rambler.ru

Semiconducting compound is used as the protective layers of cables of a high voltage. He represents a complex polymeric composition in which technical carbon is one of the basic components. Research of temperature properties of such material, in particular the thermal stability of physical and technical characteristics is one of the important and actual problems.

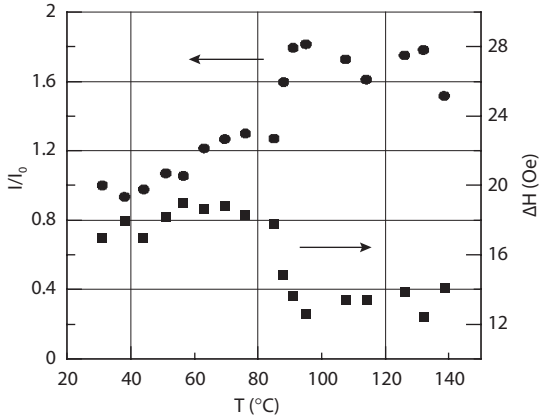

Fig. 1. Temperature dependence of relative intensity (●), and line width (■).

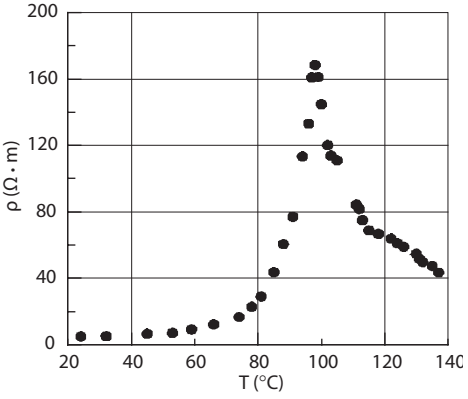

Fig. 2. Temperature dependence of specific resistance.

In this paper we have investigated the temperature dependence of the intensity I and line width ΔH of the absorption curve of the EPR, and also specific resistance ρ.

Spectra were recorded on EPR spectrometer PS 100X. The made experiments have allowed to establish sharp increase of intensity of absorption line in the range of temperatures from 80 to 100 °C (Fig. 1). Simultaneously with it appreciable reduction of the line width EPR was observed. As a result the area under the absorption curve, proportional to concentration of the paramagnetic centers, remained practically invariable.

Such behavior of parameters EPR semiconducting compound allows to draw a conclusion about change of condition EPR centers of the carbon particles, occurring in the given interval of temperatures. Temperature dependence of specific resistance semiconducting compound correlates with temperature dependence of parameters EPR and is additional acknowledgement of that in the range of temperatures 80–100 °C there is a change of a condition of an investigated material.

Effect of Frequency on the Anisotropy of the Dispersion Curves in Two-Layer Magnetic Films

A. M. Zuzin, V. V. Radaykin, S. N. Sabaev, M. A. Bakulin, and **S. V. Bezborodov**

Ogarev Mordovia State University, Saransk 430000, Russian Federation, radajkinvv@rambler.ru

The purpose of this study was to investigate the influence of the frequency of the microwave field on the dispersion dependence of the spectra of the spin-wave resonance (SWR) bilayer films with perpendicular and parallel orientations of the static magnetic field **H** relative to the film plane.

Registration of the spectra spin-wave resonance(SWR) produced by EPR spectrometer X and Q of the range EMX Plus (Bruker) at frequencies of the microwave field f = 9/3 GHz and f = 34 GHz. Single-crystal garnet-ferrite films were grown through liquid-phase epitaxy. Composition and parameters of the layers of the investigated films (thickness h, the magnetization M, α is the Gilbert damping parameter, the gyromagnetic ratio γ, the effective field of uniaxial-anisotropy H_k^{eff}) are given in the Table 1. The saturation magnetization of layers was determined from the intensity and the linewidth of the uniform ferromagnetic resonance (FMR) measured on the corresponding single-layer analogs [1].

As it is established previously [2], with the dominant dissipative mechanism of spin pinning, additional influence of reactive or dispersive properties of spin-pinning layer have lead to a change in the spatial phases of standing spin waves on the boundary between layers. This factor may lead to mismatch of the dispersion curves for normal and parallel the orientations of **H** relative to the film, because spin pinning layer can be the reactive or dispersion conditions depending on the orientation.

As the experiments have been shown, the effect of dispersive and reactive properties of the spin-pinned layer X-band the most significant for sample number 2, that leads to a significant mismatch of the dispersion curves (Fig. 1).

In work it is established that increase the frequency of the microwave field from f = 9/3 GHz to f = 34 GHz lead to the essential changes in the spectrum of SWR. The amount of observed SWR mode decreases (about twice) in both

Table 1.

Sample	Layer	Composition	h (μm)	$4\pi M$ (G)	α	γ ($\times 10^7$ Oe^{-1} s^{-1})	H_k^{eff} (Oe)
1	1*	$Y_{2.98}Sm_{0.02}Fe_5O_{12}$	0.51	1740	0.003	1.76	–1715
	2*	$Sm_{1.2}Lu_{1.8}Fe_5O_{12}$	1.4	1760	0.12	1.76	790
2	1*	$Y_{2.98}Sm_{0.02}Fe_5O_{12}$	0.34	1740	0.003	1.76	–1715
	2*	$Sm_{0.45}Er_{2.55}Fe_5O_{12}$	0.31	1330	0.2	1.38	–120

* 1 is the layer of the excitation, 2 is the spin-pinned layer.

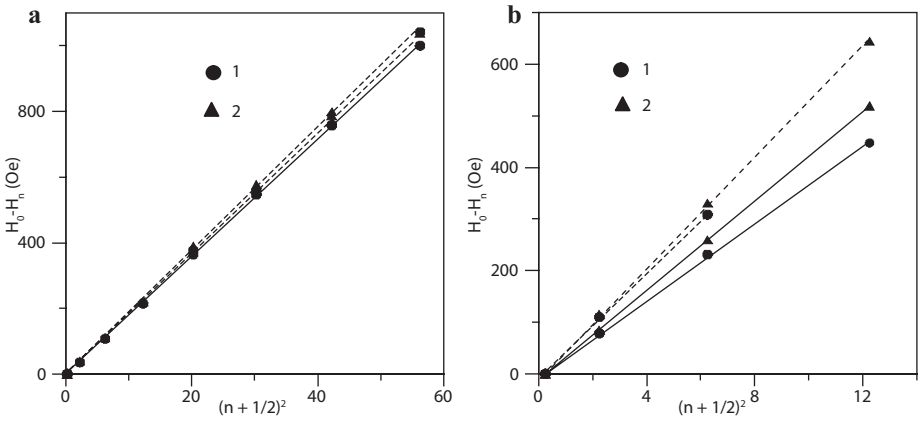

Fig. 1. Dispersion curves $H_0 - H_n = f(n + 1/2)$: **a** sample number 1, **b** sample number 2. Solid lines – X-band, dashed lines – Q-band. ● – normal orientation, ▲ – parallel orientation.

samples, also the magnitude of the mismatch of the dispersion curves for the parallel and normal orientations of the magnetic field relative to the plane film decreases. For the sample 2 has been discovered a noticeable increase angle of inclination these curves, at the same time for the sample number 1, this angle has remained practical unchanged. The increasing angle of dispersion curves in the sample number 2 with increasing frequency of the microwave field due to the strengthening of the spin pinning dissipative mechanism, that leading to a noticeable change in the spatial phase of the standing spin waves at interface between the layers and the corresponding change in the wave number k. It is shown that the absence of mismatch of the dispersion curves for sample number 1 when changing the frequency, due to the large difference between the values fields of uniform resonances $H_{01} - H_{02}$ in the excitation layer and in the spin-pinned layer.

1. Zuzin A.M., Vankov V.N., Radaykin V.V.: Technical Phys. Lett. **17**, no. 23, 65 (1991)
2. Zuzin A.M., Sabaev S.N., Radaykin V.V., Kulyapin A.V.: Physics of the Solid State **44**, no. 5, 893 (2002)

Spectra of Spin Wave Resonance in Films with a Linear Distribution of the Field Anisotropy Thickness

A. M. Zuzin, V. V. Radaykin, S. N. Sabaev, M. A. Bakulin, and **N. V. Yantsen**

Mordovian State University, Saransk 430005, Russian Federation, nikitos13rus@mail.ru

Unlike research SWR in two- and three-layered films consisting of homogeneous layers film with another character inhomogeneity of the field anisotropy, in particular the linear distribution of thickness $H_k = Bz + C$, are not fully understood.

In the work the calculation of the spectra SWR by solving the wave equation for the variable magnetization

$$\frac{2A}{M}\frac{\partial^2 m}{\partial z^2} - \left(H + Bz + C - \frac{\omega}{\gamma}\right)m = 0 \quad .$$

Constant currency A, magnetization of saturation M and g-factor corresponded to the parameters of films ferrite-garnet was assumed constant thickness. Parameters B = 1250 Oe/mkm and C = 0. The solution of this equation is a linear combination of Airy functions [1].

It is shown that unlike magnetic films with homogeneous layers, for films with a linear distribution of the field anisotropy of the distribution of peak absorption of SW-mod practically almost equidistant. On the dependence of the intensity of SW-mod from their rooms it is possible to allocate three sections.

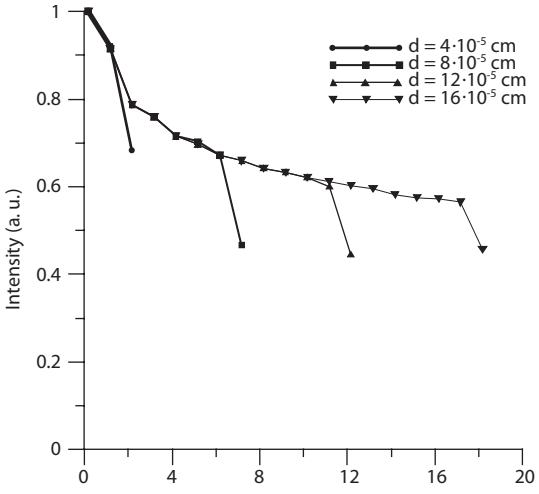

Fig. 1. Dependence of the intensity of SW-mod from their rooms at a different thickness of a film.

The first section of sufficiently rapid decreasing of intensity that corresponds to the first three modes. Then there is the plot a smooth decrease of intensity. Finally, the site of a sharp decline in the intensity of SW-mod, the beginning of which, the calculation shows that there corresponds to the transition from the excitation of localized modes to excitation of volume.

It is established that the decreasing film thickness results in consistent reduction in the number SW-mod, since mod high order on the second site, the first and third sections remain unchanged. First, with a decreasing in the thickness of the second section disappears, and then the third and first. At a certain critical thickness range is transformed into a single absorption line.

1. Hoekstra B., Stapele R.P., Robertson J.M.: J. Appl. Phys. **48**, no. 1, 382 (1977)

Spin Dynamics in Systems with Honeycomb Structure Probed by NMR and NQR

M. F. Iakovleva[1,2], E. L. Vavilova[2], M. I. Stratin[3], E. A. Zvereva[3], M. A. Evstigneeva[3], V. B. Nalbandyan[4], V. E. Kataev[2,5], and **A. Muller[6]**

[1] Kazan Federal University, Kazan 420000, Russian Federation, ymf.physics@gmail.com
[2] Zavoisky Physical-Technical Institute, Russian Academy of Sciences, Kazan 420029, Russian Federation
[3] Moscow State University, Moscow 119991, Russian Federation
[4] Southern Federal University, Rostov-on-Don 344090, Russian Federation
[5] Leibniz Institute for Solid State and Materials Research IFW Dresden, PO BOX 270116, Dresden D-01171, Germany
[6] University of Houston, Department of Chemistry and Texas Center for Superconductivity, Houston TX 77204, USA

Nontrivial topology, strong electronic, spin and orbital correlations in planar honeycomb lattice yield a rich variety of ground states. Nuclear magnetic and quadrupole resonance studies addressing to the ground states of the quasi-two-dimensional honeycomb lattice compounds $InCu_{2/3}V_{1/3}O_3$ and $Li_3Ni_2SbO_6$ are reported.

An important feature of the low-dimensional spin systems is the presence of quantum fluctuations that inhibit long-range order in the quantum spin-1/2 lattice. This effect depends on the spin coordination number z (the number of neighbors). The long-range order is possible at $T = 0$ in the 2D case in Heisenberg square lattice model with $z = 4$. The magnetic ions in the honeycomb lattice have coordination number $z = 3$. Thus quantum fluctuations are weaker than in the 1D case but stronger than in the 2D square lattice and the AFM order for the honeycomb lattice is fragile. In the $InCu_{2/3}V_{1/3}O_3$ quasi Heisenberg 2D magnetic system is realized by copper magnetic ions with spin $S = 1/2$. Uncorrelated finite size structural domains occurring in the planes are expected to inhibit the long range magnetic order. In $Li_3Ni_2SbO_6$ the magnetic system is formed by $^{2+}$Ni ions assuming high-spin configuration ($S = 1$). Due the geometry of the lattice a competition of different magnetic interactions arises, that in turn causes a magnetic frustration. It also prevents the development of the magnetic order.

Surprisingly, our experimental data show the development of two collinear antiferro-magnetic sublattices in $InCu_{2/3}V_{1/3}O_3$ below 35 and 15 K for $Li_3Ni_2SbO_6$. We have investigated the mechanism of setting the antiferromagnetic order with several methods focused on NQR and NMR results. In order to describe the experimental results some models of magnetic sublattices were considered and the most successful model was chosen.

AUTHOR INDEX

Akhmetov, M. M. 60
Akhmetzyanov, D. 52
Alfonsov, A. 36, 37
Anashkin, V. N. 53
Andreev, N. V. 38
Andrianov, V. V. 70
Anson, Ch. E. 62
Artyomov, M. Yu. 90
Atanasov, M. 16
Babaylova, E. 9
Bacher, A. 28
Badelin, A. G. 65
Bagryanskaya, E. 9
Bakirov, M. M. 60, 72, 80
Bakulin, M. A. 95, 97, 99
Bales, B. 80
Baltina, T. V. 70
Baniodeh, A. 62
Baranov, P. G. 8
Baroudi, K. 37
Barskiy, D. A. 27
Bayazitov, A. A. 53
Berezin, A. S. 63
Bezborodov, S. V. 97
Breitzke, H. 11
Büchner, B. 36, 37
Bukhtiyarova, G. A. 92
Buntkowsky, G. 11
Cava, R. J. 37
Cherepnev, G. V. 73
Chichkov, V. I. 38
Chumarov, P. 53
Chushnikov, A. I. 73
Denysenkov, V. 52
Dey, T. 36
De Zotti, M. 55
Di Mauro, E. 48
Domracheva, N. 91
Dvurechenskii, A. V. 13
Dzheparov, F. S. 12
Dzuba, S. A. 14, 77
Eisenreich, W. 28
Endeward, B. 6, 52

Eremina, R. M. 38, 62, 65
Evstigneeva, M. A. 101
Fakhrutdinov, A. R. 53
Falin, M. L. 67, 68
Fatkullin, N. 32
Fattakhov, Ya. V. 53
Fazlizhanov, I. I. 38
Fedin, M. 9
Fel'dman, E. B. 33
Fischer, M. 28
Formaggio, F. 55
Fursenko, D. A. 82
Gainutdinov, Kh. L. 70
Galeev, R. T. 62, 72, 80
Gavrilova, T. P. 38, 65
Gilmutdinov, I. F. 74
Golubeva, E. N. 21
Gorshunov, B. P. 82
Grafe, H.-J. 36, 37
Gromov, O. I. 21
Gubskaya, I. A. 22
Guedes, C. L. B. 48
Gumarov, G. G. 60
Gutmann, T. 11
Hairuzhdinov, I. T. 80
Hofmann, M. 32
Huang, Q. 37
Iafarova, G. G. 70
Iakovleva, M. 36, 101
Ibragimova, M. I. 73
Illarionov, B. 28
Isaev, N. P. 14, 55, 77
Ivanova, G. I. 74
Ivanova, T. A. 74
Ivashita, F. F. 48
Iyudin, V. S. 70
Jeschke, G. 2, 7
Kacprzak, S. 28
Kandrashkin, Yu. E. 29
Karpova, G. 9
Kataev, V. 36, 37, 101
Khaidukov, N. M. 68
Khairuzhdinov, I. T. 79
Khitrin, A. K. 86
Kirilyuk, I. 9
Klauss, H.-H. 36

Kokorin, A. I. 21
Komarovskikh, A. 75
Konov, A. B. 60
Konov, K. B. 14, 77
Konygin, G. N. 60
Koptyug, I. V. 27
Korableva, S. L. 67
Kothe, G. 28
Kovtunov, K. V. 27
Krumkacheva, O. 9
Kudryashov, V. Y. 42
Kupriyanov, I. 75
Kuzhelev, A. 9
Lapina, O. B. 26
Latypov, V. A. 67, 68
Lavrenova, L. G. 63
Leonov, D. V. 14
Likhtenshtein, G. I. 17
Link, G. 28
Lisin, V. N 56
Lomzov, A. 9
Lovchev, A. V. 68
Luetkens, H. 36
Lukaschek, M. 28
Maljuk, A. 36
Mambetov, A. E. 80
Mamedov, D. V. 38, 65
Marko, A. 6, 52
Martyanov, O. N. 92
Meier, R. 32
Mikhalitsyna, E. 50
Mingalieva, L. V. 74
Mondal, A. 62
Morozova, O. B. 15, 51
Mosca, D. H. 48
Muller, A. 101
Nadolinny, V. A. 63, 75
Nalbandyan, V. B. 42, 101
Neese, F. 16
Nenashev, A. V. 13
Nureeva, G. R. 22
Nuretdinov, I. A. 22
Nuretdinov, V. P. 22
Ovchinnikov, I. V. 74
Paesano Jr., A. 48
Palyanov, Yu. 75

Panov, M. S. 51
Petukhov, V. Yu. 60, 73
Piccinato, M. T. 48
Plackmeyer, J. 52
Polienko, Y. 9
Potapov, A. P. 90
Powell, A. K. 62
Prando, G. 37
Prisner, T. F. 3, 6, 52
Pyataev, A. V. 91
Pyshny, D. 9
Raap, J. 55
Radaykin, V. V. 95, 97, 99
Romanov, N. G. 8
Rössler, E. A. 32
Rumyantsev, E. L. 90
Rybin, D. S. 60
Sabaev, S. N. 97, 99
Saenko, N. S. 40
Salikhov, K. M. 22, 50, 72, 79, 80
Salnikov, O. G. 27
Samoilova, R. I. 55
Sarvezuk, P. W. C. 48
Savostina, L. I. 22
Savostina, S. A. 95
Schöps, P. 6
Shagalov, V. A. 53
Shakhmuratov, R. N. 49
Shakurov, G. S. 82, 93
Shegeda, A. M. 56
Shevelev, G. 9
Shubin, A. A. 26
Shukaev, I. L. 42
Shustov, V. A. 74
Skovpin, I. V. 27
Skrylnik, P. G. 83
Solovarov, N. 85
Spindler, P. E. 6
Stapf, S. 32
Stratin, M. I. 101
Sukhanov, A. 50, 62, 85
Suturina, E. A. 16
Tagirov, L. 44
Tarasov, V. 85
Terskikh, V. V. 26
Thomas, V. G. 82

Toniolo, C. 55
Tormushev, V. 9
Turanov, A. 86
Turanova, O. A. 74
Tyurin, V. 50
Ulanov, V. A. 88, 93
Useinov, N. 44
Valezi, D. F. 48
Valiullin, R. 46
Vanin, A. F. 20
Varalda, J. 48
Vasiliev, A. N. 42
Vavilova, E. 36, 37, 101
Vazhenin, V. A. 90
Vorobyeva, V. 91
Voronkova, V. 22, 50, 62
Weber, S. 28
Wu, H. 37
Wurmehl, S. 36
Yakushkin, S. S. 92
Yantsen, N. V. 99
Yatsyk, I. V. 38, 65, 73
Yim, C. 37
Yurkovskaya, A. V. 15, 51
Zainullin, R. R. 88, 93
Zaripov, R. B. 22, 79, 80, 85
Zaripov, M. M. 88
Zhiteitsev, E. R. 88
Zhivonitko, V. V. 27
Zhukova, E. S. 82
Ziatdinov, A. M. 40, 83
Zimmermann, S. 36
Zinovieva, A. F. 13
Zuzin, A. M. 95, 97, 99
Zvereva, E. A. 42, 101

Ответственный редактор В. К. Воронкова; редакторы: С. М. Ахмин, Л. В. Мосина; технический редактор О. Б. Яндуганова. Издательство КФТИ КазНЦ РАН,
420029, Казань, Сибирский тракт, 10/7, лицензия № 0325 от 07.12.2000.

BRUKER

EMX^micro

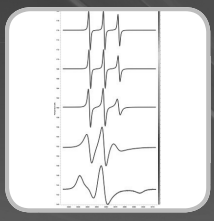

Nitrogen VT system for 100–600K

PremiumX optional microwave units for weak-pitch S/N of 2000:1

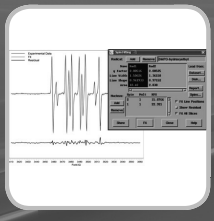

Xenon software package with SpinCount and SpinFit

- X-band continuous wave EPR spectrometer
- Compatible with L-, S- and Q-band frequencies
- Micro bay console with footprint of a PC tower
- High fidelity signal and field control
- Extensive range of accessories
- Weak-pitch signal-to-noise of 1200:1

Find out more about our cutting-edge EPR technology:
www.bruker.com/epr